CHEMICAL AND PHYSICAL INVESTIGATION OF THE EFFECT OF THE MANUFACTURING PROCESS AND STERILIZATION ON THE YARN USED IN POLY(ETHYLENE TEREPHTHALATE) VASCULAR PROSTHESES

A Thesis Presented to

The Faculty of Graduate Studies and Research

University of Manitoba

In Partial Fulfilment

of the Requirements for the Degree

Master of Science

by

Eleanor Prowse

1979

CHEMICAL AND PHYSICAL INVESTIGATION OF THE EFFECT OF THE MANUFACTURING PROCESS AND STERILIZATION ON THE YARN USED IN POLY(ETHYLENE TEREPHTHALATE) VASCULAR PROSTHESES

BY

ELEANOR RUTH PROWSE

A dissertation submitted to the Faculty of Graduate Studies of the University of Manitoba in partial fulfillment of the requirements of the degree of

MASTER OF SCIENCE

ABSTRACT

On the basis of in vivo performance, a knitted tube of Dacron® poly(ethylene terephthalate) (PET) multifilament yarn has been considered a reliable vascular prosthesis. Recently reports in the medical literature have revealed incidents where these knitted grafts have failed. These failures have been attributed to (i) alteration of the prostheses during manufacture, sterilization and/or implantation, (ii) defects in the original polymer, and/or (iii) defects in the knit construction. This study examined the physical and chemical effects of the compaction and crimping treatments during manufacture, and of gas sterilization on the PET yarns. The chemical and thermal conditions of the compaction and crimping processes were reproduced in the laboratory by following the commercial patents. As well, the PET yarns were exposed to ethylene oxide under controlled conditions in a hospital sterilization unit. Yarns unravelled from a commercially treated reference graft were also compared to the experimentally compacted and crimped yarns. Molecular weight determinations, measurements of yarn geometry, density analysis, differential scanning calorimetry, infrared spectroscopy, birefringence and tensile behavior were used to characterize the chemical and physical changes in the PET yarns.

The results indicated that significant changes occurred to the structure and properties of PET yarn during the compaction and crimping stages of manufacture and during gas sterilization. Compaction, crimping and sterilization of PET yarns resulted in changes in microstructure, surface porosity and polymer chemistry that influence the

susceptibility of PET to degradation after implantation. It is concluded that the manufacturing and sterilization conditions of the PET yarns may have a significant effect on the in vivo performance of a graft, in particular its patency, its rate of healing and the liklihood of failure.

ACKNOWLEDGEMENTS

A number of individuals contributed to the success of this study. I would especially like to thank my advisor Professor Martin W. King for his patience, encouragement and guidance throughout this research project. The advice and support from Professor Susan Hayward, Department of Clothing and Textiles, Dr. A.B. Thornton-Trump, Department of Mechanical Engineering, and Dr. M. Samanta, Department of Statistics as committee members, is also gratefully acknowledged. I would like to thank the staff of the Department of Clothing and Textiles, University of Manitoba for valuable contributions to the development of this study. Special thanks is due to Mrs. Judy Teerhuis for her assistance and support in the laboratory. Acknowledgement is due to Dr. H. Gesser, Department of Chemistry, Dr. Allan Downs and Dr. Charles Lye, Department of Surgery for their advice and support. For direction and assistance with gas sterilization I would like to thank Mrs. H. Mazerall, Director of the Central Processing Department at the Health Science Centre. The early planning phase of the study was greatly facilitated by consultation and encouragement from Dr. Robert Guidoin, Département de Chirurgie Experimentale, Centre de Biomédecine, Université Laval. I must also acknowledge the support from Mr. Lester Glantz, Executive Director of the Medical Products Institute, and Dr. Pierre Blais, Health Protection Branch, Health and Welfare Canada. I am grateful to Mr. Danny Buksak, Department of Chemistry, for his help with the Differential Scanning Calorimeter, Mr. Bryn Easterbrook, Department of Chemistry, for making the density beads, and to Mr. Clive

Healy, Central Instruments Service, for constructing the compaction apparatus. In addition I wish to acknowledge the assistance of E.I. du Pont de Nemours and Company Inc for supplying the Dacron Type 56 yarn and to Rohm and Haas Co for supplying the Triton X-100.

TABLE OF CONTENTS

LIST OF TABLES

LIST OF FIGURES

LIST OF PLATES

Chapter 1

INTRODUCTION

The basic healing pattern of vascular prostheses involves several steps. Upon implantation of the graft the interstices of the fabric are sealed and the surfaces are coated by an absorbed protein layer of whole-blood thrombus (coagulated blood). Next the whole-blood thrombus is converted to fibrin which decreases the thrombogenicity of the surface. After approximately 24 hours an inner and outer layer of fibrin forms around the prosthesis. During the first few weeks after implantation the outer fibrin layer is organized by granulation tissue. An outer encapsulating sheath of fibrous tissue is formed which gives rise to discrete tufts that grow between the yarn bundles and organize the inner layer of fibrin (Wesolowski, 1968: 328). The ultimate aim is to promote the development of a good fibrin lining that is moderately resistant to whole-blood thrombus and does not slough off to cause embolization. This condition is to be distinguished from the desirable initial state of forming a thin whole-blood thrombus layer. Researchers have identified some important factors involved in the healing of vascular prostheses or vascular grafts, but there are still a number of gaps in understanding the in vivo interaction with synthetic materials (Wesolowski, 1968; Bruck, 1978; and Sauvage et al., 1974).

Satisfactory performance of a material is dependent on whether its properties ensure its function in a specific environment. In particular, fibers which comprise surgical implants should be selected to give optimum performance in the body environment. This is especially

true for vascular prostheses, which must remain viable while in the circulatory system.

A knitted tube made of poly(ethylene terephthalate) (PET) yarn has been adopted as the preferred vascular prosthesis, in the majority of applications (Golaski, 1968; Sauvage et al., 1976; and Guidoin et al., 1977). Specifically, poly(ethylene terephthalate) yarn has been desired for its overall performance, good handling properties and availability. The knitted construction was chosen for: (i) ease in handling; (ii) non-fraying property; (iii) good elongation; (iv) good elastic recovery; and (v) flexibility. In addition, the porosity and performance characteristics of the knitted tube have been improved by compacting and crimping techniques (See Appendix A for a definition of these terms) (Smith, 1974; and Jeckel, 1967). Nevertheless, with longer term implantation of the prostheses, some previously unforeseen problems have arisen (Guidoin et al., 1978).

In the past few years, incidents of the failure of knitted arterial grafts have been reported in the medical literature (Yashar et al., 1978; Blumenberg and Gelfand, 1977; Perry, 1975; Hayward and Korompal, 1976; and Hussey, 1976). Some of these failures have been thought to be due to alteration of the prostheses during manufacture, sterilization or implantation. Others have been attributed to defects in the original polymer and/or knit construction. A number of surgeons and researchers working with vascular prostheses have indicated that there is a gap in the knowledge of how the manufacturing process and sterilization of these products affect their life within the body (Guidoin et al., 1977; King and Lyman, 1975; Blumenberg and Gelfand, 1977; and Hayward and Korompal,1976).

Researchers did not believe that the PET graft was vulnerable to degradation in the body. This belief was reflected in the approach of previous studies which have focussed on the effect of the fabric construction of the grafts upon the body (Wesolowski, Fries and Sawyer, 1961; Guidoin et al., 1977; and King and Lyman, 1975). Wesolowski, Fries and Sawyer (1961) suggested that the porous wall, rather than the chemical reactivity, governed the fate of the graft. Almost no consideration has been given to the history of the graft prior to its implantation, or to how the PET fibers might change during manufacture and/or sterilization (King and Lyman, 1975). Consequently there has been ample justification for this exploratory study which has examined the poly(ethylene terephthalate) yarn structure and properties before and after the compaction and crimping stages of manufacture, and before and after sterilization.

OBJECTIVES

1. The main objective of this study was to analyze the relationships between the chemical and physical properties of the yarn samples to determine whether measurable differences existed between the untreated, the treated and the commercially treated samples. If differences did exist between the untreated and treated samples then it was intended:

(i) To characterize the changes in fiber structure during compaction by comparing the chemical and physical properties of the untreated sample before and after compaction.

(ii) To characterize the changes in fiber structure during crimping by comparing the chemical and physical properties of the compacted sample before and after crimping.

(iii) To characterize the changes in fiber structure during sterilization by comparing the chemical and physical properties of the compacted, crimped samples before and after sterilization.

Further objectives were:

2. To characterize the fiber structure, and suggest possible manufacturing conditions for the commercial reference (Milliknit®) graft by comparing the chemical and physical properties of the commercial reference sample with those of the compacted and crimped yarn samples,and

3. To compare the chemical and physical properties of the compacted, crimped and sterilized samples to the untreated sample.

ASSUMPTIONS

1. There was no difference between the three experimentally prepared batches of compacted yarn.

2. The selected chemical and physical tests were sufficiently sensitive to measure the structural changes that occurred in the yarn during processing and sterilization.

3. The information given in United States Patents 3,853,462 (Smith, 1974) and 3,337,673 (Jeckel, 1967), which describe the compaction and crimping processes respectively approximate the actual manufacturing conditions for Milliknit® vascular prostheses.

4. The conditions for treatment of the yarn in the study were the same as those outlined in United States Patent 3,853,462 (Smith, 1974) for the compaction process, and United States Patent 3,337,673 (Jeckel, 1967) for the crimping process.

5. Vascular prostheses are manufactured from yarn similar to that used in this study.

SCOPE AND LIMITATIONS

Due to the exploratory nature of this study, the sample size was small in that the treated and untreated yarn was selected from within a single bobbin and the commercial reference yarn was unravelled from two prostheses. Therefore, consideration of inherent differences between individual filaments and lack of uniformity in the yarns were not included in the analysis.

Chapter 2

REVIEW OF LITERATURE

This chapter describes the elements in the design of poly(ethylene terephthalate) (PET) grafts, and the recently reported failures experienced with their use. Chemical, microstructural, and biological degradation of PET are then reviewed.

ELEMENTS IN THE DESIGN OF POLY(ETHYLENE TEREPHTHALATE) GRAFTS

A knitted vascular prosthesis has been developed from poly(ethylene terephthalate) (PET) yarn (Golaski, 1968; Sauvage et al., 1976; and Guidoin et al., 1977). This graft, with various refinements in structure, has been adopted by the majority of surgeons. The basic design consists of three major elements: (1) the PET polymer; (2) the warp or weft knitted tube of continuous multifilament yarns; and (3) the crimped tube.

An important design criteria has been that the PET polymer should be suitable for implantation in the body environment. It has been generally accepted that PET retains its tensile strength in the body and experiences negligible degradation (Guidoin et al., 1977; Lyman, 1968; and Skelton, 1974). It has possessed good handling properties during manufacture and for the surgeon (Guidoin et al., 1977). In addition, PET yarn has been available in a wide range of types and constructions (Golaski, 1968).

A knitted construction with multifilament yarns has enabled the

porosity required for vascular implantation to be achieved. Laboratory and in vivo experimental trials have shown that porosity or permeability of knitted arterial grafts is an important factor in their performance in the body environment. The porosity has been measured in terms of the number of cubic centimeters of water which pass through one square centimeter of graft fabric per minute at 120 mm H_g pressure. The porosity should be high enough to promote tissue ingrowth and long-term healing and low enough to prevent undue hemorrhaging at implantation (Golaski, 1968; Sauvage et al., 1976; and Guidoin et al., 1977). Multifilament yarns with little or no twist allow openings between filaments, which increase the porosity (Golaski, 1968). The knitted structure has contributed interstitial spaces between yarns. Chemical and thermal processing techniques are used during manufacture to shrink the yarn longitudinally, which swells the yarn laterally, and hence compacts the knit structure to the desired porosity (Golaski, 1968; Smith, 1974; and Jeckel, 1976).

The knitted construction has had several other useful design features. The knitted prostheses have been desired for their non-ravelling characteristics, ease of handling and flexibility. It has been important to the surgeon that the grafts do not fray when cut to the required length for implantation. The elongation, elastic recovery and crease resistance of the knitted fabric have contributed to ease in handling of the prostheses. The flexibility of the tube has allowed it to be twisted to help prevent kinking during surgical insertion (Golaski, 1968; and Guidoin et al., 1977).

In 1955 Sterling Edwards suggested that crimping vascular prostheses along their length would improve their performance within the

body. Specifically, corrugations provide non-collapsible grafts and have helped to eliminate occlusion caused by kinking (Takebayaski, 1975). The accordion-like pleats have also contributed the necessary elasticity and extensibility of normal blood vessels (Golaski, 1968). The tubing has been uniformly crimped by a heat setting process (Jeckel, 1967).

FAILURE OF POLY(ETHYLENE TEREPHTHALATE) GRAFTS

Descriptions of the failed PET grafts revealed that they have "deteriorated" (Perry, 1975: 320), "are very fragile" and can be "easily pulled apart" (Hayward and Korompal, 1976: 582). Blumenberg and Gelfand (1977: 495) considered the problem may be one of "manufacture, material, or both." Guidoin et al. (1977: 201), who studied a number of brands of PET vascular prostheses, concluded that: "as far as the prosthesis is concerned, it might be not only a problem in the design of the prosthesis but also in the catalysts and chemicals employed to manufacture them." Perry (1975) stated that the manufacturers could not determine the cause of the failure of the weakened grafts. Likewise independent laboratories have been unable to establish why knitted PET grafts lose tensile strength (Hayward and Korompal, 1976). Clearly, chemical and physical analysis of the polymer material could contribute to a better understanding of the performance of the graft.

Sauvage et al. (1976) have outlined three stages in the life of a graft. The first stage involves textile processing necessary to produce the "fiber framework," which the surgeon implants in stage two, and which the body utilizes in stage three to form a fully healed graft. King and Lyman (1975) have also outlined the environments to which the

graft is exposed: processing, storage, sterilization, and implantation within the body. Each environment has the potential to affect the performance of the prosthesis in all subsequent environments. Sawyer et al. (1978: 218) after studying seven different chemical compacting methods, for a number of evaluation criteria, concluded from the findings that: "...it is imperative for the vascular surgeon to have some idea of the various modifications introduced into the manufacture of a dacron [Dacron®] prosthetic graft if one expects similar performance characteristics among the grafts following implantation." Thus, it would be unrealistic to consider the biochemical or biomechanical in vivo behavior without having regard for the previous history of the material.

DEGRADATION OF POLY(ETHYLENE TEREPHTHALATE)

Chemical Degradation

Environmental conditions over a period of time can lead to degradation of the exposed polymer. Degradation of polymers has been considered "any type of modification of a polymer chain involving the main-chain backbone or side groups or both" (Reich and Stivala, 1971: xiv). This modification has often been of a chemical nature where primary or secondary valency bonds are broken within or between chains. When the various polymer properties such as crystallinity, molecular weight and mechanical properties have been affected the polymer is said to have "degraded." The degradation of polyesters can be initiated by any of the following mechanisms; thermal, oxidative, radiative, mechanical, chemical or biological (King and Lyman, 1975; and Reich and Stivala, 1971). With reference to the manufacturing process and sterilization of

PET vascular prostheses, the relevant mechanisms are expected to be chemical and/or thermal in nature.

The repeat unit of PET is;

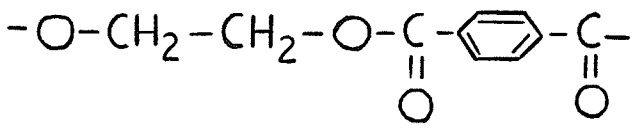

molecular weight 192.

The high molecular weight, and the configuration of the chains, have made it difficult to study the degradation of the PET polymer directly. Studies of a number of simpler model systems representing specific segments of the PET chain have allowed identification of the probable sites prone to degradation (Buxbaum, 1968). Possible degradation mechanisms in the manufacturing process and sterilization of vascular prostheses are: (1) the chemical reactions involved in compaction; (2) the effect of heat due to crimping; and (3) the chemical reactions or effect of heat upon sterilization.

Since an acidic solvent is used in the compaction process, it is possible that PET is subject to hydrolysis. Although PET is known to resist attack by water, acids and bases due to its aromatic nature and tight packing of chains (Buxbaum, 1968), hydrolysis in neutral or acid media can occur as outlined below:

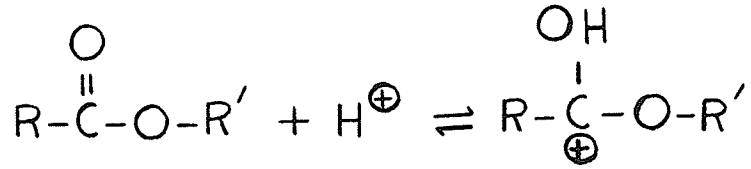

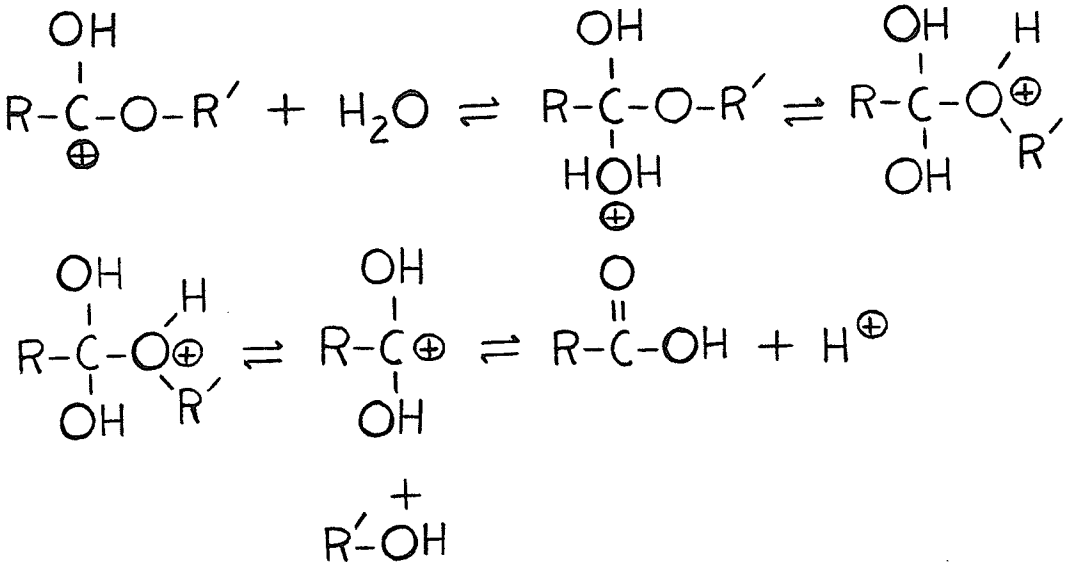

(Buxbaum, 1968: 189).

Moreover, the PET is exposed to three heat treatments during manufacture and sterilization: (1) during drying after compaction; (2) during crimping; and (3) during gas or steam sterilization. Thermal degradation of PET involves random chain scission at the ester links (Buxbaum, 1968; and Pohl, 1951). The main thermal reaction has been summarized as follows:

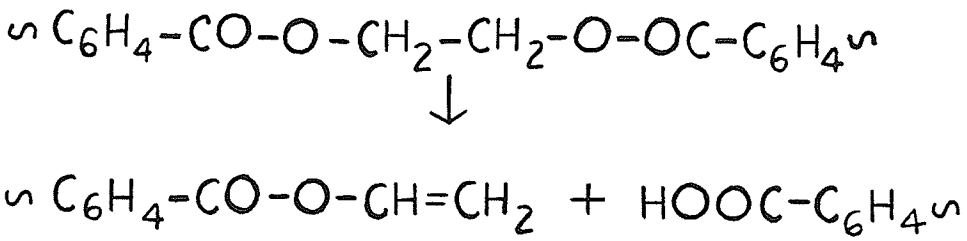

(Buxbaum, 1968: 185).

This reaction occurs especially at temperatures greater than 200°C (Buxbaum, 1968; and Carter, 1971). According to Carter (1971: 134) at 100°C, 4.0×10^{-8} ester links are broken per day per 10^6 g of polymer while at 282°C, 3.1×10^{-2} ester links are broken per day per 10^6 g of polymer.

Plester (1970) indicated that PET is suitable for gas sterilization treatment, while King and Lyman (1975) pointed out that the effects of sterilization on polymeric materials are very seldom given proper attention. Bruck (1971) suggested that above room temperature polyesters can react with ethylene oxide. The three membered ring of ethylene oxide is highly strained and opens readily (Roberts, Stewart and Caserio, 1971). Evidence from the literature indicates that macromolecules, such as PET, containing hydroxyl and carboxyl groupings may react with ethylene oxide to form crosslinks or pendant chains (Battaered and Tregear, 1967: 41). In addition, ethylene oxide can react with carboxyl and hydroxyl endgroups of PET (Stevens, 1975; Bruck, 1971; and Roberts, Stewart and Caserio, 1971). The reaction mechanisms are outlined below:

(1) carboxyl endgroup addition

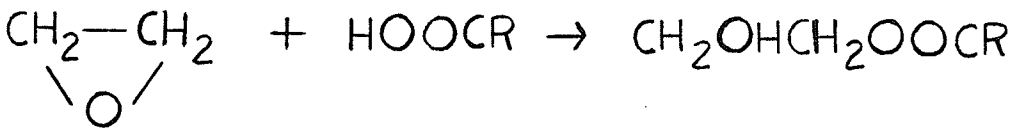

(adapted from Bruck, 1971: 151).

(2) hydroxyl endgroup addition

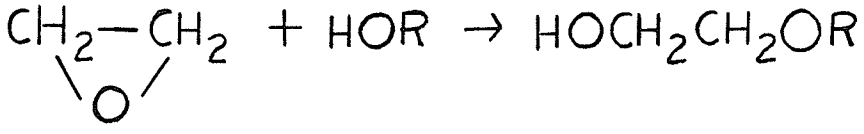

(Adapted from Roberts, Stewart and Caserio, 1971: 266).

Changes in Microstructure

An understanding of the chemical and thermal effects which occur during the manufacture and sterilization of PET grafts requires some knowledge of the microstructure of the fibers. Unfortunately, none of the current models for fiber structure explain all the fiber properties (Walczek, 1977). In spite of this fact some representative models have been used to examine the microstructure of fibers. The following descriptions explain how specific models apply to PET fibers and what microstructural changes may take place during the compaction, crimping and sterilization treatments.

A general view presented by Morton and Hearle (1975: 33) included the following elements: (i) the "degree of order"; (ii) the "degree of localization of order"; (iii) the "length/width ratio of localized units"; (iv) the "degree of orientation"; and (v) the "size of localized units." The term "order" refers to the correlation of neighbouring chains in direction, distance apart, and relative position (Hearle and Greer, 1970: 2). In most textile fibers there is a wide range of degrees of order from a highly ordered (perfectly crystalline) to a wholly random (amorphous). "Orientation is the extent to which the chain direction is correlated over the whole fiber" (Hearle and Greer, 1970: 2). This is usually expressed relative to the fiber axis.

Drawn PET fibers generally exhibit a high degree of order, and the chains are predominently oriented in the longitudinal direction of the fiber. From previous studies of PET, it has been suspected that the drawn fibers ". . . behave as if they contain two conterminous types of structural organization, crystalline and amorphous" (Goodman

and Rhys, 1965: 38). Recently researchers have suggested a three phase model in which drawn PET fibers also contain an intermediate (oriented amorphous) phase of nearly extended molecular chains along the fiber axis (Prevorsek et al., 1974; and Gupta and Kumar, 1978). For the purpose of this study a three phase model is utilized. Therefore, drawn PET is referred to as a semicrystalline, oriented fiber with crystalline, intermediate and amorphous phases.

When drawn PET is exposed to certain chemicals, or to temperatures in excess of its glass transition temperature, a decrease in length is observed. It has been suggested that this longitudinal shrinkage is caused by localized disruption of the van der Waals forces, thereby allowing an increase in the mobility of the chain segments (Ribnick, Weigmann, and Rebenfeld, 1973).

According to Wilson (1974), thermally induced shrinkage is a two stage process. It involves a rapid initial stage associated with disorientation in the amorphous zones. Contraction occurs when thermal energy frees the intermolecular bonds between neighbouring extended chains (Ribnick, 1969: 748). Prevorsek et al. (1974) explained this stage of contraction by reference to the intermediate phase where chains within the phase reorganize themselves to minimum energy positions. This increases the amount of the intermediate phase (Deopura, Sinha and Varma, 1977). The second stage, described by Wilson (1974), involves chain folding and an increase in the amount of crystallization. At relatively low temperatures drawn PET chains are freed from intermolecular bonds, and so can contract from an extended to a folded configuration. At higher temperatures these nucleating regions grow into larger folded crystallites which eventually replace the extended chain

configuration (Ribnick, 1969). In terms of the two phase model, Peters (1963), explained that those segments of the molecular chain which possess sufficient energy will break away from the amorphous regions. Thus the size of the crystalline regions grows at the expense of the amorphous regions. Eventually an entangled state is produced in the amorphous regions which resists random thermal motion. A dynamic equilibrium is thereby established since further growth of the crystallites is limited by the lack of available molecules in the amorphous regions. At the same time the void space in the fiber is increasing due to the breakage of intermolecular bonds (Statton, 1971).

In chemically induced shrinkage it is thought that the solvent swells the polyester structure and disrupts the van der Waals forces between the PET chains (Weigmann et al., 1977). According to Weigmann et al. (1977), a high degree of shrinkage occurs, because the solvent disorientates the intermediate phase.

Disorientation due to chemically induced shrinkage is similar to that experienced by heat induced shrinkage, since in both instances the random thermal motion of the chains leads to lateral swelling and the formation of crystallites. With the heat induced shrinkage, however, larger crystallites are formed. Weigmann et al. (1977: 753) have concluded that "at the same level of disorientation obtained by heat or solvent treatment, the structure produced by the solvent treatment is much more accessible to the dyestuff." It is suspected that this is caused by the formation of voids in the solvent treated structure (Weigmann et al., 1977).

Only a few studies have considered the effect of solvent treatment on PET followed by heat. Weigmann, Scott and Ribnick (1977) found

that the void structure in solvent treated PET partially collapsed on subsequent heating. The degree of collapse was dependent on the heating temperature. They concluded that:

> Thermal treatments at temperatures beyond the temperature of the thermal stability of the solvent-induced crystallites completely eliminates any memory of the prior solvent treatment and results in a fiber structure essentially identical with that produced by heat treatment alone (Weigmann, Scott and Ribnick, 1977: 770).

IMPLICATIONS FOR DEGRADATION IN THE BODY ENVIRONMENT

Chemical and microstructural changes occurring during manufacture and sterilization are expected to affect the likelihood of polymer degradation, as well as the rate of healing and the mechanical performance of the implanted graft. Surface and internal chemical degradation of the polymer weakens the grafts and alters their mechanical performance. Chemical changes to the PET chain, involving chain scission, cross-linking or addition reactions are likely to change the susceptibility of the polymer to degradation in the body as well as effect the healing process. Furthermore, changes in the crystalline, intermediate, and amorphous phases, and the creation of void spaces, will affect the chemical reactivity and hence the healing properties of the material. Until recently, neither the conditions that promote biological degradation, nor those that affect healing of the PET graft, have received much attention in the literature.

Reed, Gilding and Wilson (1977), in studying the biodegradability of elastomeric biomaterials, concluded that extracellular enzymes with known ester cleavage ability, such as esterase and leucine amino peptidase, could degrade PET. Chemical hydrolysis has been found to be the

main mechanism in causing degradation when either of these two enzymes have been present in high concentrations. Potts (1978: 645) stated that, "although aromatic polyesters are generally considered to be resistant to biological degradation, there have been no published studies on their level of bioresistance." Furthermore, little is known about the blood/polymer interface. According to Merrill (1977: 15):

> . Since the sequence of moieties on the protein are rarely known, one is nearly completely ignorant of how to design the polymer surface to thwart activation of activatable proteins that arrive on the surface. One does know that polymeric substances become coated with protein molecules after exposure to blood in vivo and that in some instances a stable layer of protein is finally achieved that renders the polymer passive.

Sawyer et al. (1978) have evaluated the patency, handling characteristics, long-term function, pathology, complications and acceptability to the host of the PET grafts after seven different chemical modification treatments during manufacture. Two of the main points they presented in their discussion were that the ". . . crimping and compaction of a dacron [Dacron®] prosthesis appears to affect long-term function of these prostheses following implantation," and that chemical treatment along with porosity and construction determine the nature of the inner fibrous capsule formation (Sawyer et al., 1978: 218). The character of this capsule determines the success or failure of the prostheses.

Chapter 3

METHOD

The research design and procedures are presented in this chapter in the following sequence: the selection and description of samples, the compaction, crimping and sterilization procedures, the evaluation procedures, and the analysis of data. Six measures are included in the evaluation procedure: viscometry, yarn geometry, thermal analysis, infrared spectroscopy, birefringence, and tensile properties. Yarn geometry includes shrinkage, filament diameter, linear density and density. The tensile properties of interest are tenacity, breaking toughness and initial modulus.

SELECTION AND DESCRIPTION OF SAMPLES

Seven samples of polyester yarn were selected for the study. They each represented a different stage in the manufacture and sterilization of PET vascular grafts. Samples one to six were 4.4 tex/27 filament Type 56 Dacron®* yarn (*Dacron® - registered United States Trademark for poly(ethylene terephthalate) from E.I. du Pont de Nemours and Company Inc.) (Plate 1 and Table 1). Sample seven was 11.1 tex/54 filament Type 57 Dacron® yarn unravelled from a Milliknit®* graft (*Milliknit® - registered United States Trademark for knitted vascular prostheses from Golaski Laboratories Inc.) (Plate 1 and Table 1). Two strands of the Dacron® yarn from the bobbin were wound together so

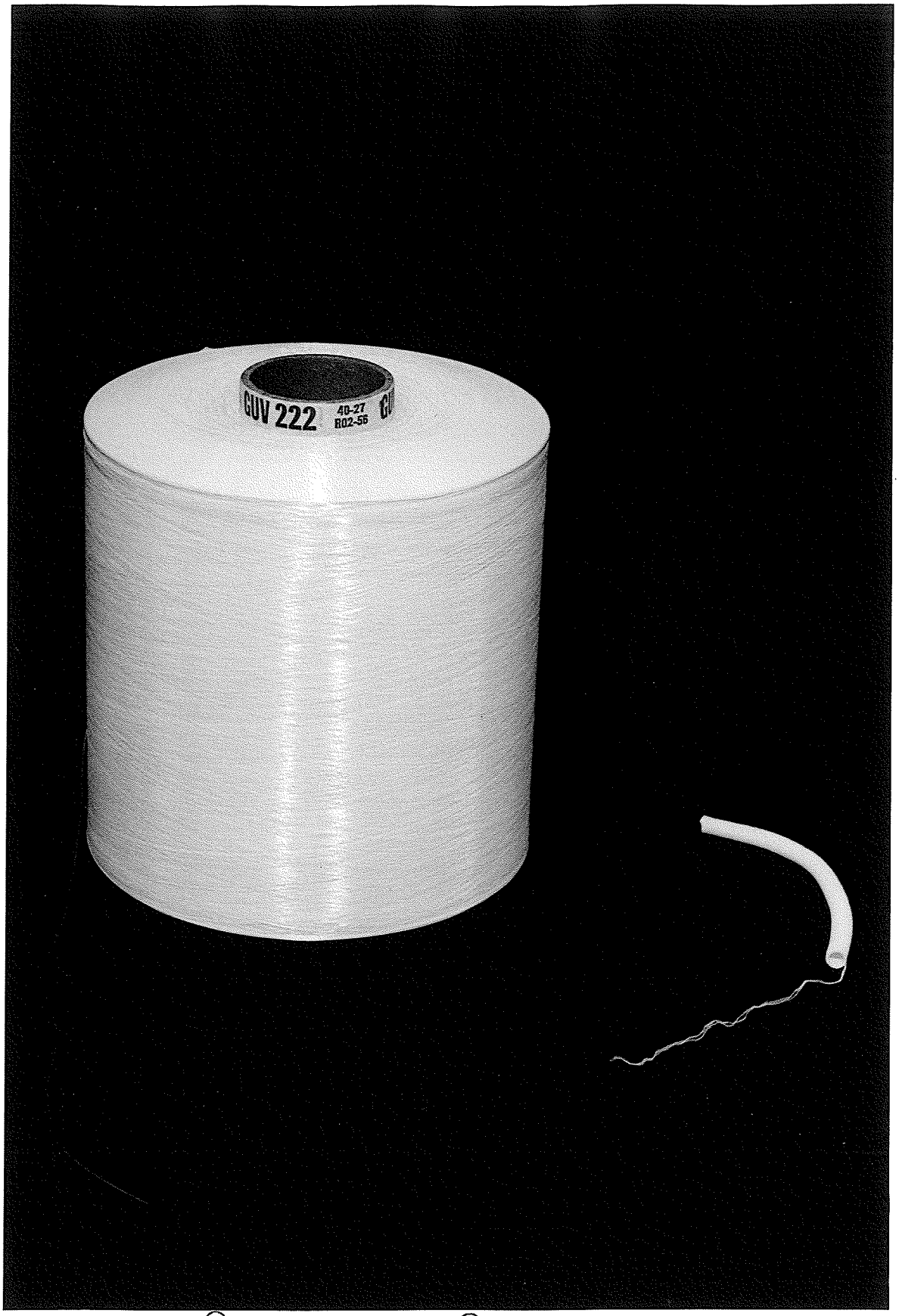

Plate 1. Dacron ® Yarn and Milliknit ® Graft

comparison could be made with the commercial reference yarn unravelled from the vascular grafts. Although the tex values were different, the yarns were comparable because the Milliknit® graft contained yarn shrunk by 25% during compaction. It is believed that Type 56 and Type 57 are both normal tenacity filament Dacron®. They differ in that Type 56 is semi-dull, and Type 57 is dull (Burlington Industries Inc., 1970: 34). The filaments in the dull yarn contain more TiO_2 which is used as a delusterant.

Table 1. Description of Samples

Sample	Description
One	Untreated yarn, 4.4 tex f27 t0 Dacron® polyester.
Two	Sample one compacted.
Three	Sample two crimped at 94°C (200°F).
Four	Sample two crimped at 154°C (300°F).
Five	Sample three sterilized.
Six	Sample four sterilized.
Seven	Commercial reference sample - unravelled from the Milliknit® grafts, 11.1 tex f54 t0 Dacron® polyester.

COMPACTION, CRIMPING AND STERILIZATION PROCEDURES

Compaction Process

A brass compaction apparatus was constructed to restrain the yarn and thereby control the amount of shrinkage during compaction (Plate 2). A special winding instrument was built to wind two strands

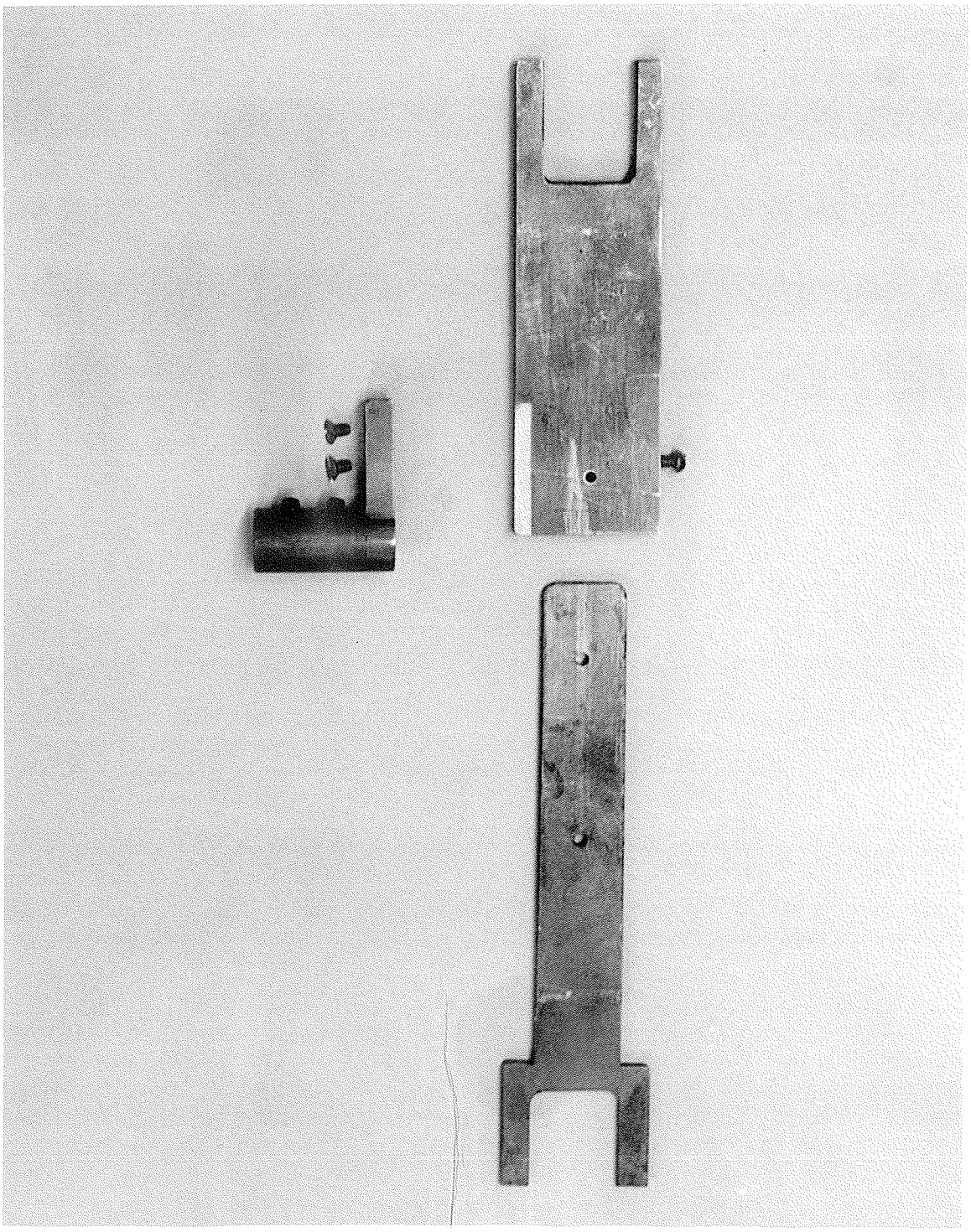

Plate 2. Compaction Apparatus

of yarn onto the compaction apparatus (Plate 3). After winding the samples at controlled speed and tension, the apparatus was used to restrain the yarn bundle at 25% of its original length. This was done in accordance with United States Patent 3,853,462 (Smith, 1974) which specified that 70 denier tubing shrinks 33% in the wale direction during chemical treatment. This corresponds to a 25% length reduction in the yarn (Hearle, Grosberg, and Backer, 1969; and Munden, 1959).

The compaction process was performed on three batches of yarn which were later divided into six 4.0 ± 0.2 g samples (Smith, 1974: example III). A 6% hexafluoro-2-propanol and 94% methylene chloride compaction solution was prepared. Each yarn batch was treated for 5 min in a 250 ml cylinder in a controlled temperature bath at 20.0 ± 0.1^{o}C using a 25:1 solution: sample ratio (Plate 4). The yarn was then washed in a 1% solution of Triton X-100, to remove surface chemicals, and rinsed in tap water for 5 min (Smith, 1974: example I). Following washing, the samples were dried still wrapped on the apparatus at 100^{o}C ± 2^{o}C for 5 min in a hot air oven.

Crimping Process

The crimping process was simulated by heating four compacted yarn samples for 1 hour in an unrestained state in a hot air oven. Two were heated to 94^{o}C and the other two were heated to 154^{o}C. These temperatures are the two extremes recommended in the patent (Jeckel, 1967: section 15, page 2). One hour was chosen because according to Ribnick (1969) most of the shrinkage that would take place at these temperatures would occur within 1 hour.

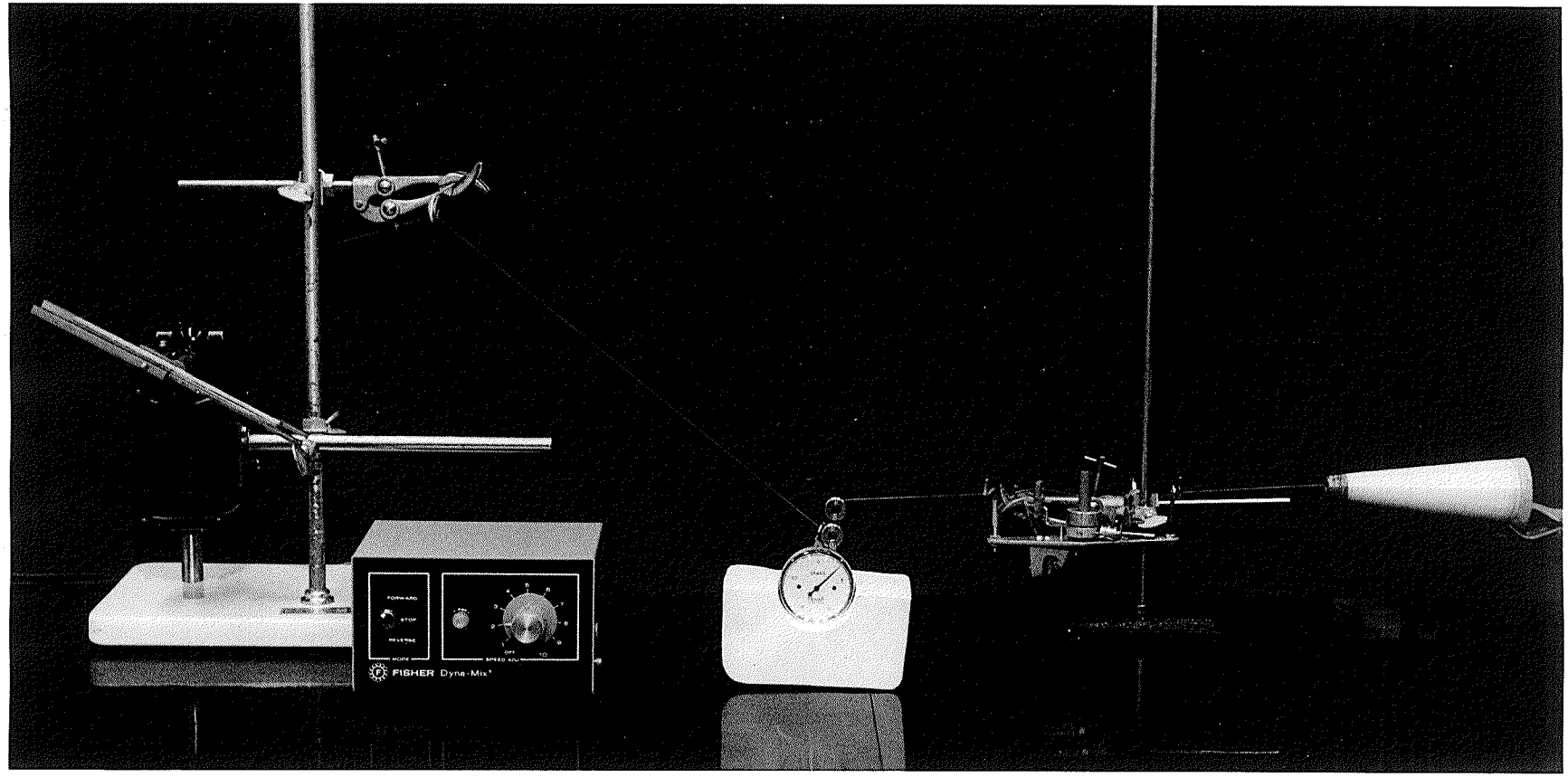

Plate 3. Winding Instrument

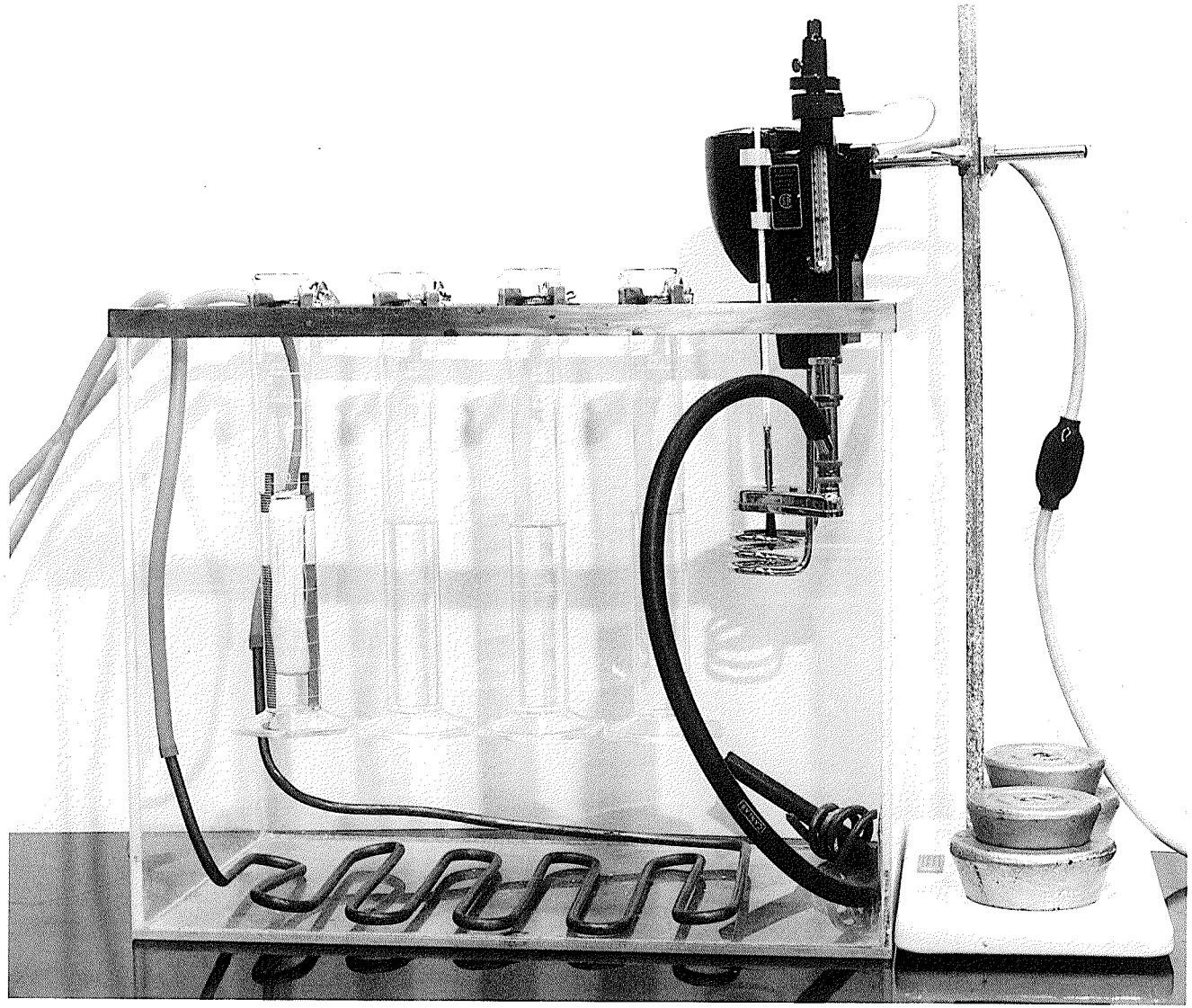

Plate 4. Compaction Processing Equipment

Sterilization

Two of the four compacted and crimped yarn samples were heat sealed into polyethylene and paper sterilization pouches, and sterilized in a Castle Gas Sterilizer: with 12% ethylene oxide and 88% freon at 56°C for 5 hours utilizing 10 lb pressure and 40% relative humidity (Ernst, 1973). This was followed by 3 hours aeration.

EVALUATION PROCEDURE

Each of the seven samples were tested by the procedures described below. The tests were performed in the standard testing atmosphere (65 ± 2% R.H. and 21 ± 1°C) unless otherwise stated. Yarns were randomly selected from each sample for testing.

Viscometry

The viscosity average molecular weight ($\overline{M}_v$) was determined by a method adapted from ASTM (1977) Designation: D2857-70. Specimens were ground in a Wiley Mill using a #10 mesh, dried at 110°C for 3 hours, and then dissolved for 3 hours in purified o-chlorophenol at 95°C. The specimen solution concentration was .00500 ± .00002 g/ml (.125 g in 25 ml of o-chlorophenol). After filtration the rates of flow through a Cannon 150K300 Ubbelohde dilution viscometer were timed. The viscometer was kept at a controlled temperature by immersing it in a constant temperature bath maintained at 25.0 ± 0.1°C. A series of solutions with different polymer concentrations were prepared and timed by adding 1,1,1,2 and 5 ml aliquots of polymer solution to the solvent. The viscosity average molecular weight for o-chlorophenol at 25°C was calculated from the intrinsic viscosity by the following equation:

$$\overline{M}_v = \sqrt[.81]{\frac{[\eta]}{.00019}}$$

(Moore and Sanderson, 1968).

Yarn Geometry

Shrinkage. The lengths of selected yarns from each sample were measured with a ruler before and after the compaction, crimping and sterilization treatments. The average length was calculated from twenty-five specimens, and the percentage shrinkage was computed according to the formula:

$$S = \frac{\text{Initial length} - \text{Final length}}{\text{Initial length}} \times 100$$

(Wilson, 1974: 278).

Filament diameter. An Olympus Binocular Microscope at 400 times magnification, an Olympus Eyepiece Fiber Micrometer, and an Olympus Stage Micrometer (0.01 mm) were used to measure the diameter of thirty filaments selected from each yarn sample (Heyn, 1954; Barron, 1965; Stoves, 1957; and Schwarz, 1934). Glycerol mounting media was used.

Linear density. The linear density in tex (g/1000 m) was determined according to ASTM (1977) Designation: D1059-76. A Shirley Crimp Tester was used to measure the length of fifteen 25.4 cm specimens at 3 g applied load. The specimens were weighed on a Sartorius Balance to five decimal places of a gram.

Density. Density is the mass per unit volume (Morton and Hearle, 1975: 154). There are limits to its use in assessing the degree of

crystallinity of polymers because it must be assumed that the structure consists solely of two completely defined, discrete phases; amorphous and crystalline. Farrow and Ward (1960) have concluded that the measurement of crystallinity by density is unreliable because the density of the non-crystalline material cannot be assumed to be constant. There has also been a problem with measuring the density of solvent treated fibers because the heavier component of the density gradient column may diffuse preferentially into the fiber structure and exchange with the residual solvent, thereby causing abnormally high density values (Weigmann, Scott and Ribnick, 1978). Yet, density has been used in conjunction with other tests to measure overall changes in the level of order. Wilson (1974) used density to study the overall structural change in PET yarn due to thermal shrinkage. Weigmann, Scott and Ribnick (1977) measured the changes in fiber structure due to solvent and/or heat treatment. Both studies found that density increased after treatment (Wilson, 1974; and Weigmann, Scott and Ribnick, 1977).

Values for nominal and hydrostatic density were obtained for the yarn samples. Hydrostatic densities were measured in a calibrated density column containing a mixture of xylene and carbon tetrachloride (Morton and Hearle, 1975; Preston and Nimkar, 1950; and Hall, 1976). Standardized glass beads were used to calibrate the column over a range of densities from 1.340 to 1.430 g/cm^3. The column was immersed in a constant temperature water bath held at 23.0 ± 0.1°C. After the yarn samples were inserted the column was allowed to stabilize for 24 hours before the readings were taken.

The nominal density of individual filaments was calculated in g/cm^3 using the data obtained for linear density and filament diameter as follows:

$$\text{Nominal density} = \frac{M}{\pi r^2 \ell}$$

where, $\frac{100{,}000M}{\ell}$ = average linear density of an individual filament in tex.

$2r$ = average filament diameter in cm.

Thermal Analysis

Polymeric materials undergo physical changes when heated or cooled through their transition temperatures. These changes are accompanied by the absorption or release of energy in the form of heat. In differential scanning calorimetry (DSC) the sample and the reference material are subjected to a closely controlled temperature program. Thermal energy is added to or subtracted from the sample or reference material in order to maintain both at the same temperature (Perkin - Elmer, 1967). The thermogram produced yields a direct calorimetric measurement of the transition energy. Thus structural variations in the material can be observed through measurement of the temperature of transition, the energy of transition, and the slope of the transition curve.

There are two transition peaks of interest for the purposes of this study; the melt peak, and the premelt endotherm peak (PEP). "Melting is a first-order crystalline-amorphous transition; the transition temperature and the accompanying heat effect define the chemical composition and crystallinity of the polyester" (Ke, 1962: 624). Solvent and heat treatments lead to secondary crystallization in PET polymers. This is observed by the presence of a PEP at temperatures below the melting point. The area under a thermogram peak is proportional to the amount of heat accompanying the transition, so the heat of transition can be measured

directly by calibration with a reference material (Perkin-Elmer, 1967; and Ke, 1962). The sum of the integrated area of the PEP (the heat of premelt crystallization ($\Delta H'$)) and the integrated area of the melt peak (the heat of fusion ($\Delta H''$)) gives the overall heat of fusion (ΔH). When this value is divided by the heat of fusion of an ideal PET crystal the apparent degree of crystallinity (W_c(d.s.c.)) is determined. This measure represents the volume fraction of the crystalline phase within the polymer (Fakirow et al., 1977: 1122).

Weigmann, Scott and Ribnick (1978) have examined premelt endotherm peaks to study the number and size distribution of crystallites of PET exposed to heat and solvent treatments. A distinct peak suggests a relatively narrow distribution of crystallite size. Whereas a broad and diffuse PEP suggests fewer crystallites with a wider range of crystallite sizes. Measurements of these characteristics before and after heat and solvent treatments help to identify changes in crystalline structure of PET fibers (Weigmann, Scott and Ribnick, 1978).

A Perkin-Elmer differential scanning calorimeter model DSC - 1B was used to measure the thermal behavior of the seven samples. Each yarn specimen was cut to 6.5 mm in length and packed into an aluminium sample pan. An aluminium lid was crimped on each. The specimen weight was recorded. To prevent oxidation of the PET at high temperatures an N_2 purge was connected to generate a 20 cc/min flow of gas. A Fisher Recordall Series 5000 was used to record the thermograms.

For the assessment of the melt peak the calorimeter was run from 221°C (494°K) to 281°C (554°K) at a scan speed of 10°C/min and range 1. The melting points of the samples were indicated by the peak temperatures (Manche and Carroll, 1972). The heats of fusion ($\Delta H''$) were computed

from the area under the curves which were calibrated against the heat of fusion of a known weight of indium. The premelt endotherm peaks (PEP) were run from 12°C (285°K) to 281°C (554°K) at a scan speed of 20°C/min and range 1. The PEP temperatures were read from the thermogram peaks. The heat of premelt crystallization ($\Delta H'$) was computed from the heat of fusion of a known weight of indium. The characteristics of the PEP's were described in terms of their shape, height and position. From the overall heat of fusion (ΔH) an apparent degree of crystallinity W_c(d.s.c.) was determined according to:

$$W_c(\text{d.s.c.}) = \frac{\Delta H}{\Delta H^o}$$

where, $\Delta H = \Delta H'' + \Delta H'$

ΔH^o = 24.3 kJ/mole (The heat of fusion of an ideal PET crystal).

Infrared Spectroscopy

Infrared spectroscopy has been used to determine the molecular structure of PET. "It is based upon the concept that if a material is subjected to radiation of the same frequency as the vibrations experienced by the atoms within the material then the result of such motion would be some form of interaction with the incident radiation" (Hearle and Greer, 1970: 139). The recorded spectrum is a plot of the percentage transmittance of radiation from the sample versus the frequency of the wavelength of incident radiation. The spectrum obtained from a range of transmission frequencies is a characteristic of the chemical structure of the material.

More recently an infrared technique called attenuated total reflectance (ATR) has been used to obtain information about the

surface chemistry of fibers (Carlsson, Suprunchuk and Wiles, 1970). "The ATR spectra of organic molecules corresponds closely to the conventional transmission infrared spectra" (Carlsson, Suprunchuk and Wiles, 1970: 73). This technique is particularly suited for studying changes in surface chemistry of vascular grafts, since as Merrill (1977: 15) concluded ". . . it is the material in the first few hundred angstrom units below a blood interface that govern what blood will do . . . ."

The surface chemistry and structural characteristics of the samples were analyzed by the attenuated total reflectance method (ATR) (Carlsson, Suprunchuk and Wiles, 1970; Manning, 1970; Wilks and Iszard, 1964; and Sibilia, 1975). A Beckman 18A Infrared Spectrophotometer was used with a Wilks Model 9 ATR attachment. The yarn samples were wrapped around resilient rubber pads and mounted on each side of the KRS-5 crystal. The assembly was held together by screws tightened to 3 inch lb with a constant torque wrench. Four 20 min scans were run for each sample. The initial percentage transmission was set to 50% to facilitate sample comparison. A polystyrene film was scanned in transmitted light as a calibration reference for each sample. The wavenumber ranged from 4,000 to 600 cm^{-1}.

For the purpose of the present investigation there were three important aspects of the fiber structure which were considered using the infrared spectra: endgroups, crystallinity and chain folding. Generally, infrared spectra have been used to determine the acid endgroups present in PET. If degradation causes chain scission then shorter molecules are formed and the number of acid endgroups usually increases. Polyester may have both hydroxyl and carboxyl endgroups. The amount of each is dependent on the conditions of polymerization. Patterson

and Ward (1957) attributed the absorption band at 3535 cm^{-1} to alcoholic hydroxyl endgroups of PET. Day and Wiles (1972) have connected the broad absorption band at approximately 3290 cm^{-1} with the presence of carboxyl endgroups within the polymer. The concentration of such endgroups can be quantified by measuring the intensity of these bands (Addleman and Zichy, 1972).

The baseline technique was used to measure the level of absorbance of the 3290 cm^{-1} and 3535 cm^{-1} frequency bands corresponding to the carboxyl and hydroxyl endgroups respectively (Kendall, 1966; and Clark and Hickie, 1975: 245). These absorptions correspond to their respective endgroup concentrations.

There are several bands in the infrared spectrum of PET which change their intensities as the crystallinity of the sample changes. It has been established that those near 1470, 1337, 973 and 845 cm^{-1} increase in intensity during crystallization while at the same time, those near 1453, 1370, 1040 and 895 cm^{-1} decrease in intensity (Bahl, Cornell and Boerio, 1974). The accepted explanation for this comes from Miyake (1959), who believes that rotational isomerism in the ethylene glycol segments of the PET molecules controls these changes. He studied the spectral changes caused by an increase in crystallization on heating PET at 230^{o}C for 5 min and found the bands relating to the trans configuration (1470, 1337, 973 and 845 cm^{-1}) increased in intensity, while those relating to the gauche configuration (1453, 1370, 1040 and 895 cm^{-1}) decreased in intensity. The bands 1470, 1337, 973 and 845 cm^{-1} have been related to the trans ethylene glycol segments or the trans configuration of the crystalline and the intermediate phases. The bands near 1453, 1370, 1040 and 895 cm^{-1} have been assigned to gauche ethylene

glycol segments as found in the amorphous phase. An alternative explanation by Liang and Krimm (1959) relates these spectral changes to symmetry and resonance characteristics of the substituted benzenoid ring framework. This explanation has not yet been widely accepted.

The baseline technique was also used to measure the level of absorbance of the trans configuration frequency bands at 1470, 1337, 973 and 845 cm^{-1} and the gauche configuration bands at 1453, 1370, 1040 and 895 cm^{-1} (Kendall, 1966; and Clark and Hickie, 1975). The peak at 794 cm^{-1} which corresponds to the aromatic hydrogen-carbon inplane vibrations was used as a standard (Miyake, 1959). It was assumed that the absorption level of this peak would remain unchanged by the chemical and thermal treatments in this study.

The absorption at 988 cm^{-1} in the spectra of PET has been assigned to chain folding (Wilson, 1974). Some researchers have reported that thermal contraction leads to an increase in the intensity of the 988 cm^{-1} band (Wilson, 1974; and Prevorsek et al., 1974). In fact, Wilson (1974) evaluated the intensity increase for various treatment temperatures. Prevorsek et al. (1974) calculated an absorptivity ratio of the 988 cm^{-1} to 973 cm^{-1} bands to quantify the increase in the degree of chain folding. In this investigation it was found that the frequency band relating to chain folding, 988 cm^{-1}, could not be clearly distinguished using the ATR technique.

Birefringence

Birefringence is the difference between the refractive indices in the longitudinal and the transverse directions of a fiber ($n_{||}-n_{\perp}$). It is regarded as a measure of the mean molecular orientation in the

crystalline, intermediate and amorphous phases (Morton and Hearle, 1975). Thus birefringence will be highest when the molecules all lie parallel to the fiber axis, and it will be lowest when they are randomly directed. Commercially drawn PET fibers have high birefringence due to the high degree of molecular orientation that is possible, and the presence of the benzene ring in the main chain (Morton and Hearle, 1975). Prevorsek et al. (1974) observed that thermal contraction leads to a decrease in birefringence. Wilson (1974) also found a fall in birefringence due to heat induced shrinkage. At temperatures up to 100°C a fall in birefringence was noted, but beyond this temperature any further fall in birefringence was offset by a rise accompanying crystallization. Some researchers have suggested that the initial decrease in birefringence is in part due to disorientation in the intermediate phase (Wilson, 1974; Prevorsek et al., 1974, Deopura, Sinha and Varma, 1977; and Goodman and Rhys, 1965).

An Olympus Polarizing Microscope at 400 times magnification and a Leitz Wetzler Berek Compensator were used to measure the birefringence of twenty-five filaments from each yarn sample (The Textile Institute, 1975; Leitz-Wetzler, 1960; Heyn, 1954; Barron, 1965; Stoves, 1957; and Schwarz, 1934). Glycerol was used as the mounting media.

Tensile Properties

Tenacity. The tenacity of a fiber is the tensile stress at the point of failure expressed as force per unit linear density of the unstrained specimen (ASTM, 1977: D2256). Molecular weight, type of crystallinity (crystalline, intermediate or amorphous phases), degree of intermolecular entanglements and degree of molecular orientation are

important factors which affect fiber tenacity. It was found that by increasing the number average molecular weight of PET from 8,000 to 30,000 large increases in fiber tenacity are obtained (Walczak, 1977: 269). Intermolecular entanglements in the form of linked molecules may increase the mechanical strength of the structure.

The following researchers have found losses in the tenacity of drawn PET fibers due to thermally and chemically induced shrinkage. Ribnick, Weigmann and Rebenfeld (1972) found that shrinkage induced by methylene chloride treatment resulted in decreased tenacity. Prevorsek et al. (1974) found that the decrease in tenacity upon thermal contraction was accompanied by a decrease in molecular orientation. Statton (1971) explained that a thermally induced decrease in tenacity is likely caused by the relatively few molecules passing through the fiber structure due to chain folding.

Yarn tenacity was determined by the single-strand method adapted from ASTM (1977) Designation: D2256-75. An Instron Tester was used with a 13 cm gauge length and a crosshead speed of 12.5 cm/min. Thirty yarn specimens were tested from each sample. The specimens were centrally mounted in rubber faced, pneumatic jaws, pretensioned with a 3.1 g weight, and strained until the first filament breakage, which was observed as a discontinuity on the load/elongation curve. The average yarn tenacity was then calculated in mN/tex.

Breaking toughness. Breaking toughness is the energy required to break a material (Nielsen, 1962: 102). The toughest materials have high tenacities accompanied by high elongations to break. The average breaking toughness of thirty yarn specimens was calculated in mN.m/tex.m from the area under the load/elongation curves obtained by the single-strand

method described above as directed in ASTM (1977) Designation: D2101-72. The areas were measured by a Gelman Planimeter.

Initial modulus. Initial modulus is the slope of the initial straight-line portion of a stress-strain curve. The modulus is the ratio of the change in stress to the change in strain (ASTM, 1977:D2101). It depends on the degree of crystallinity, the degree of orientation, and on the proportion and distribution of the intermediate and amorphous phases. This has been emphasized by Walczak who stated that " . . . the type of transition between crystalline and amorphous areas is suspected to have a very important influence in the overall effect" (Walczak, 1977: 264). Initial modulus also depends on chain configuration. When PET has fully extended chains (trans configurations) it requires a greater force to produce unit extension than when the chains are less fully extended (Walczak, 1977). Thus polymer crystallites may be treated as undeformable in comparison with the amorphous regions of the polymer (Meares, 1965).

Ribnick, Weigmann and Rebenfeld (1972) have reported that PET yarn has a lower initial modulus after methylene chloride induced shrinkage. Wilson (1974) has found similar results for thermally induced shrinkage. These findings are "consistent with the view that initial modulus is determined by elements in the amorphous regions, the progressive disorientation of which produces both increasing shrinkage and decreasing modulus" (Wilson, 1974:282).

The average initial modulus of thirty specimens was calculated in N/tex for each sample as directed in ASTM (1977) Designation: D2101-72. The load required to produce 8% elongation was measured from each of the single-strand, load/elongation curves.

STATISTICAL ANALYSIS

Parametric and non-parametric one-way analyses of variance were used to assess whether there were significant differences between the untreated, the five treated and the commercially treated samples. In the parametric analysis of variance the fixed effect model was used to determine whether significant differences existed between the observed means of the following measures; filament diameter, linear density, birefringence, tenacity, breaking toughness and initial modulus (Snedecor and Cochran, 1967: 258). The non-parametric Kruskal-Wallis test was also performed (Gibbons, 1971: 198). In it no assumption is made about the parent populations except for continuity. The parametric Scheffē test on multiple comparisons was used in five separate analyses to consider the effects of compaction, crimping and sterilization, the comparison of the commercial reference sample with the compacted and crimped samples, and the effect of compaction, crimping and sterilization.

The fixed effect model for one-way analysis of variance, is described as follows:

$$Y_{ij} = \mu + \alpha_i + \xi_{ij} \qquad \begin{matrix} i = 1, 2, \ldots a \\ j = 1, 2, \ldots n \end{matrix}$$

where, Y_{ij} = jth observation for the ith treatment.

μ = overall mean.

α_i = the effect of the ith treatment such that

$$\alpha_1 + \alpha_2 + \ldots \alpha_a = 0.$$

ξ_{ij}'s are independent normal random variables with mean 0 and variance σ^2.

The null hypothesis of interest is, Ho ($\alpha_1 = \alpha_2 \ldots = \alpha_a = 0$).

The alternative hypothesis is, H_a ($\alpha_i \neq \alpha_j$ for some $i \neq j = 1, \ldots, a$).

An analysis of variance table was used to summarize the quantities involved in the computation of the test statistic (See Table 2).

Table 2. Analysis of Variance (ANOVA) Table

Source of Variation	Degree of Freedom	Sum of Squares	Mean Square
Between Sample	a-1	S_B*	$s_B = \frac{S_B}{a-1}$
Error	a(n-1)	S_E*	$s_E = \frac{S_E}{a(n-1)}$
Total	an-1	S_T*	

*The ANOVA has used the usual definition of the sums of squares due to the different components of variation.

To test H_o ($\alpha_1 = \alpha_2 \ldots \alpha_a = 0$) the F ratio $F = \frac{s_B}{s_E}$ was used with degrees of freedom a-1, a(n-1) as the test statistic.

The next step in studying the results was to examine the treatment means and the sizes of differences among them by using the technique of multiple comparisons. Any linear combination, $L = \lambda_1 \bar{X}_1 + \lambda_2 \bar{X}_2 + \ldots \lambda_k \bar{X}_k$, where the λ's are fixed numbers with $\sum_{i=1}^{k} \lambda_i = 0$, is called a comparison of treatment means, where $k \leq a$ (Snedecor and Cochran, 1967: 269). The estimated standard error (S_L) of the comparison L is $\sqrt{\Sigma\lambda^2}(s_E/\sqrt{n})$, when n is the number of observations in each sample. For Scheffé's test L/S_L is declared significant at the .05 level if it numerically exceeds $\sqrt{(a-1)\ F_{0.05}}$ where $F_{0.05}$ is the .05 level of F for degrees of freedom $f_1 = a-1$, $f_2 = a(n-1)$ (Snedecor and Cochran, 1967: 271).

For the non-parametric Kruskal-Wallis one-way ANOVA test it is assumed that there are "a" independent sets of observations, one from each of "a" continuous populations $F_1(x)$, $F_2(x)$, . . ., Fa(x), where the ith random sample is of size n_i, i = 1, 2, . . . a, and where there are a total of $\sum_{i=1}^{a} n_i = N$ observations (Gibbons, 1971: 194). The null hypothesis is, H_0 $F_1(x) = F_2(x) = \ldots F_a(x)$ for all x. The alternative hypothesis is, H_a $F_i(x) \neq F_j(x)$ for some $i \neq j$ and for at least one x.

For the test statistic the N observations are arranged in order of magnitude and R_i is denoted as the actual sum of ranks assigned to the elements of the ith sample in this combined arrangement. In case of a tie the midrank method was used (Gibbons, 1971: 97). The test statistic M due to Kruskal and Wallis is defined by:

$$M = \frac{12}{N(N+1)} \sum_{i=1}^{a} \frac{R_i^2}{n_i} - 3(N+1)$$

If no n_i is small then under the null hypothesis M is distributed approximately as the chi square random variable with a-1 degrees of freedom. The rejection region of this test is $M \geq \chi^2_{\alpha,\ a-1}$ corresponding to a level of significance α.

An Olivetti table computer P602 was used to perform the parametric one-way analysis of variance. The other analyses were calculated manually.

Chapter 4

RESULTS AND DISCUSSION

This chapter reports the results of the chemical and physical measurements on the PET yarn before and after compaction, crimping and sterilization. These results are used to indicate the changes that occurred in the PET fiber structure. In addition the likely manufacturing conditions of the commercial reference sample are discussed. The properties of the sterilized samples are compared to those for the control sample, and predictions are made about their future in vivo performance.

The average results for the chemical and physical measures of the treatments and comparisons are summarized in Tables 3 to 11 and some are presented graphically in Figures 1 to 15, Appendix D. The DSC thermograms, infrared spectra, and stress-strain curves are presented in Figures 16 to 51, Appendix D. The individual data for the seven samples are to be found in Tables 12 to 27, Appendix B.

The mean values of the filament diameter, linear density, birefringence, tenacity, breaking toughness and initial modulus measurements for all seven samples were compared using the one-way analysis of variance, the fixed effect model, and the Kruskal-Wallis one-way ANOVA test. Both statistical techniques found that significant differences (at the .01 level) existed between all the untreated, treated and commercially treated samples (Tables 28 and 29, Appendix C). The critical values for the multiple comparisons are found in Table 30, Appendix C.

EFFECT OF COMPACTION

To analyze the effect of compaction the untreated sample(number one) was compared to the compacted sample (number two) (Table 3).

Molecular Weight and Endgroup Analysis

The visosity average molecular weight of the untreated PET was 31,200. The value of 22,200 obtained for sample two was substantially lower than the original value. This indicated that chain scission occurred during the compaction process. It is proposed that the 1, 1, 1, 3, 3, 3 hexafluoro - 2 - propanol solvent initiated these chain scission reactions by the following acid hydrolysis mechanism:

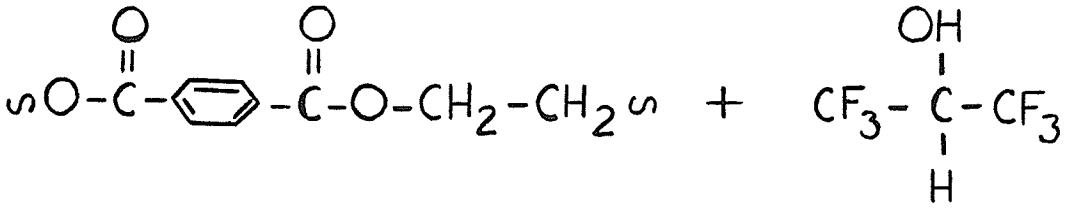

PET 1,1,1,3,3,3 Hexafluoro-2-propanol

Step 1

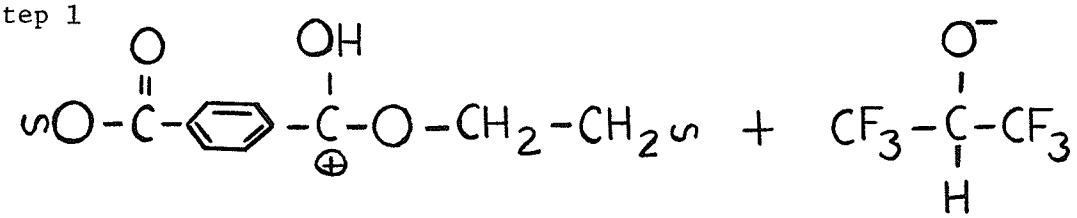

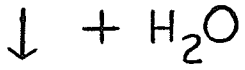

Step 2

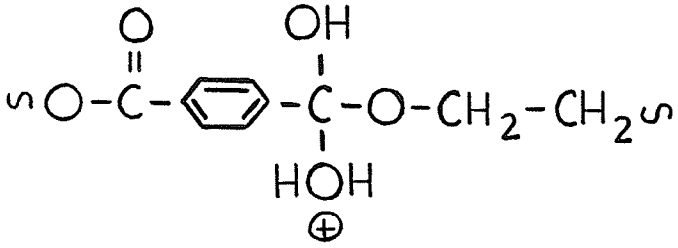

Table 3. Effect of Compaction on the PET Yarn

Measure	Units	Untreated(Sample One)	Compacted(Sample Two)	Change**	% Change
Molecular Weight		31,200	22,200	-	
Carboxyl Endgroup	absorbance	0.030	0.000	Same	
Hydroxyl Endgroup	absorbance	0.010	0.000	Same	
Length	cm	25.40	19.05	-	25
Filament Diameter	μm	12.6	14.2*	+	11
Linear Density	tex	8.7	11.8*	+	26
Hydrostatic Density	g/cm^3	1.369	1.397	+	
Nominal Density	g/cm^3	1.293	1.389	+	
DSC $\Delta H'$ (PEP)	cal/g	None	8.6	Appears	
DSC $\Delta H''$ (Melt Peak)	cal/g	12.0	11.0	Same	
DSC $\Delta H=\Delta H'+\Delta H''$	cal/g	12.0	19.6	+	
DSC Degree of Crystallinity		0.49	0.81	+	
DSC PEP Temperature	^oC	None	146	Appears	
DSC Melt Peak Temperature	^oC	260	260	Same	
I.R. Trans Bands	absorbance	Appendix B, Tables 22 and 23		-	
I.R. Gauche Bands	absorbance	Appendix B, Tables 22 and 23		Same	
Birefringence		0.190	0.163*	-	86
Tenacity	mN/tex	290	185*	-	36
Breaking Toughness	mN.m/tex.m	175	70*	-	60
Initial Modulus	N/tex	7.86	3.16*	-	60

*Significantly different at the .05 level.

**Denoted 'same' if not significantly different at the .05 level; otherwise + increase, - decrease.

Rearrangement

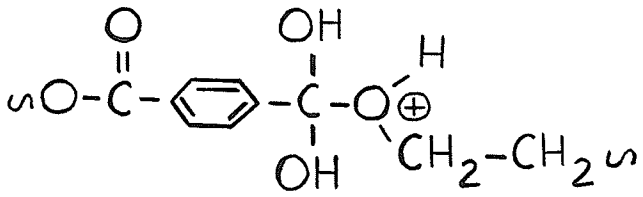

Step 3
Chain Scission

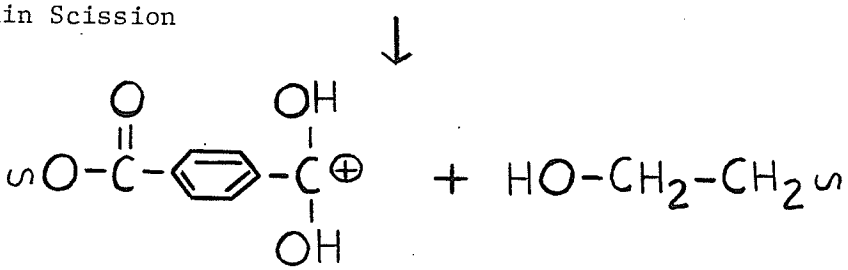

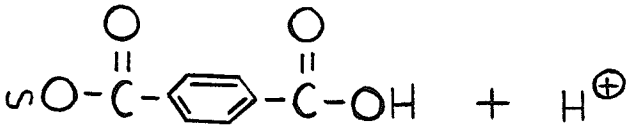

(adapted from Buxbaum, 1968:189).

The water necessary to proceed from step one to step two would have been present inside the fibers themselves, or from the aqueous rinse baths.

The infrared spectra for samples one and two showed similar levels of absorbance for both hydroxyl and carboxyl endgroups. Any increases in the levels of absorbance due to hydrolytic chain scission were not detected by the ATR technique. This can be explained by the fact that this technique was not capable of distinguishing between absorbances of less than 12%, whereas the change in molecular weight corresponded to increases in endgroup content from about 0.3 to 0.5%.

Yarn Geometry

The apparatus used during compaction limited the longitudinal yarn shrinkage to 25%. Consequently sample two had a greater filament diameter than sample one which was significant at the .05 level. That is, lateral swelling occurred during compaction. The 26% increase in linear density was also significant at the .05 level. The hydrostatic density increased from 1.369 to 1.397 g/cm^3. Similarly, the nominal density increased from 1.293 to 1.389 g/cm^3. These increases were consistent with the findings of Weigmann et al. (1977: 751). They detected an increase in hydrostatic density from 1.3775 to 1.3837 g/cm^3 when drawn PET was shrunk 19.5% in methylene chloride. In this research an increase in density was found despite the increase in filament diameter. These results suggested that in addition to forming a more compact structure, residual solvent remained in the compacted yarns. The density of methylene chloride is 1.333 g/cm^3.

Microstructure

The results of the thermal analysis were used to suggest changes in microstructure during compaction. The DSC thermogram for sample one did not show a premelt endotherm peak (PEP), as can be seen in Figure 16. The thermogram for sample two had a broad and diffuse PEP($\Delta H'$) of 8.6 cal/g at 146°C. This was consistant with the temperature range of 125 - 180°C for the crystallization endotherm of PET, as reported by Carter (1971: 131). The appearance of this peak demonstrated that secondary crystallization occurred during compaction. The shape of the PEP suggested that a wide range in crystallite size was formed. The size and placement of the PEP indicated that the secondary crystallites formed were fewer in number, smaller and less perfect than the primary

crystallites of the melt.

The melting point for both samples was 260°C (Figure 17). This falls within the range 255-260°C as reported by Ludewig (1971: 373) for polyesters. The heat of fusion ($\Delta H''$) for sample two was similar to that obtained for sample one, 11.0 cal/g and 12.0 cal/g respectively. These values fall within the range 9 to 16 cal/g reported by Goodman and Rhys (1965: 47) for the heat of fusion of PET. The overall heat of fusion (ΔH) was 12.0 cal/g for sample one, and increased to 19.6 cal/g for sample two. The DSC degree of crystallinity was therefore higher for sample two (0.81) compared to sample one (0.49), indicating that the volume fraction of crystalline material increased upon compaction. The increase was due to the formation of secondary crystallites.

The infrared bands relating to crystallinity showed a decrease in absorbance for the trans bands 1470, 1337 and 845 cm^{-1} (Figure 18). This loss in trans absorption suggested that the number of extended chains decreased. This could mean that the amount of crystalline regions decreased and/or the degree of crystalline perfection decreased (Morton and Hearle, 1975: 604). But having observed that the DSC volume fraction of crystalline material increased, the loss of trans absorption suggested that the compaction treatment was responsible for reducing the degree of crystalline perfection.

The overall orientation as measured by birefringence showed a decrease of 86% which was significant at the .05 level. Morton and Hearle (1975: 577) reported that PET has a birefringence of 0.188, which is similar to the value of 0.190 obtained for sample one. The decrease in orientation during compaction was due to the longitudinal shrinkage and lateral swelling within the fiber. Weigmann et al.

(1977: 753) explained that in solvent induced shrinkage ". . . more extensive shrinkage coincides with the disorientation of the more non-crystalline regions . . . ." This loss in orientation may be associated with the decrease in crystalline perfection discussed earlier.

Tensile Properties

Sample two had a lower tenacity (36%), breaking toughness (60%) and initial modulus (60%) than sample one. These differences were significant at the .05 level (Figure 19). The radical change in the shape of the stress/strain curve indicates that the PET polymer has been plasticized. The solvent was presumably responsible for this change. Chain scission, longitudinal shrinkage, lateral swelling, and loss of orientation would explain this inferior tensile behavior. Similar trends have been observed by Ribnick, Weigmann and Rebenfeld (1972: 722) who reported a decrease in the tenacity and initial modulus of PET yarn after being shrunk longitudinally 16.9% in methylene chloride.

Summary

The compaction process produced a considerable deterioration in the tensile properties of the PET yarn. This was due to chain scission, longitudinal shrinkage, lateral swelling, and possibly the presence of residual solvent. Compaction also provided an opportunity for the growth of secondary crystallites, and resulted in the formation of a denser, more compact, though less perfect crystalline microstructure.

EFFECT OF CRIMPING

In order to discuss the effect of the crimping process, the

compacted sample (number two) was compared with samples three and four that had been compacted and crimped at 94°C and 154°C respectively (Tables 4 and 5).

Molecular Weight and Endgroup Analysis

The viscosity average molecular weight of 22,200 for sample two was similar to the values of 22,100 and 21,900 obtained for samples three and four respectively. Any marginal loss in $\overline{M}_v$ was probably due to thermally induced chain scission reactions (Buxbaum, 1968; and Carter, 1971). The infrared spectra did not indicate any significant changes in hydroxyl or carboxyl endgroup content.

Yarn Geometry

Following compaction, crimping did not result in significant additional longitudinal shrinkage. The filament diameters for both samples showed no change at the .05 significance level. The linear density of sample four was 4% lower than that of sample two. This difference was significant at the .05 level. This may have been due to a greater loss of residual solvent at the higher crimping temperature. The measured values for hydrostatic density were 1.397 g/cm^3 for the compacted sample and 1.395 g/cm^3 after both crimping treatments. This difference was not considered significant. Samples three and four had higher nominal densities (1.448 and 1.429 g/cm^3 respectively) than that of 1.389 g/cm^3 for sample two. The increase in the nominal densities, as compared to no change in the hydrostatic densities, reflected a reduction in porosity. This was consistent with the finding of Weigmann, Scott and Ribnick (1977) who reported that the void structure in solvent treated PET collapses during subsequent heat treatment. The higher

Table 4. Effect of Crimping at 94°C on the PET Yarn

Measure	Unit	Compacted (Sample Two)	Compacted, Crimped 94°C (Sample Three)	Change**	% Change
Molecular Weight		22,200	22,100	Same	
Carboxyl Endgroup	absorbance	0.000	0.035	Same	
Hydroxyl Endgroup	absorbance	0.000	0.000	Same	
Length	cm	19.05	18.55	Same	
Filament Diameter	μm	14.2	13.7	Same	
Linear Density	tex	11.8	11.5	Same	
Hydrostatic Density	g/cm^3	1.397	1.395	Same	
Nominal Density	g/cm^3	1.389	1.448	+	
DSC ΔH' (PEP)	cal/g	8.6	3.3	-	
DSC ΔH" (Melt Peak)	cal/g	11.0	11.2	Same	
DSC ΔH=ΔH'+ΔH"	cal/g	19.6	14.5	-	
DSC Degree of Crystallinity		0.81	0.60	-	
DSC PEP Temperature	°C	146	157	+	
DSC Melt Peak Temperature	°C	260	260	Same	
I.R. Trans Bands	absorbance	Appendix B, Tables 22 and 23		+	
I.R. Gauche Bands	absorbance	Appendix B, Tables 22 and 23		Same	
Birefringence		0.163	0.171*	+	5
Tenacity	mN/tex	185	203*	Same	
Breaking Toughness	mN.m/tex.m	70	80*	+	13
Initial Modulus	N/tex	3.16	2.58	-	18

*Significantly different at the .05 level.

**Denoted 'same' if not significantly different at the .05 level; otherwise + increase, - decrease.

Table 5. Effect of Crimping at 154°C on the PET Yarn

Measure	Unit	Compacted (Sample Two)	Compacted, Crimped 154°C (Sample Four)	Change**	% Change
Molecular Weight		22,200	21,900	Same	
Carboxyl Endgroup	absorbance	0.000	0.000	Same	
Hydroxyl Endgroup	absorbance	0.000	0.000	Same	
Length	cm	19.05	19.05	Same	
Filament Diameter	μm	14.2	13.6*	Same	
Linear Density	tex_3	11.8	11.3*	-	4
Hydrostatic Density	g/cm_3	1.397	1.395	Same	
Nominal Density	g/cm^3	1.389	1.429	+	
DSC ΔH' (PEP)	cal/g	8.6	2.3	-	
DSC ΔH" (Melt Peak)	cal/g	11.0	9.4	-	
DSC ΔH=ΔH'+ΔH"	cal/g	19.6	11.7	-	
DSC Degree of Crystallinity		0.81	0.48	-	
DSC PEP Temperature	°C	146	172	+	
DSC Melt Peak Temperature	°C	260	260	Same	
I.R. Trans Bands	absorbance	Appendix B, Tables 22 and 23		+	
I.R. Gauche Bands	absorbance	Appendix B, Tables 22 and 23		Same	
Birefringence		0.163	0.177*	+	8
Tenacity	mN/tex	185	214*	+	14
Breaking Toughness	mN.m/tex.m	70	92*	+	24
Initial Modulus	N/tex	3.16	3.56*	+	11

*Significantly different at the .05 level.

**Denoted 'same' if not significantly different at the .05 level; otherwise + increase, - decrease.

nominal density for sample three as compared to sample four may have been related to the presence of a greater amount of residual solvent in sample three.

Microstructure

Previously it was mentioned that the DSC thermogram for sample two exhibited a broad and diffuse PEP of 8.6 cal/g at 146°C. Sample three produced a smaller, but similar broad shaped PEP of 3.3 cal/g at 157°C (Figure 20). Sample four revealed a smaller PEP, than either samples two or three, of 2.3 cal/g at 172°C, which was skewed to the right (Figure 22). Both samples showed peak sizes and distributions that indicated a large proportion of the secondary crystallites, particularly the smaller ones, were lost during crimping. Thus, the effect of crimping was to reduce the number of secondary crystallites in the PET yarn.

The heat of fusion ($\Delta H''$) was similar for samples two and three (11.0 cal/g and 11.2 cal/g respectively) but was lower for sample four (9.4 cal/g) (Figure 21 and 23). This difference in thermal behavior supports the earlier suggestion that the compacted yarn (sample two) contains residual solvent. Any such solvent would be more effectively removed by crimping at a higher temperature. Consequently sample four would have experienced more extensive rearrangement of chains than sample three, which accounts for its lower $\Delta H''$ value. Both crimped samples had lower overall heats of fusion (ΔH) than the compacted sample. Thus the DSC degree of crystallinity ratios were lower for the crimped samples (0.48 and 0.60) than for sample two (0.81).

The infrared spectra for both samples three and four showed an

increase in the trans 1337 and 845 cm^{-1} bands (Figures 24 and 25) which corresponds to a larger proportion of the ethylene glycol units being in the extended chain configuration. These results were not inconsistent with the decrease in the overall heat of fusion (ΔH) mentioned previously, since the volume fraction of crystalline material could have decreased while its level of perfection, increased.

Samples three and four had 5% and 8% higher birefringence respectively than sample two. These increases were significant at the .05 level. The higher the temperature of crimping, the greater was the increase in orientation, since crimping is accompanied by a collapse the void structure, and an increase in the degree of crystalline perfection.

Tensile Properties

Crimping at both temperatures produced some significant changes in tensile properties (Figures 26 and 27). Sample four revealed increases in tenacity (14%), breaking toughness (24%) and initial modulus (11%) which were significant at the .05 level. Figures 26 and 27 also show that the yield point increases and the degree of plasticization decreases at higher crimping temperatures. These observations can be explained by the collapsed surface pores, the increases in the degree of orientation and the degree of crystalline perfection, as well as removal of residual solvent. Sample three showed less predominant, but similar trends, except for initial modulus. It is proposed that the loss in initial modulus was due to the presence of small, isolated pockets of residual solvent within the microstructure which acted locally as plasticizers at low stresses (Meares, 1965: 233).

Summary

The crimped yarns (samples three and four) generally had superior tensile properties to those of the compacted sample (sample two). This was attributed to the fact that crimping collapsed the surface pores, increased the orientation and increased the degree of crystalline perfection, as well as driving off some or all the residual solvent. The one exception was a decrease in the initial modulus of the 94°C crimped sample (sample three). This was explained by the continued presence of residual solvent within the fibers, which had a plasticizing effect on the polymer at low stresses. At, 154°C (sample four), it is thought that most, if not all of the solvent had been removed. Reductions in residual solvent caused increases in orientation and hydrostatic density, and losses in surface porosity. The effect of crimping at both temperatures was to increase the crystalline perfection and to reduce the volume fraction of crystalline material, which partly resulted from a loss of secondary crystallites. Some of the property changes that occurred during compaction were partially reversed during crimping.

EFFECT OF STERILIZATION

To analyze the effect of sterilization, the properties of the compacted, crimped and sterilized samples (numbers five and six) were compared to those of the compacted and crimped samples (numbers three and four) (Tables 6 and 7).

Molecular Weight and Endgroup Analysis

Sterilization increased the viscosity average molecular weight of both samples: sample three increased from 22,100 to 28,300, and sample four increased from 21,900 to 25,800. This could be explained by the ethylene oxide serving as a crosslinking agent between neighbouring chains. Approximately two chains out of every five or six would have to crosslink in order to give this increase in the $\overline{M}_v$. The more extensive crosslinking in the sample crimped at 94°C (sample five) might have indicated that the structure had greater free space than the sample crimped at 154°C (sample six). This may suggest that sample three contained more residual solvent than sample four. Some increase in $\overline{M}_v$ could have occurred through endgroup addition reactions between the ethylene oxide and the PET as outlined below:

(1) carboxyl endgroup addition

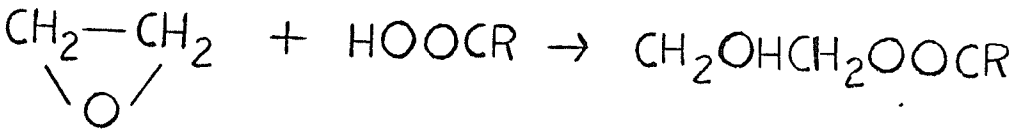

(adapted from Bruck, 1971: 151).

Table 6. Effect of Sterilization on the PET Yarn Crimped at 94°C

Measure	Unit	Compacted, Crimped 94°C (Sample Three)	Compacted, Crimped 94°C, Sterilized (Sample Five)	Change**	% Change
Molecular Weight		22,100	28,300	+	
Carboxyl Endgroup	absorbance	0.035	0.000	Same	
Hydroxyl Endgroup	absorbance	0.000	0.000	Same	
Length	cm	18.55	18.55	Same	
Filament Diameter	µm	13.7	13.8	Same	
Linear Density	tex_3	11.5	12.3*	+	7
Hydrostatic Density	g/cm_3	1.395	1.396	Same	
Nominal Density	g/cm^3	1.448	1.523	+	
DSC ΔH' (PEP)	cal/g	3.3	4.7	+	
DSC ΔH'' (Melt Peak)	cal/g	11.2	9.7	-	
DSC ΔH=ΔH'+ΔH''	cal/g	14.5	14.4	Same	
DSC Degree of Crystallinity		0.60	0.59	Same	
DSC PEP Temperature	°C	157	148	-	
DSC Melt Peak Temperature	°C	260	260	Same	
I.R. Trans Bands	absorbance	Appendix B, Tables 22 and 23		-	
I.R. Gauche Bands	absorbance	Appendix B, Tables 22 and 23		Same	
Birefringence		0.171	0.169	Same	
Tenacity	mN/tex	203	195	Same	
Breaking Toughness	mN.m/tex.m	80	77	Same	
Initial Modulus	N/tex	2.58	3.73*	+	31

*Significantly different at the .05 level.

**Denoted 'same' if not significantly different at the .05 level; otherwise + increase, - decrease.

Table 7. Effect of Sterilization on the PET Yarn Crimped at 154°C

Measure	Unit	Compacted, Crimped 154°C (Sample Four)	Compacted, Crimped 154°C, Sterilized (Sample Six)	Change**	% Change
Molecular Weight		21,900	25,800	+	
Carboxyl Endgroup	absorbance	0.000	0.000	Same	
Hydroxyl Endgroup	absorbance	0.000	0.000	Same	
Length	cm	19.05	19.05	Same	
Filament Diameter	μm	13.6	13.2	Same	
Linear Density	tex_3	11.3	11.3	Same	
Hydrostatic Density	g/cm_3	1.395	1.396	Same	
Nominal Density	g/cm^3	1.429	1.543	+	
DSC ΔH' (PEP)	cal/g	2.3	4.1	+	
DSC ΔH" (Melt Peak)	cal/g	9.4	10.6	+	
DSC ΔH=ΔH'+ΔH"	cal/g	11.7	14.7	+	
DSC Degree of Crystallinity		0.48	0.60	+	
DSC PEP Temperature	°C	172	174	Same	
DSC Melt Peak Temperature	°C	260	260	Same	
I.R. Trans Bands	absorbance	Appendix B, Tables 22 and 23		-	
I.R. Gauche Bands	absorbance	Appendix B, Tables 22 and 23		Same	
Birefringence		0.177	0.182*	+	3
Tenacity	mN/tex	214	191*	-	11
Breaking Toughness	mN.m/tex.m	92	85*	Same	
Initial Modulus	N/tex	3.56	2.89*	-	19

*Significantly different at the .05 level.

**Denoted 'same' if not significantly different at the .05 level; otherwise + increase, - decrease.

(2) hydroxyl endgroup addition

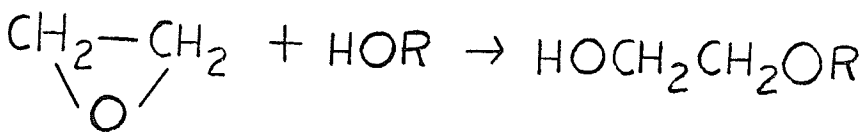

(adapted from Roberts, Stewart and Caserio, 1971: 266). Alternatively the ethylene oxide might have formed pendant chains from the PET. These mechanisms might have caused changes in carboxyl and hydroxyl endgroup concentrations, but such changes were not observed by infrared spectroscopy, because the ATR technique used was not sufficiently sensitive.

Yarn Geometry

No shrinkage was detected after sterilization of the crimped samples. The filament diameters did not change significantly at the .05 level. The hydrostatic densities for samples five and six were similar before and after sterilization (1.395 and 1.396 g/cm^3 respectively). Sample five had a 7% higher linear density than sample three. This difference was significant at the .05 level. The nominal density of both samples increased (from sample three at 1.448 g/cm^3 to sample five at 1.523 g/cm^3, and from sample four at 1.429 g/cm^3 to sample six at 1.543 g/cm^3). This indicated that the surface porosity of the fibers in both samples decreased upon sterilization. The greater decrease occurred in the sample that had been crimped at the higher temperature (sample four).

Microstructure

Both samples five and six produced larger PEP's on the DSC

thermogram indicating net gains in the amount of secondary crystallization after sterilization (Figures 28 and 30). The PEP for sample three increased from 3.3 cal/g at 157°C to 4.7 cal/g at 148°C, while that for sample four increased from 2.3 cal/g at 172°C to 4.1 cal/g at 174°C. The two samples however experienced different mechanisms for crystallite growth. The distribution of the sample five curve indicated that more smaller secondary crystallites had formed compared with sample six where the increase was mainly due to the formation of larger secondary crystallites.

The heat of fusion ($\Delta H''$) for sample three decreased from 11.2 cal/g to 9.7 cal/g after sterilization whereas the heat of fusion ($\Delta H''$) for sample four increased from 9.4 cal/g to 10.6 cal/g (Figures 29 and 31). The total heat of fusion (ΔH) and the DSC degree of crystallinity ratio were not significantly different for samples three and five because although the secondary crystallization increased during sterilization the primary crystallization decreased. The DSC degree of crystallinity ratios were 0.60 for sample three and 0.59 for sample five. The increases in the total heat of fusion (ΔH) and the DSC degree of crystallinity ratio for sample six (0.60) compared to sample four (0.48) were due to increases in the number of both secondary and primary crystallites. This suggested that to produce the structure in sample six the primary crystallites in sample four were not undergoing much change due to the sterilization conditions. For sample five a rearrangement was occurring after the removal of the residual solvent; similar to that which occurred after crimping at 154°C.

The trans bands 1337 and 845 cm^{-1} decreased for both samples during sterilization (Figures 32 and 33), which indicates a decrease

in the amount of crystallinity and/or in the degree of crystalline perfection. Since the DSC results for sample five showed that its volume fraction of crystalline material remained the same, the degree of crystalline perfection must have decreased. Similarly, since the DSC results showed an increase in the volume fraction of crystalline material for sample six, the degree of crystalline perfection must have decreased to obtain a decrease in the absorption of the trans configuration bands.

There was an increase in birefringence during the sterilization of sample four (3%) but no increase for sample three that was significant at the .05 level. For sample six this suggested that the growth in primary and secondary crystallites was predominantly oriented. Any effect due to the growth of secondary crystallites in sample five however was offset by the loss of oriented primary crystallites.

Tensile Properties

Except for the initial modulus of sample five there appears to be a general trend towards inferior tensile behavior following sterilization despite increases in crystallinity, birefringence and molecular weight (Figures 34 and 35). Thus, there must have been an overriding effect due to the sterilization environment which masked trends due to changes in microstructure. A clue to the explanation may be found in sample three whose initial modulus increased significantly at the .05 level by over 30% during sterilization. It is suggested that during sterilization much of the residual methylene chloride was replaced by ethylene oxide which then crosslinked the PET and increased the initial modulus. In sample six with a smaller free volume, crosslinking was less extensive and more ethylene oxide endgroup or pendant chain addition reactions may have occurred. These would have decreased

intermolecular cohesion and could have contributed to small reductions in tenacity (11%) and initial modulus (19%).

Summary

The trend toward inferior mechanical properties for the sterilized PET yarn (sample five and six) could not be explained in terms of the structural changes that were measured. It is therefore concluded that these unexpected trends were due to addition and crosslinking reactions with ethylene oxide, and due to the further loss of residual solvent from the sample crimped at 94°C (sample three) during sterilization. For both samples the decrease in surface porosity and the increase in secondary crystallization were accompanied by a decrease in the degree of crystalline perfection. Some of the property changes that had been observed during crimping, such as tenacity, breaking toughness and birefringence, were reversed during sterilization.

COMMERCIAL REFERENCE COMPARISON

Sample seven was obtained by unravelling the yarn from a commercial Milliknit® graft. In order to characterize the fiber structure, and suggest possible manufacturing conditions for the Milliknit® graft, the chemical and physical properties of this reference yarn were compared to those of the compacted and crimped samples (numbers three and four) (Tables 8 and 9). This comparison involved samples three and four because the Milliknit® graft was not sterilized.

Molecular Weight and Endgroup Analysis

The viscosity average molecular weight of 20,700 for the reference sample was lower than the values of 22,100 and 21,900 obtained for

Table 8. Commercial Reference Comparison to the PET Yarn Crimped at 94°C

Measure	Unit	Compacted, Crimped 94°C (Sample Three)	Commercial Reference (Sample Seven)	Difference**	% Difference
Molecular Weight		22,100	20,700	-	
Carboxyl Endgroup	absorbance	0.035	0.000	Same	
Hydroxyl Endgroup	absorbance	0.000	0.000	Same	
Filament Diameter	μm	13.7	13.9	Same	
Linear Density	tex_3	11.5	11.2	Same	
Hydrostatic Density	g/cm_3	1.395	1.379	-	
Nominal Density	g/cm^3	1.448	1.341	-	
DSC ΔH' (PEP)	cal/g	3.3	None	-	
DSC ΔH'' (Melt Peak)	cal/g	11.2	12.4	Same	
DSC ΔH=ΔH'+ΔH''	cal/g	14.5	12.4	-	
DSC Degree of Crystallinity		0.60	0.51	-	
DSC PEP Temperature	°C	157	None	-	
DSC Melt Peak Temperature	°C	260	260	Same	
I.R. Trans Bands	absorbance	Appendix B, Tables 22 and 23		+	
I.R. Gauche Bands	absorbance	Appendix B, Tables 22 and 23		Same	
Birefringence		0.171	0.159*	-	7
Tenacity	mN/tex	203	24*	-	88
Breaking Toughness	mN.m/tex.m	80	5*	-	94
Initial Modulus	N/tex	2.58	.894*	-	65

*Significantly different at the .05 level.

**Denoted 'same' if not significantly different at the .05 level; otherwise + increase, - decrease.

Table 9. Commercial Reference Comparison to the PET Yarn Crimped at 154°C

Measure	Unit	Compacted, Crimped 154°C (Sample Four)	Commercial Reference (Sample Seven)	Difference**	% Difference
Molecular Weight		21,900	20,700	-	
Carboxyl Endgroup	absorbance	0.000	0.000	Same	
Hydroxyl Endgroup	absorbance	0.000	0.000	Same	
Filament Diameter	μm	13.6	13.9	Same	
Linear Density	tex_3	11.3	11.2	Same	
Hydrostatic Density	g/cm_3	1.395	1.379	-	
Nominal Density	g/cm^3	1.429	1.341	-	
DSC ΔH' (PEP)	cal/g	2.3	None	-	
DSC ΔH" (Melt Peak)	cal/g	9.4	12.4	+	
DSC ΔH=ΔH'+ΔH"	cal/g	11.7	12.4	+	
DSC Degree of Crystallinity		0.48	0.51	Same	
DSC PEP Temperature	°C	172	None	-	
DSC Melt Peak Temperature	°C	260	260	Same	
I.R. Trans Bands	absorbance	Appendix B, Tables 22 and 23		-	
I.R. Gauche Bands	absorbance	Appendix B, Tables 22 and 23		Same	
Birefringence		0.177	0.159*	-	10
Tenacity	mN/tex	214	24*	-	89
Breaking Toughness	mN.m/tex.m	92	5*	-	95
Initial Modulus	N/tex	3.56	.894*	-	75

*Significantly different at the .05 level.

**Denoted 'same' if not significantly different at the .05 level; otherwise + increase, - decrease.

samples three and four respectively. Since the greatest loss in $\overline{M}_v$ occurred during compaction, this suggests that the commercial reference sample might have been compacted under more severe conditions than those used in this study. No significant difference was observed between the concentrations of carboxyl and hydroxyl endgroups of sample seven and those of samples three and four.

Yarn Geometry

Neither the filament diameter nor the linear density of the commercial reference sample (sample seven) were significantly different from the compacted and crimped samples (samples three and four) at the .05 level. Samples three and four had higher hydrostatic densities than sample seven (1.395 g/cm^3 and 1.395 g/cm^3 compared with 1.379 g/cm^3), and higher nominal densities than sample seven (1.448 g/cm^3 and 1.429 g/cm^3 compared with 1.341 g/cm^3). This suggests that sample seven may have been compacted under less severe conditions than the samples in this study.

Microstructure

The DSC thermograms indicate major differences between sample seven and the compacted and crimped samples (samples three and four). Sample seven produced an endotherm peak of .8 cal/g at 229°C (Figures 36 and 38), which fell outside the usual temperature range of 125-180°C for PEPs (Carter, 1971: 131). For example, samples three and four had PEP's at 157 and 172°C respectively. It is therefore suggested that this small distinct peak was not a PEP, but corresponds to the heat of fusion of low molecular weight oligomers present in the commercial reference sample. This suggestion is consistent with the low molecular

weight results and supports the earlier conclusion that the commercial reference sample experienced more extensive chain scission than either of the experimentally compacted and crimped samples. This might have been due to more severe compaction, the knitting process and/or post-crimping finishing treatments.

The heat of fusion ($\Delta H''$) for sample seven (12.4 cal/g) was higher than that for both samples three and four (11.2 and 9.4 cal/g respectively) (Figures 37 and 39). However, the total heat of fusion (ΔH) and the DSC crystallinity ratio were similar for samples seven and four (DSC crystallinity ratios: 0.51 and 0.48 respectively) because sample four contained more secondary crystallites, while sample seven contained more primary crystallites. Both these sets of values were lower than those for sample three (DSC crystallinity ratio: 0.60). This DSC behavior suggests that a more extreme crimping time or temperature were used to manufacture sample seven than to prepare samples three and four experimentally.

The levels of the trans infrared absorbances for sample seven were higher than those for sample three, yet lower than those for sample four, which suggests that the commercial reference sample had an intermediate degree of crystalline perfection (Figures 40 and 41). It is therefore concluded that sample seven could have been crimped under less severe conditions than sample four because crimping caused an increase in the trans band absorbances. Alternatively, sample seven could have been compacted under more severe conditions than sample four because compaction caused a decrease in the absorbances of the trans bands.

The commercial reference sample (sample seven) showed less birefringence at the .05 significance level than samples three and four

(7% and 10% less respectively). This may mean that the commercial conditions for compaction were more severe than those used experimentally in this study.

Tensile Properties

Sample seven had considerably lower tenacity, breaking toughness and initial modulus than both samples three and four (Figures 42 and 43). The differences lay between 65 and 95%, and all were significant at the .05 level. The initial portion of the stress/strain curve of sample seven was concave rather than convex as found for the other six samples. These inferior tensile properties could have resulted from the commercial compaction and crimping conditions being more severe than those used in this study and/or the damage that was inevitably caused by the knitting process.

Summary

The majority of the properties measured, such as the reduction in molecular weight, the DSC results, the lower amount of birefringence and the inferior tensile properties were evidence that the commercial reference sample (sample seven) was compacted and/or crimped under more severe conditions than those used in this study. The density results suggested that sample seven might have been compacted under less severe conditions. The presence of two melt peaks, and the very low molecular weight indicating extensive chain scission suggests evidence for oligomers in sample seven.

EFFECT OF COMPACTION, CRIMPING AND STERILIZATION

The chemical and physical properties of the compacted, crimped

and sterilized samples (numbers five and six) were compared to those of the untreated sample (number one) in order to assess the overall changes that occurred to the original yarn during compaction, crimping and sterilization (Tables 10 and 11).

Molecular Weight and Endgroup Analysis

The viscosity average molecular weights for samples five and six (28,300 and 25,800 respectively) were lower than that for sample one (31,200). These reductions reflect the overwhelming importance of chain scission reactions during compaction despite the occurrence of cross-linking and/or additions to the chain during sterilization. The concentrations of carboxyl and hydroxyl endgroups, as measured by the infrared spectra, were not found to change significantly between the untreated (sample one) and the sterilized samples (samples five and six). This is because the infrared spectral analysis were not sufficiently sensitive to measure the changes in endgroup concentrations that accompanied the experimentally measured changes in molecular weight.

Yarn Geometry

The overall longitudinal shrinkage of 20-30% during compaction, crimping and sterilization was accompanied by lateral swelling in sample five (9%) and increases in linear density for samples five (29%) and six (23%). The hydrostatic density increased from 1.369 g/cm^3 for sample one to 1.396 g/cm^3 for samples five and six, while the nominal density increased from 1.293 g/cm^3 (sample one) to 1.523 g/cm^3 and 1.543 g/cm^3 for samples five and six respectively. These results confirm that a more compact structure was produced by the processing and sterilization treatments.

Table 10. Comparison of PET Yarn Compacted, Crimped at 94°C and Sterilized to the Untreated PET Yarn

Measure	Unit	Untreated (Sample One)	Compacted, Crimped 94°C, Sterilized (Sample Five)	Change**	% Change
Molecular Weight		31,200	28,300	-	
Carboxyl Endgroup	absorbance	0.030	0.000	Same	
Hydroxyl Endgroup	absorbance	0.010	0.000	Same	
Length	cm	25.40	18.55	-	27
Filament Diameter	μm	12.6	13.8*	+	9
Linear Density	tex	8.7	12.3*	+	29
Hydrostatic Density	g/cm_3	1.369	1.396	+	
Nominal Density	g/cm^3	1.293	1.523	+	
DSC ΔH' (PEP)	cal/g	None	4.7	Appears	
DSC ΔH" (Melt Peak)	cal/g	12.0	9.7	-	
DSC ΔH=ΔH'+ΔH"	cal/g	12.0	14.4	+	
DSC Degree of Crystallinity		0.49	0.59	+	
DSC PEP Temperature	°C	None	148	Appears	
DSC Melt Peak Temperature	°C	260	260	Same	
I.R. Trans Bands	absorbance	Appendix B, Tables 22 and 23		-	
I.R. Gauche Bands	absorbance	Appendix B, Tables 22 and 23		Same	
Birefringence		0.190	0.169*	-	11
Tenacity	mN/tex	290	195*	-	33
Breaking Toughness	mN.m/tex.m	175	77*	-	56
Initial Modulus	N/tex	7.86	3.73*	-	53

*Significantly different at the .05 level.

**Denoted 'same' if not significantly different at the .05 level; otherwise + increase, - decrease.

Table 11. Comparison of PET Yarn Compacted, Crimped at 154°C and Sterilized to the Untreated PET Yarn

Measure	Unit	Untreated (Sample One)	Compacted, Crimped 154°C, Sterilized (Sample Six)	Change**	% Change
Molecular Weight		31,200	25,800	+	
Carboxyl Endgroup	absorbance	0.030	0.000	Same	
Hydroxyl Endgroup	absorbance	0.010	0.000	Same	
Length	cm	25.40	19.05	-	25
Filament Diameter	μm	12.6	13.2*	Same	
Linear Density	tex_3	8.7	11.3*	+	23
Hydrostatic Density	g/cm_3	1.369	1.396	+	
Nominal Density	g/cm^3	1.293	1.543	+	
DSC ΔH' (PEP)	cal/g	None	4.1	Appears	
DSC ΔH" (Melt Peak)	cal/g	12.0	10.6	-	
DSC ΔH=ΔH'+ΔH"	cal/g	12.0	14.7	+	
DSC Degree of Crystallinity		0.49	0.60	+	
DSC PEP Temperature	°C	None	174	Appears	
DSC Melt Peak Temperature	°C	260	260	Same	
I.R. Trans Bands	absorbance	Appendix B, Tables 22 and 23		-	
I.R. Gauche Bands	absorbance	Appendix B, Tables 22 and 23		Same	
Birefringence		0.190	0.182*	-	4
Tenacity	mN/tex	290	191*	-	34
Breaking Toughness	mN.m/tex.m	175	85*	-	51
Initial Modulus	N/tex	7.86	2.89*	-	63

*Significantly different at the .05 level.

**Denoted 'same' if not significantly different at the .05 level; otherwise + increase, - decrease.

Microstructure

Compaction, crimping and sterilization produced secondary crystallization and caused loss of some primary crystallites. PEP's appeared at 148 and 174^{o}C in the DSC scans for samples five and six respectively (Figures 44 and 46). At the same time the heats of fusion ($\Delta H''$) decreased from 12.0 cal/g for sample one to 9.7 and 10.6 cal/g for samples five and six respectively (Figures 45 and 47). The net effect was an increase in the degree of crystallinity which was in line with the observed increase in density. The DSC crystallinity ratio increased from 0.49 for sample one to 0.59 and 0.60 for samples five and six respectively. The overall loss in the level of infrared trans absorption suggests less crystalline perfection was present in the sterilized samples (Figures 48 and 49).

The birefringence decreased overall. The losses of 11% for sample five, and 4%, for sample six, were significant at the .05 level. Such losses in orientation point to the overriding importance of longitudinal shrinkage and lateral swelling during compaction, which out weighed any subsequent improvements in orientation during crimping and/or sterilization.

Tensile Properties

The overall effect of compaction, crimping and sterilization was to produce lower tenacities, reductions in breaking toughness and lower initial moduli. These losses ranged between 33 and 63% and all were significant at the .05 level (Figures 50 and 51). The important factors that influence this deterioration in tensile behavior during compaction, crimping and sterilization appear to be the chain scission reactions, the longitudinal shrinkage and loss of orientation, and the

addition of ethylene oxide to form pendant chains. These factors out weighed the opposing trends such as the formation of a denser, more compact structure, and the crosslinking of the PET with ethylene oxide.

IMPLICATIONS FOR IMPLANTATION OF MANUFACTURED AND STERILIZED POLY(ETHYLENE TEREPHTHALATE) YARN

Initial interaction between the PET yarn and the chemical species in the body is either adsorption onto the surface, or absorption into the fiber. Interaction with proteins from the blood at the polymer surface and subsequent changes that occur in the adsorbed proteins " . . . are influenced by several factors, including surface smoothness, surface-free energy, chemical structure, electrical properties, enzymatic influences, species-related hematological properties of test animals, and hemorheological factors" (Bruck, 1978: 70). In this study the nature of the surface smoothness, was considered in terms of surface porosity, and the chemical structure and microstructure were examined.

The initial steps in healing are crucial because in the short term they affect thrombus formation, and in the long term they affect the formation of the inner fibrin capsule. Over time a stable layer which renders the polymer passive is most desirable. It is not known how the microstructure effects this process (Merrill, 1977), but surface porosity has been related to thrombus formation. A decrease in surface porosity was obtained after manufacture and sterilization. Merrill (1977: 7) reported that a smooth surface (with fewer pores) will avoid excessive clotting and so prevent excessive thrombus development. This means that the manufactured and sterilized prostheses may be less likely to generate thrombi which, if produced, might block the lumen of the graft and cause early graft failure.

The other factor to consider is surface chemistry. This may influence which species in the blood are absorbed and thus whether thrombi are formed (Merrill, 1977: 14). The reduction in average molecular weight by chain scission reactions, and the additions to the chains will have provided more available endgroups and possibly alter the sites for chemical interaction. Also residual chemicals from processing may affect the long-term in vivo function of the grafts (Sawyer et al., 1978: 218).

As mentioned previously, the tensile properties of the PET yarn were significantly lower after compaction, crimping and sterilization than they were originally. This loss in yarn tenacity and initial modulus may make PET grafts manufactured by this compaction process more susceptible to permanent deformation under continuously applied stress cycles such as the systolic blood pressure.

Polymer degradation may involve either the surface or the internal structure of the PET fibers or both. Any alteration of the surface chemistry will influence the subsequent chemical interaction with the internal structure. It is the non-crystalline areas of the surface rather than the crystalline areas which are more permeable to the components of the blood and other chemical species in the body (Merrill, 1977: 9). Since this study found that the non-crystalline areas decreased, it follows that the permeability may also have decreased. In addition, since the surface porosity decreased there would be a decreased area for surface adsorption. On the other hand, chain scission, the growth of branched chains, and the alteration of available endgroups may have increased the reactivity of the PET surface. Such an increase might change the type of chemical species absorbed and so alter the mechanism of internal PET degradation.

Chapter 5

CONCLUSIONS

In answering the objectives of this study the relationships between the chemical and physical properties of the PET yarn before and after compaction, crimping and sterilization have been analyzed. The main objective was to identify differences in properties between the untreated yarn and the treated yarn samples. The second objective involved an assessment of the structural characteristics of the commercial reference sample and an attempt has been made to suggest how this commercial product was manufactured. The third objective examined the overall effect of processing and sterilization. Implications for implantation of the sterilized grafts have been considered, and areas for further research have been defined.

CHANGES IN YARN PROPERTIES AND STRUCTURE

This study found that significant changes occurred in the structure and properties of PET multifilament yarns (i) during the compaction and (ii) crimping stages of manufacture into vascular prostheses and (iii) during sterilization in ethylene oxide. These three sets of changes did not all proceed in the same direction. In general, similar trends were observed during compaction and sterilization, but these were partially reversed during crimping.

Of particular concern was the overall loss of approximately 33% in yarn tenacity, which was due mainly to the loss of orientation and to the chain scission reactions that occurred during chemical compaction.

The temperature of crimping was important because it controlled the degree of fiber recrystallization and the extent to which the compaction solvent was removed from the yarns. At low crimping temperatures, sufficient quantities of solvent remained to plasticize the structure. The improvements in tensile properties during crimping could be explained in terms of the observed changes in microstructure. The changes in the structure and properties of the PET yarn due to sterilization in ethylene oxide were to some extent dependent on the thermal history of the yarn. Consequently it was concluded that ethylene oxide reacts with PET by addition and/or crosslinking mechanisms.

COMMERCIAL REFERENCE COMPARISON

The structure and properties of the knitted yarn removed from the commercial vascular prostheses did not correspond with those of the two experimentally compacted and crimped yarns. The commercial reference yarn was considerably weaker than the experimental yarns. It was less oriented, had other inferior tensile properties, and a lower molecular weight. These observations suggest that the commercial reference yarn experienced some damage during knitting, and was compacted and/or crimped under more severe conditions than those used in this study.

EFFECT OF COMPACTION, CRIMPING AND STERILIZATION

Inferior tensile properties were produced when the compaction, crimping and sterilization treatments were combined. This was due to the overall loss in orientation, longitudinal shrinkage and chain scission reactions. This decrease out weighed any increases in strength

that might have been expected from a more compact structure and/or crosslinking with ethylene oxide. The overall trends during the manufacturing and sterilization procedures showed an increase in the volume fraction of crystalline material, a growth of secondary crystallites and a loss in crystalline perfection.

IMPLICATIONS FOR IMPLANTATION OF MANUFACTURED AND STERILIZED POLY(ETHYLENE TEREPHTHALATE) YARN

There appeared to be a decrease in surface porosity of the fibers due to manufacturing and sterilization which would be accompanied by the formation of a smoother surface. Since a smooth surface helps to prevent thrombus development, the manufacturing and sterilization treatments may help in the prevention of excessive thrombus development which contribute to graft failure. The chemical changes occurring within the PET during manufacturing and sterilization may have altered the sites for chemical interaction. The losses in yarn tenacity and initial modulus may make these vascular prostheses more susceptible to permanent deformation. The evidence from this study did not indicate conclusively that the manufacturing and sterilization procedures promote chemical reactivity and polymer degradation. The permeability of the polymer to liquids would have decreased due to the decrease in non-crystalline areas but the chemical changes during processing may have altered the endgroups of the PET so as to increase their chemical reactivity. Further work is needed to clarify the relative importance of changes in microstructure and surface porosity and to relate these to the accompanying chemical changes in order to draw further conclusions about the effect of manufacturing and sterilization on the in vivo performance of PET grafts.

AREAS FOR FURTHER RESEARCH

To clarify the findings of this study further research is needed in a number of areas. It would be desirable to evaluate alternative conditions for compacting, crimping and sterilizing the PET yarn, to examine the effect of additional manufacturing, and a variety of in vivo environments, to use other techniques to measure additional chemical and physical properties of the PET polymer and fibers, and to explain the unexpected results concerning residual methylene chloride and ethylene oxide obtained in this study.

By considering alternative times, temperatures, and chemicals for compaction further insights into the fibers structural changes may be forthcoming. For instance the effect of the other acidic solvent, trichloroacetic acid should be evaluated (Smith, 1974). By exposing the PET yarn to the compaction chemicals separately, their individual effects will be clarified. It would be of value to consider other compaction techniques, such as the use of vapor phase halogenated hydrocarbons (Sawyer et al., 1978). The effect of repeated sterilization treatments and different types of sterilization (eg. steam and gamma radiation) should also be evaluated. More information is needed about the behavior of PET in other environments such as the knitting process and storage.

Other techniques such as X-ray diffraction, transmission infrared spectroscopy and dye penetration studies may more clearly describe the internal phases and void spaces within PET fibers. In this study the infrared spectroscopy attenuated total reflectance technique was not sensitive enough to accurately measure the endgroup concentrations or the amount of chain folding. Titration techniques or transmission

infrared spectroscopy might prove to be more sensitive methods for end-groups analysis (Ludewig, 1971: 133). Future studies that evaluate the properties of vascular grafts rather than those of the yarn should include additional measurements such as the longitudinal stretch and recovery, creep and fatigue, the resistance to compression, the flexibility or bending properties, as well as the bursting strength. Bursting strength has been used by Guidoin et al. (1978) to predict in vivo performance.

Since the results of this study indicated that residual solvent is likely to be present in the compacted fibers, gas chromatography studies would be valuable to determine the amount of residual solvent and other compaction chemicals. It would be useful to examine the amount of residual ethylene oxide that remains after gas sterilization, and how this amount is affected by an aeration cycle. In the future clinical studies should use grafts whose manufacturing and sterilization histories are known in detail. This would enable researchers to obtain a clearer understanding of how the chemical and mechanical changes occurring during manufacture and sterilization influence the patency and healing rates of implanted grafts.

LITERATURE CITED

Addleman, R.L. and Zichy. 1972. Accurate measurement of carboxyl and hydroxyl end-group concentrations in poly(ethylene terephthalate) film by infra-red spectroscopy. Polymer. 13:391-398.

American Society for Testing and Materials. 1977. Annual Book of ASTM Standards, parts 32 and 35. Philadelphia: American Society for Testing and Materials.

Bahl, S.K., Cornell, D.D. and Boerio, F.J. 1974. Interpretation of the vibrational spectra of poly(ethylene terephthalate). J. Polym. Sci. B-12:13-19.

Barron, A.L.E. 1965. Using the Microscope. London: Chapman and Hall. Ltd.

Battaerd, H.A.J. and Tregear, G.W. 1967. Graft Copolymers. New York: Interscience Publishers.

Blumenberg, R.M. and Gelfand, M.L. 1977. Failure of knitted dacron as an arterial prosthesis. Surgery. 81(5):493-496.

Bruck, S.D. 1978. Some current problems and new dimensions of polymeric biomaterials for blood-contacting applications. Biomat., Med. Dev., Art. Org. 6(1):57-76.

Bruck, S.D. 1971. Sterilization problems of synthetic biocompatible materials. J. Biomed. Mater. Res. 5:139-158.

Burlington Industries, Inc. 1970. Textile Fibers and Their Properties. North Carolina: Burlington Industries, Inc.

Buxbaum, T.H. 1968. The degradation of poly(ethylene terephthalate). Angew. Chem. Intl. Ed. 7(3):182-190.

Carlsson, D.J., Suprunchuk, T. and Wiles, D.M. 1970. The uses of ATR infrared spectroscopy in fiber science. Can. Textile J. 87:73-78.

Carter, M.E. 1971. Essential Fiber Chemistry. New York: Marcel Dekker Inc.

Chamot, E.M. and Mason, C.W. 1958. Handbook of Chemical Microscopy. Vol. I 3d. ed. New York: John Wiley and Sons Inc.

Clark, M.J. and Hickie, T.S. 1975. The quantitative analysis of some binary mixtures of fibers by methods of infra-red spectroscopy. J. Textile Inst. 66(7):243-248.

Day, M. and Wiles, D.M. 1972. Photochemical degradation of poly(ethylene terephthalate) I. irradiation experiments with xenon and carbon arc. J. of Appl. Polym. Sci. 16:175-189.

Deopura, B.L., Sinha, T.B. and Varma, D.S. 1977. Dependence of mechanical properties on crystalline, intermediate and amorphous phases in poly(ethylene terephthalate) fibers. Textile Res. J. 47(4):267-271.

Dumbleton, J.H. 1969. The effect of oil and air annealing on the structure of drawn poly(ethylene terephthalate). Polymer. 10(7):539-542.

Ernst, R.R. 1973. Ethylene oxide gaseous sterilization for industrial applications. Industrial Sterilization. ed. Briggs Phillips, G. and Miller, W.S. Durham, North Carolina: Duke University Press.

Fakirow, S. et al. 1977. Structure and properties of poly(ethylene terephthalate) crystallized by annealing in the highly oriented state: 2 melting behavior and the mosaic block structure of the crystalline layers. Polymer. 18(11):1121-1129.

Farrow, G. and Ward, I.M. 1960. Crystallinity in poly(ethylene terephthalate) a comparison of x-ray, infra-red and density measurements. Polymer. 1:330-339.

Gibbons, J.D. 1971. Nonparametric Statistical Inference. New York: McGraw-Hill Book Co. Inc.

Golaski, W.M. 1968. Engineering design factors in the construction and evaluation of knitted arterial prostheses. Materials conference, American Institute Chemical Engineers. Philadelphia (April).

Goodman, I. and Rhys, J.A. 1965. Polyesters. London: Iliffe Books Ltd.

Grosberg, P. 1969. The geometry of knitted fabrics. Structural Mechanics of Fibers, Yarns and Fabrics. ed. Hearle, J.W., Grosberg, P. and Backer, S. Vol. I New York: Wiley - Interscience.

Guidoin, R.C. et al. 1978. Structural and mechanical properties of Dacron^{R} prostheses as arterial substitutes. Laboratoire de Chirurgie Expérimentale, Centre du Biomédecine et Département de Chirurgie Université Laval, Quebec and Bureau of Medical Devices, National Health and Welfare, Ottawa.

Guidoin, R.C. et al. 1977. Dacron as arterial prosthetic material: nature, properties, brands, fate and perspective. Biomat. Med. Dev., Art. Org. 5(2):177-203.

Gupta, V.B. and Kumar, S. 1978. Third phase in poly(ethylene terephthalate). Polymer. 19(8):953-955.

Hall, D.M. 1976. Practical Fiber Identification. Alabama: Auburn University.

Hayward, R.H. and Korompal, F. 1976. Degeneration of knitted dacron grafts. Surgery. 79(5):581-583.

Hearle, J.W.S. and Greer, R. 1970. Fiber structure. Textile Progress. 2(4):1-203.

Heyn, A.N.J. 1954. Fiber Microscopy. New York: Interscience Publishers.

Hussey, H.H. 1976. Arterial replacement: failure of synthetic prostheses. J. Am. Med. A. 235(8):848.

Jeckel, N.C. 1967. Uniformly corrugated prostheses and process for making same. United States Patent 3,337,673; assigned to U.S.C.I. Corp.

Ke, B. 1962. Differential thermal analysis of high polymers. IV Saturated linear polyesters. J. Appl. Polym. Sci. 6(24):624-628.

Kendall, D.N. 1966. Applied Infrared Spectroscopy. New York: Reinhold Publishing Corp.

King, R.N. and Lyman, D.J. 1975. Polymers in contact with the body. Environmental Health Perspectives. 11:71-74.

Leitz Wetzlar. 1960. Berek Compensator Directions for Use. Ontario: Ernst Leitz (Canada) Ltd.

Liang, C.Y. and Krimm, S. 1959. Infrared spectra of high polymers part IX polyethylene terephthalate. J. Mol. Spec. 3:554-574.

Ludewig, H. 1971. Polyester Fibres. London: Wiley - Interscience.

Lyman, D.J. 1968. Biomedical polymers. Ann. N.Y. Acad. Sci. 146:30-47.

Makarewicz, P.J. and Wilkes, G.L. 1978. Structural rearrangements in the liquid-induced crystallization of cold-drawn poly(ethylene terephthalate). Textile Res. J. 48(3):136-143.

Manche, E.P. and Carroll, B. 1972. Thermal methods. Physical Methods in Macromolecular Chemistry. ed. Carroll, B. Vol. II. New York: Marcel Dekker Inc.

Manning, R.J. 1970. Reflectance techniques in infrared spectroscopy. Beckman Technical Report No. 565.

Meares, P. 1965. Polymers: Structure and Bulk Properties. London: D. Van Nostrand Company Ltd.

Merrill, E.W. 1977. Properties of materials affecting the behavior of blood at their surfaces. Ann. N.Y. Acad. Sci. 283:6-16.

Miyake, A. 1959. The infrared spectrum of polyethylene terephthalate I. the effect of crystallization. J. Polym. Sci. 38:479-495.

Moore, W.R. and Sanderson, D. 1968. Viscosities of dilute solutions of polyethylene terephthalate. Polymer. 9:153-158.

Morton, W.E. and Hearle, J.W.S. 1975. Physical Properties of Textile Fibers. New York: John Wiley and Sons.

Munden, D.L. 1959. The geometry and dimensional properties of plain-knit fabrics. J. Textile Inst. 50:T448-T471.

Nielsen, L.E. 1962. Mechanical Properties of Polymers. New York: Reinhold Publishing Corporation.

O'Connor, R.T. 1968. Absorption spectroscopy. Analytical Methods for a Textile Laboratory. AATCC Monograph number 3. North Carolina.

Patterson, D. and Ward, I.M. 1957. The assignment of the carboxyl and hydroxyl absorptions in the infrared spectrum of polyethylene terephthalate. Trans. Farad. Soc. 53:291-294.

Perkin-Elmer, 1967. Instructions differential scanning calorimeter Norwalk, Connecticut.

Perry, M.O. 1975. Early failure of dacron prosthetic grafts. J. Cardiovas. Surg. 16(3):318-321.

Peters, R.H. 1963. Textile Chemistry. Vol. I. The Chemistry of Fibers. New York: Elsevier Publishing Co.

Plester, D.W. 1970. The effects of sterilization process on plastics. Biomed. Eng. 5 (September):443-447.

Pohl, H.A. 1951. The thermal degradation of polyesters. J. Amer. Chem. Soc. 73 (December):5660-5661.

Potts, J.E. 1978. Biodegradation. Aspects of Degradation and Stabilization of Polymers. ed. Jellinek, H.H.G. Amsterdam: Elsevier Scientific Publishing Co.

Preston, J.M. and Nimkar, M.V. 1950. The use of density gradient tubes in fiber studies and their applications to the analysis of fiber mixtures. J. Textile Inst. 41:T446-T454.

Prevorsek et al. 1974. Effects of thermal contraction on structure and properties of PET fibers. J. Macromol. Sci-Phys. B9(4):733-759.

Reed, A.M., and Gilding, D.K. and Wilson, J. 1977. Biodegradability elastomeric biomaterials. Trans. Am. Soc. Artif. Intern. Organs. 23:109-115.

Reich, L. and Stivala, S.S. 1971. Elements of Polymer Degradation. New York: McGraw-Hill Inc.

Ribnick, A. 1969. The thermal shrinkage of an oriented polyester yarn as a function of time, temperature and stress. Textile Res. J. 39(8):742-748.

Ribnick, A.S., Weigmann, H.D. and Rebenfeld, L. 1972. Interactions of nonaqueous solvents with textile fibers. part I: effects of solvents on the mechanical properties of a polyester yarn. Textile Res. J. 42(12):720-726.

Ribnick, A.S., Weigmann, H.D. and Rebenfeld, L. 1973. Interactions of nonaqueous solvents with textile fibers. part II: isothermal kinetics of polyester yarn. Textile Res. J. 43(3):176-183.

Roberts, J.D., Stewart, R. and Caserio, M.C. 1971. Organic Chemistry. California: Benjamin.

Sauvage, L.R. et al. 1976. Healing of Arterial Prostheses. Seattle: Providence Medical Center.

Sauvage, L.R. et al. 1974. Future directions in the development of arterial prostheses for small and medium caliber arteries. Surg. Cl. N.A. 54(1):213-228.

Sawyer, P.N. et al. 1978. Evaluation of chemical compacting techniques on the performance, thrombosis rate, histology, and healing of experimental similarly fabricated Dacron prostheses. Trans. Am. Soc. Artif. Intern. Organs. 24:215-218.

Scheffé, H. 1959. The Analysis of Variance. New York: John Wiley and Sons, Inc.

Schwarz, E.R. 1934. Textiles and the Microscope. 1st. ed. New York: McGraw-Hill.

Sibilia, J.P. 1975. Applications of the ATR technique to the study of fiber and fabric surfaces. Surface Characteristics of Fibers and Textiles. ed. Schick, M.J. part I. New York: Marcel Dekker Inc.

Skelton, J. 1974. Textiles in biomedical devices some unrecognized variables. Biomed., Med. Dev., Artif. Org. 2(4):345-352.

Smith, R.E. 1974. Compaction of polyester fabric materials. United States Patent 3,853,462; assigned to Meadox Medicals Inc.

Snedecor, G.W. and Cochran, W.G. 1967. Statistical Methods. 6th ed. Iowa: The Iowa State University Press.

Statton, W.O. 1971. Synthetic fibers: structure and setting. The setting of Fibers and Fabrics. ed. Hearle, J.W.S. and Miles, L.W.S. England: Merrow Publishing Co. Ltd.

Stevens, M.P. 1975. Polymer Chemistry an Introduction. Massachusetts: Addison - Wesley Publishing Co., Inc.

Stoves, J.L. 1957. Fiber Microscopy. London: National Trade Press.

Takebayaski, J. 1975. A comparative study on the patency of crimping and noncrimping vascular prostheses with emphasis on the earliest morphological changes. J. Surg. Res. 19(3):209-218.

The Textile Institute. 1975. Identification of Textile Materials. 7th ed. Manchester: The Textile Institute.

Ward, I.M. 1961. The molecular structure and mechanical properties of polyethylene terephthalate fibers. Textile Res. J. 31(7):650-664.

Watson, E.W. et al. 1964. A differential scanning calorimeter for quantitative differential thermal analysis. Anal. Chem. 36(7):1233-1238.

Weigmann, H.D., Scott, M.G. and Ribnick, A.S. 1978. Interactions of nonaqueous solvents with textile fibers part X: effects of thermal history on polyester-solvent interactions. Textile Res. J. 48(1):4-13.

Weigmann, H.D., Scott, M.G. and Ribnick, A.S. 1977. Interactions of nonaqueous solvents with textile fibers. part IX: thermal stability of solvent-induced modifications on polyester fiber structure. Textile Res. J. 47(12):761-771.

Weigmann, H.D. et al. 1977. Interactions of nonaqueous solvents with textile fibers. part VIII: mechanism of dye diffusion in solvent-treated polyester yarns. Textile Res. J. 47(11):745-754.

Weigmann, H.D. et al. 1976. Interactions of nonaqueous solvents with textile fibers. part VII: dyeability of polyester yarns after heat and solvent-induced structural modifications. Textile Res. J. 46(8):574-587.

Wesolowski, S.A. et al. 1968. Arterial prosthetic materials. Ann. N.Y. Acad. Sci. 146:325-344.

Wesolowski, S.A., Fries, C.C. and Sawyer, P.N. 1961. The importance of biological reactivity of the synthetic vascular graft wall. Trans. Am. Soc. Artif. Intern. Organs. 7:296-300.

Wilks, P.A. and Iszard, M.R. 1964. The identification of fibers and fabrics by internal reflection spectroscopy. Wilks Scientific Corporations. Fifteenth Mid-American Spectroscopy Symposium. Chicago, Illinois. June.

Willard, H.H., Merritt, L.L. and Dean, J.A. 1974. Instrumental Methods of Analysis. 5th ed. New York: D. Van Nostrand Company.

Wilson, M.P.W. 1974. Shrinkage and chain folding in drawn poly(ethylene terephthalate) fibers. Polymer. 15(5):277-282.

Yashar, J.J. et al. 1978. Failure of dacron prostheses caused by structural defect. Surgery. 84(11):659-663.

APPENDIXES

APPENDIX A

DEFINITION OF TERMS

AND

LIST OF ABBREVIATIONS

DEFINITION OF TERMS

Compaction process. The chemical treatment used to reduce the porosity of knitted tubing fabric according to United States Patent 3,853,462 (Smith, 1974).

Crimping process. The heat treatment used to produce uniformly crimped prostheses according to United States Patent 3,337,673 (Jeckel, 1967).

Other terms used in this study follow the definition of textile terms in ASTM(1977) Designation: D123-77.

LIST OF ABBREVIATIONS

DSC	Differential scanning calorimetry.
$\Delta H'$	Heat of premelt crystallization.
$\Delta H''$	Heat of fusion.
ΔH	Overall heat of fusion.
M	Test statistic due to Kruskal and Wallis.
$\bar{M}_v$	Viscosity average molecular weight.
η	Intrinsic viscosity.
PEP	DSC premelt endotherm peak.
PET	poly(ethylene terephthalate).
W_c(d.s.c.)	DSC apparent degree of crystallinity.

APPENDIX B

EXPERIMENTAL RESULTS

Table 12. Viscosity Measurements; Average Rates of Flow of Polymer Concentrations and Solvent, and Intrinsic Viscosity for Each Sample

Sample	Average Rate of Flow of Solvent(sec)	Average Rate of Flow of Polymer Concentration(sec)					Intrinsic Viscosity
	2 ml	1 ml	2 ml	3 ml	5 ml	10 ml	
1	76.7	86.7	90.2	93.0	94.5	97.7	.8300
2	76.4	84.7	89.0	90.8	94.7	97.2	.6291
3	77.4	85.6	90.0	92.2	95.0	98.6	.6269
4	79.9	87.6	89.9	91.8	94.0	96.3	.6238
5	77.5	86.6	90.2	92.7	93.9	96.9	.7665
6	76.4	85.1	90.0	91.8	94.0	96.5	.7119
7	75.2	82.6	86.7	88.7	92.7	94.1	.5747

Table 13. Viscosity Average Molecular Weight for Each Sample

Sample	1	2	3	4	5	6	7
Viscosity Average Molecular Weight	31,200	22,200	22,100	21,900	28,300	25,800	20,700

Table 14. Infrared Spectra Endgroup Analysis for Each Sample

Groups		Carboxyl	Hydroxyl
Band Frequency(cm^{-1})		3290	3535
		Absorbance	
Sample	1	0.030	0.010
	2	0.000	0.000
	3	0.035	0.000
	4	0.000	0.000
	5	0.000	0.000
	6	0.000	0.000
	7	0.000	0.000

Table 15. Mean Length and Shrinkage for Each Sample

Sample	1	2	3	4	5	6
Mean Length(cm)	25.40	19.05	18.55	19.05	18.55	19.05
Shrinkage (%)		25	2*	0*	0*	0*

*Percentage of the previous treatment.

Table 16. Filament Diameter for Each Specimen

Sample	1	2	3	4	5	6	7
Filament Diameter (Microns)	13.2	14.5	12.9	14.3	13.3	12.7	13.8
	14.1	13.9	13.9	13.2	14.2	12.9	14.7
	14.6	14.1	14.5	13.6	14.1	13.1	14.4
	13.3	13.9	13.6	14.2	14.1	13.2	13.0
	12.5	14.2	14.7	13.2	14.7	13.5	16.3
	11.4	14.7	13.5	14.0	13.2	12.6	14.8
	11.1	14.2	13.4	12.8	13.2	13.2	12.0
	12.0	14.3	13.8	13.2	13.5	14.2	16.3
	12.8	14.6	13.5	13.9	13.8	12.8	12.8
	11.7	14.4	13.2	13.9	13.5	13.4	13.6
	11.3	14.0	12.9	14.1	13.7	13.1	14.0
	12.1	13.9	12.9	13.5	13.6	13.5	12.4
	12.7	14.3	14.3	13.7	14.5	13.6	14.4
	12.3	14.4	14.1	13.3	14.0	13.8	13.2
	14.2	14.2	13.5	12.9	13.1	13.1	14.6
	12.1	13.8	13.1	13.5	14.0	12.7	13.0
	13.0	13.8	13.5	14.0	13.2	13.5	14.0
	11.2	14.4	14.3	14.2	14.2	14.3	14.5
	12.9	13.9	13.8	15.5	14.7	14.3	13.7
	11.8	14.2	13.9	14.2	14.5	13.1	15.4
	10.4	13.6	13.6	13.4	13.9	13.1	13.5
	13.0	13.8	13.2	12.8	14.2	12.6	14.0
	13.5	14.6	14.3	12.6	13.8	12.6	14.6
	14.7	14.4	13.5	13.8	13.7	12.7	13.7
	13.5	14.2	14.0	12.9	13.9	13.2	15.1
	12.6	13.9	13.2	13.6	13.8	13.6	14.1
	12.8	13.8	13.6	14.4	12.9	12.8	13.8
	12.4	13.8	14.0	14.0	13.5	12.4	13.0
	11.5	14.6	14.2	13.6	13.7	12.5	13.1
	12.6	14.6	14.3	13.0	13.5	13.4	12.6
Mean	12.6	14.2	13.7	13.6	13.8	13.2	13.9
Standard Deviation	1.1	0.3	0.5	0.6	0.5	0.5	1.0
Coefficient of Variation	8.4	2.2	3.6	4.5	3.4	3.9	7.4

Table 17. Linear Density for Each Specimen

Sample	1	2	3	4	5	6	7
Linear Density (tex)	8.9	12.4	11.4	11.3	12.1	11.7	11.2
	8.4	12.3	11.5	11.2	12.2	11.6	11.1
	8.6	12.0	11.6	11.3	13.4	11.5	11.2
	8.6	12.1	11.7	11.1	12.6	11.5	11.4
	8.4	11.6	11.6	11.3	12.6	11.5	10.9
	8.7	12.1	11.1	11.1	12.6	11.4	11.0
	8.7	11.8	11.6	11.3	12.3	11.3	12.0
	8.7	11.5	11.3	11.4	12.1	11.4	12.0
	8.7	11.8	11.6	11.2	12.1	11.4	10.9
	8.8	11.5	11.6	11.5	12.3	10.9	11.0
	8.8	11.4	11.6	11.0	12.1	11.2	10.8
	8.4	11.6	11.5	11.3	12.0	11.4	11.5
	8.8	11.6	11.5	11.3	12.1	11.4	11.0
	8.7	11.5	11.4	11.2	11.9	10.9	10.8
	8.7	12.2	11.4	11.4	11.7	11.0	11.0
Mean	8.7	11.8	11.5	11.3	12.3	11.3	11.2
Standard Deviation	0.2	0.3	0.2	0.1	0.4	0.2	0.4
Coefficient of Variation	1.8	2.8	1.3	1.2	3.3	2.1	3.4

Table 18. Hydrostatic and Nominal Density for Each Sample

Sample	1	2	3	4	5	6	7
Hydrostatic Density (g/cm^3)	1.369	1.397	1.395	1.395	1.396	1.396	1.379
Nominal Desnity (g/cm^3)	1.293	1.389	1.448	1.429	1.523	1.543	1.341

Table 19. DSC Premelt Endotherm Results for Each Sample

Sample	1	2	3	4	5	6	7
Heat of Premelt Crystallization ($\Delta H'$) (cal/g)	None	8.6	3.3	2.3	4.7	4.1	None
Premelt Endotherm Peak Temperature(^oC)	—	146	157	172	148	174	—

Table 20. DSC Melt Results for Each Sample

Sample	1	2	3	4	5	6	7
Heat of Fusion ($\Delta H''$) (cal/g)	12.0	11.0	11.2	9.4	9.7	10.6	12.4
Melt Peak(^oC)	260	260	260	260	260	260	260

Table 21. Overall Heat of Fusion and DSC Degree of Crystallinity for Each Sample

Sample	1	2	3	4	5	6	7
Overall Heat of Fusion (ΔH)	12.0	19.6	14.5	11.7	14.4	14.7	12.4
DSC Degree of Crystallinity	0.49	0.81	0.60	0.48	0.59	0.60	0.51

Table 22. Infrared Spectra Crystallinity Analysis for Each Sample

Bands		Trans	Gauche	Trans	Gauche	Trans	Gauche	Trans	Gauche	Calibration Standard
Band Frequency (cm^{-1})		845	895	973	1040	1337	1370	1470	1453	794
Absorbance										
Sample	1	.450	.070	.050	.030	.310	.110	.230	.090	.090
	2	.060	.000	.000	.000	.020	.000	.000	.000	.035
	3	.215	.000	.000	.020	.165	.050	.035	.005	.065
	4	.190	.000	.010	.000	.130	.020	.010	.030	.060
	5	.180	.000	.015	.010	.110	.030	.000	.000	.060
	6	.165	.000	.005	.000	.100	.000	.000	.000	.050
	7	.200	.000	.010	.000	.145	.005	.045	.010	.040

Table 23. Spectra Changes Due to Crystallization

	Compaction	Crimping		Sterilization		Comparison		Effect of Compaction, Crimping and Sterilization	
		Crimped	Crimped	Crimped	Crimped	Crimped	Crimped	Crimped	Crimped
Sample	2 vs 1	94°C 3 vs 2	154°C 4 vs 2	94°C 5 vs 3	154°C 6 vs 4	94°C 7 vs 3	154°C 7 vs 4	94°C 5 vs 1	154°C 6 vs 1
Bands(cm^{-1})									
Trans 1470	-*							-	-
Gauche 1453									
Trans 1337	-	+	+	-	-	+	-	-	-
Gauche 1370									
Trans 973									
Gauche 1040									
Trans 845	-	+	+	-	-	+	-	-	-
Gauche 895									

* + intensity increase of more than .12.
- intensity decrease of more than .12.

Table 24. Birefringence for Each Specimen

Sample	1	2	3	4	5	6	7
Birefringence	0.189	0.163	0.172	0.169	0.171	0.181	0.162
	0.189	0.166	0.172	0.174	0.168	0.181	0.155
	0.193	0.163	0.172	0.174	0.168	0.184	0.159
	0.189	0.163	0.172	0.177	0.171	0.184	0.164
	0.193	0.163	0.174	0.177	0.168	0.181	0.151
	0.189	0.163	0.172	0.174	0.168	0.184	0.163
	0.189	0.163	0.174	0.177	0.172	0.184	0.159
	0.189	0.163	0.174	0.178	0.168	0.184	0.161
	0.189	0.162	0.172	0.180	0.168	0.179	0.157
	0.193	0.164	0.172	0.174	0.173	0.184	0.158
	0.189	0.164	0.173	0.177	0.168	0.181	0.161
	0.189	0.163	0.169	0.178	0.168	0.181	0.144
	0.189	0.162	0.169	0.177	0.168	0.181	0.163
	0.189	0.162	0.169	0.174	0.168	0.184	0.159
	0.189	0.163	0.169	0.177	0.168	0.184	0.164
	0.189	0.162	0.169	0.178	0.171	0.184	0.158
	0.193	0.162	0.174	0.180	0.168	0.184	0.163
	0.189	0.162	0.168	0.178	0.168	0.179	0.158
	0.189	0.166	0.172	0.180	0.168	0.181	0.157
	0.189	0.163	0.167	0.180	0.168	0.181	0.158
	0.189	0.163	0.166	0.178	0.168	0.184	0.161
	0.189	0.166	0.168	0.178	0.168	0.179	0.158
	0.189	0.166	0.169	0.178	0.168	0.179	0.157
	0.189	0.160	0.172	0.178	0.168	0.179	0.159
	0.189	0.162	0.169	0.178	0.168	0.181	0.161
Mean	0.190	0.163	0.171	0.177	0.169	0.182	0.159
Standard Deviation	0.001	0.001	0.002	0.002	0.002	0.002	0.004
Coefficient of Variation	0.789	0.914	1.387	1.431	0.898	1.110	2.709

Table 25. Tenacity for Each Specimen

Sample	1	2	3	4	5	6	7
Tenacity (mN/tex)	272	193	239	235	196	188	45
	297	180	239	259	232	210	20
	263	185	217	196	170	125	27
	308	153	224	238	220	117	29
	305	170	186	259	204	164	38
	297	176	233	248	224	242	17
	320	212	183	227	200	205	14
	294	172	211	240	198	164	13
	320	214	215	196	198	203	28
	322	166	213	207	174	192	17
	337	170	200	218	190	171	14
	280	191	207	177	180	199	18
	311	186	209	216	186	223	27
	334	185	200	187	236	214	9
	291	164	220	227	186	141	32
	260	143	222	248	218	167	19
	280	207	192	203	194	192	11
	255	195	213	220	180	156	16
	283	176	203	257	208	186	25
	297	176	181	225	214	212	16
	277	216	205	209	226	227	24
	269	180	213	207	222	231	30
	249	230	213	183	186	186	14
	283	197	226	185	182	212	28
	289	220	196	196	164	234	14
	280	162	175	196	180	197	39
	283	164	168	161	176	188	18
	291	197	168	198	164	212	39
	283	189	192	205	164	190	34
	260	172	141	196	192	195	38
Mean	290	185	203	214	195	191	24
Standard Deviation	23	21	22	26	21	31	10
Coefficient of Variation	8	11	11	12	11	16	41

Table 26. Breaking Toughness for Each Specimen

Sample	1	2	3	4	5	6	7
Breaking Toughness (mN.m/tex.m)	154	67	93	113	78	86	8
	180	73	93	68	93	91	3
	155	74	85	142	71	73	5
	201	69	86	86	88	69	7
	184	65	77	110	81	81	8
	182	74	85	105	85	75	3
	201	69	79	92	78	81	2
	183	71	84	95	73	88	5
	195	64	81	108	80	81	6
	208	66	76	97	83	87	4
	212	71	83	91	86	98	5
	164	80	84	90	86	99	6
	191	80	84	85	74	96	3
	209	69	87	87	72	92	12
	179	69	78	88	68	84	3
	154	64	89	107	88	82	4
	166	79	77	99	81	103	3
	149	72	84	103	80	92	3
	165	70	84	92	79	82	6
	176	68	84	94	72	92	4
	163	74	76	89	72	81	4
	157	66	77	78	70	75	4
	144	80	79	86	71	82	5
	169	70	75	81	90	89	2
	171	76	83	90	70	88	6
	166	60	67	79	70	80	10
	169	58	66	70	65	78	4
	171	70	65	80	63	87	7
	166	72	75	81	61	78	7
	153	61	60	80	72	80	7
Mean	175	70	80	92	77	85	5
Standard Deviation	19	6	8	15	8	8	2
Coefficient of Variation	11	8	10	16	11	9	45

Table 27. Initial Modulus for Each Specimen

Sample	1	2	3	4	5	6	7
Initial Modulus (N/tex)	7.59	3.07	2.53	3.77	3.95	2.35	.844
	8.28	3.43	2.77	3.85	4.14	2.67	.888
	8.14	3.05	2.71	3.77	4.04	2.22	.985
	7.93	2.97	2.47	4.06	3.99	3.04	.899
	8.07	2.92	3.00	3.71	4.04	2.56	.629
	8.21	3.33	2.47	3.50	4.38	2.43	.801
	7.78	3.20	2.66	3.77	3.95	2.19	.866
	8.14	3.02	2.74	3.53	3.51	2.22	.660
	8.28	3.15	2.77	3.79	3.36	2.94	1.06
	8.35	3.43	2.66	3.88	3.80	2.40	.768
	8.49	3.30	2.63	3.93	3.99	2.91	1.04
	7.59	3.17	2.71	3.26	3.90	2.94	.920
	7.73	3.40	2.37	3.82	4.09	2.48	.888
	8.28	3.28	2.74	3.01	3.90	2.56	.671
	7.66	3.20	2.79	3.71	2.92	2.51	1.13
	7.93	3.12	2.45	3.63	3.65	2.22	.801
	8.14	2.94	2.55	3.66	3.07	3.07	.844
	7.59	3.17	2.74	3.23	3.45	2.48	.725
	7.52	3.02	2.29	3.77	3.60	2.51	.899
	7.66	2.94	2.42	3.98	3.99	2.94	.682
	7.31	3.66	2.58	3.39	3.70	3.79	1.05
	7.73	3.48	2.95	3.90	3.90	3.34	.985
	7.04	3.51	2.45	3.63	3.99	3.85	.866
	7.45	3.33	2.42	4.09	3.75	3.55	1.08
	7.59	3.15	2.27	3.58	3.90	3.74	1.13
	8.28	3.07	2.66	3.07	3.40	3.04	1.07
	7.93	2.94	2.42	2.80	3.21	3.39	.649
	8.28	2.56	2.32	2.80	3.58	3.42	.877
	7.11	2.94	2.47	3.01	3.16	3.47	1.13
	7.59	2.94	2.27	2.93	3.45	3.50	.996
Mean	7.86	3.16	2.58	3.56	3.73	2.89	.894
Standard Deviation	.382	.230	.195	.378	.352	.522	.153
Coefficient of Variation	5	7	8	11	9	18	17

APPENDIX C

STATISTICAL ANALYSIS

Table 28. One-Way Analysis of Variance for Filament Diameter, Linear Density, Birefringence, Tenacity, Breaking Toughness and Initial Modulus

Source of Variation	Degrees Freedom	Sum of Squares	Mean Square	F Ratio	Critical Value $F_{.01}$
Filament Diameter	6	51.33	8.56	17.83**	2.90
Error	203	98.35	.48		
Linear Density	6	121.31	20.22	252.75**	2.99
Error	98	7.61	0.08		
Birefringence	6	.0173	.0029	483.33**	2.92
Error	168	.0010	.000006		
Tenacity	6	1148233.5	191372.3	373.63**	2.90
Error	203	103971.6	512.2		
Breaking Toughness	6	442292.4	73715.4	642.12**	2.90
Error	203	23314.1	114.8		
Initial Modulus	6	814632695.1	135772115.9	1189.50**	2.90
Error	203	23170937.4	114142.5		

**Significant at the .01 level.

Table 29. Kruskal-Wallis One-Way Analysis of Variance for Filament Diameter, Linear Density, Birefringence, Tenacity, Breaking Toughness and Initial Modulus

Measure	Degrees Freedom	M	Critical Value $\chi^2_{.01}$
Filament Diameter	6	67.383**	16.812
Linear Density	6	80.358**	16.812
Birefringence	6	165.386**	16.812
Tenacity	6	142.646**	16.812
Breaking Toughness	6	162.849**	16.812
Initial Modulus	6	177.085**	16.812

**Significant at the .01 level.

Table 30. Scheffé's Test - Multiple Comparisons

Treatment	Compaction	Crimping		Sterilization	
Comparison	Sample 2 vs Sample 1	Sample 3 vs Sample 2	Sample 4 vs Sample 2	Sample 5 vs Sample 3	Sample 6 vs Sample 4
Measure					
Filament Diameter	8.89*	2.78	3.33	.56	2.22
Linear Density	31.00*	3.00	5.00*	8.00*	0.00
Birefringence	39.36*	11.66*	20.41*	2.92	7.29*
Tenacity	18.17*	3.11	5.02*	1.38	3.98*
Breaking Toughness	38.46*	3.66*	8.06*	1.10	2.56
Initial Modulus	54.45*	6.72*	4.63*	13.32*	7.76*

*Significant at the .05 level.

Table 30. Scheffē's Test - Multiple Comparisons (Cont.)

Treatment	Reference Comparison		Effect of Compaction, Crimping and Sterilization		5% Critical Value
Comparison	Sample 7 vs Sample 3	Sample 7 vs Sample 4	Sample 5 vs Sample 1	Sample 6 vs Sample 1	
Measure					
Filament Diameter	1.11	1.67	6.67*	3.33	3.58
Linear Density	3.00	1.00	36.00*	26.00*	3.62
Birefringence	17.49*	26.24*	30.61*	11.66*	3.60
Tenacity	30.97*	32.87*	16.44*	17.13*	3.58
Breaking Toughness	27.47*	31.87*	35.90*	32.97*	3.58
Initial Modulus	19.53*	30.89*	47.85*	57.58*	3.58

*Significant at the .05 level.

APPENDIX D

FIGURES

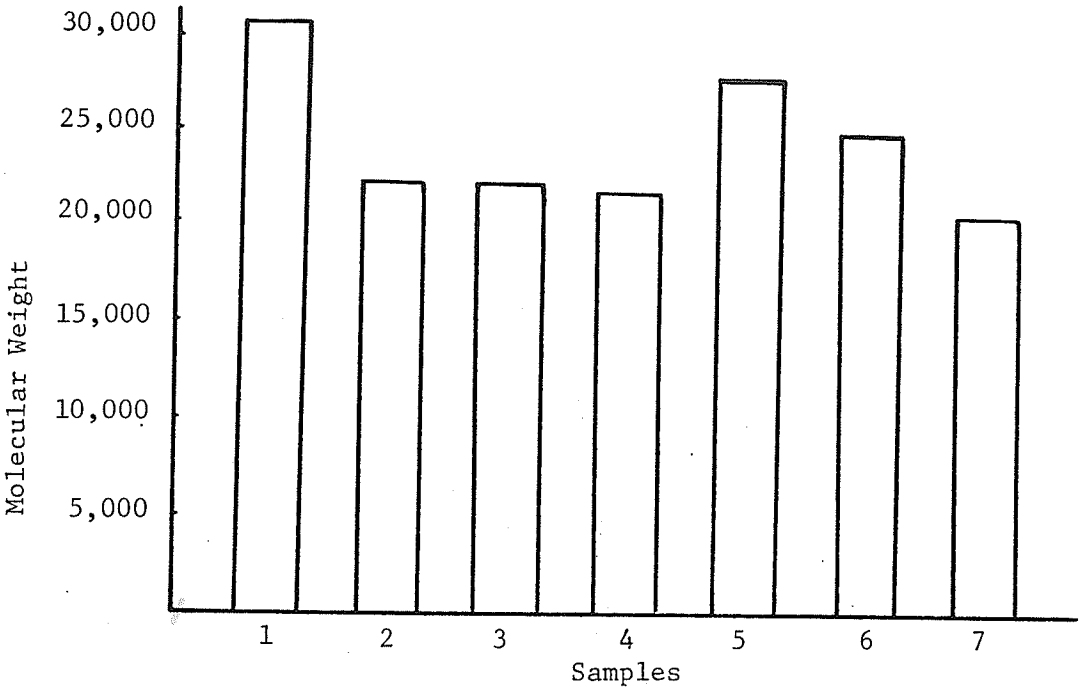

Figure 1. Molecular Weight for Each Sample

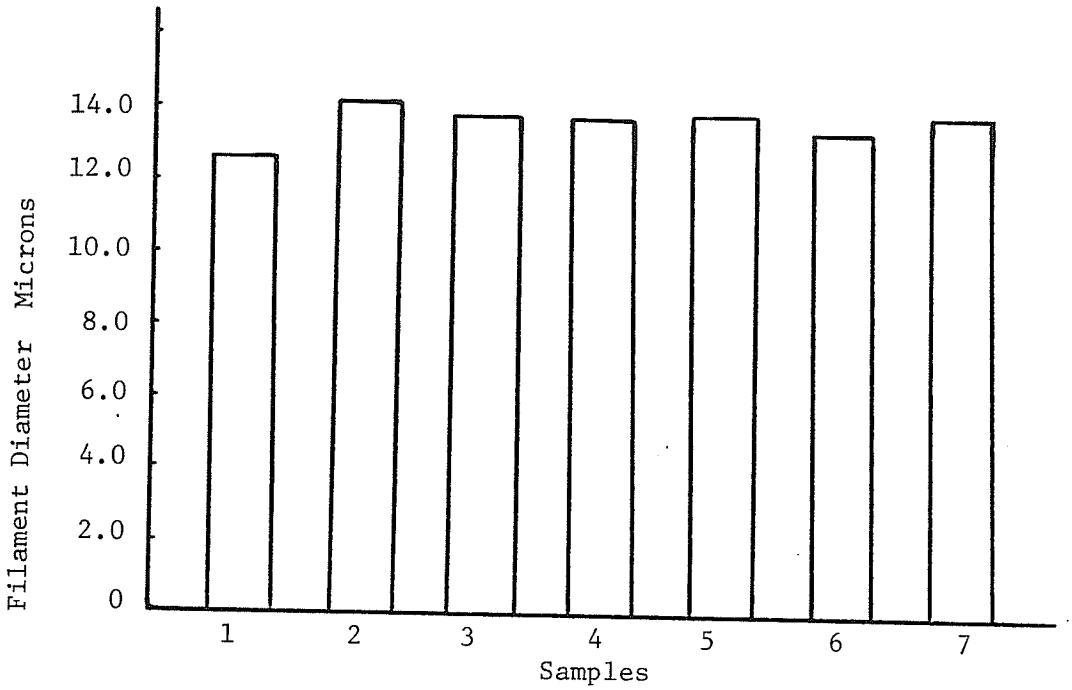

Figure 2. Sample Means for Filament Diameter

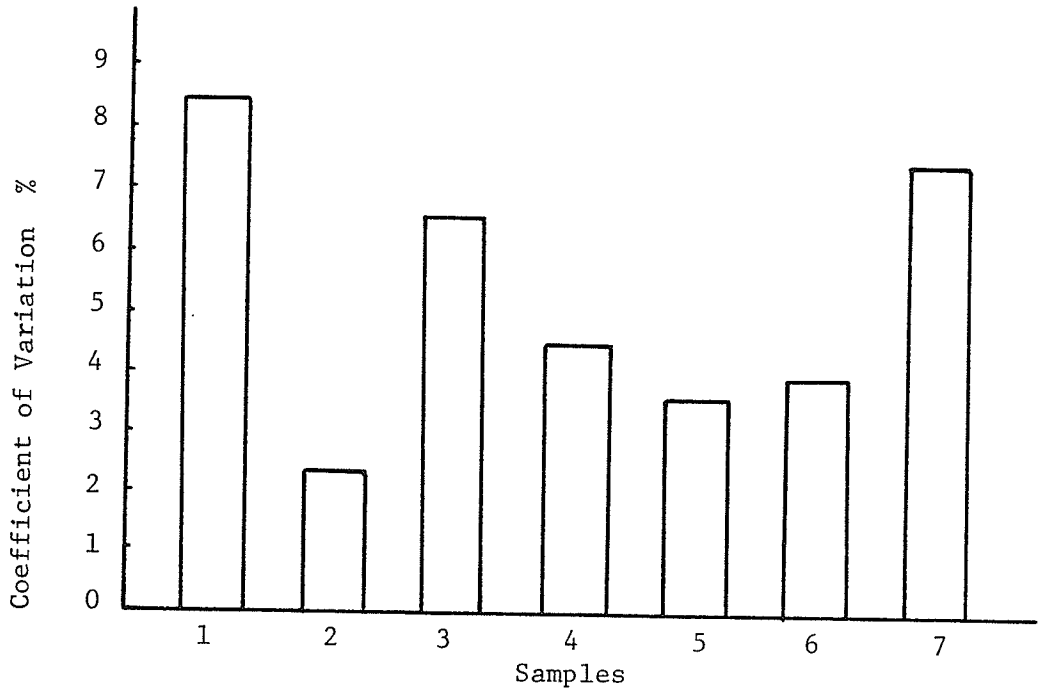

Figure 3. Sample Coefficients of Variation for Filament Diameter

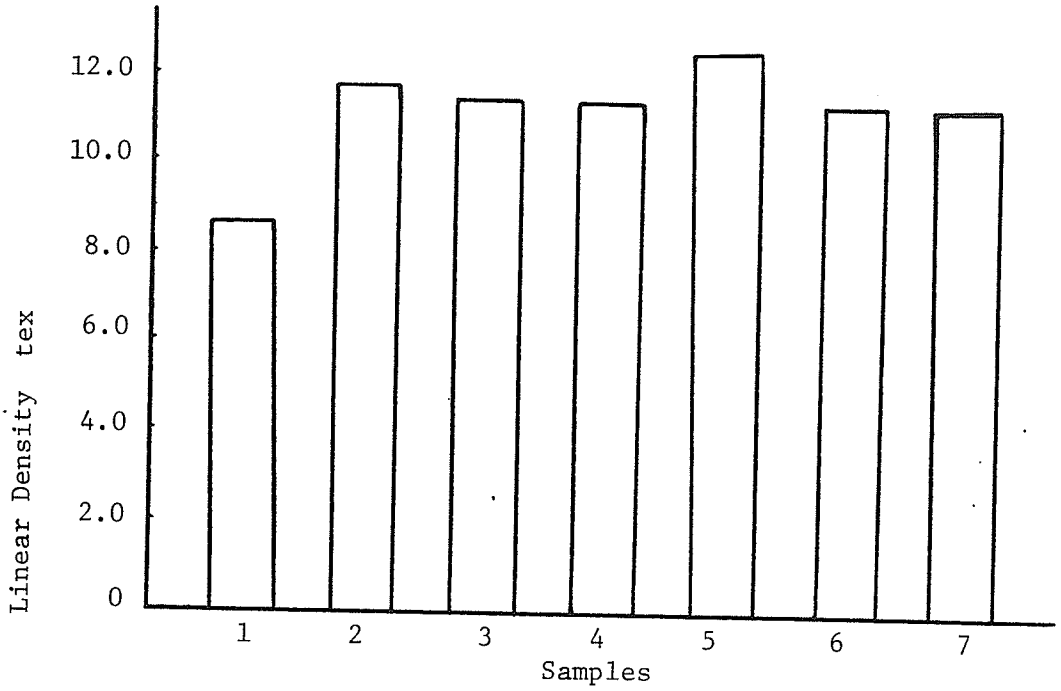

Figure 4. Sample Means for Linear Density

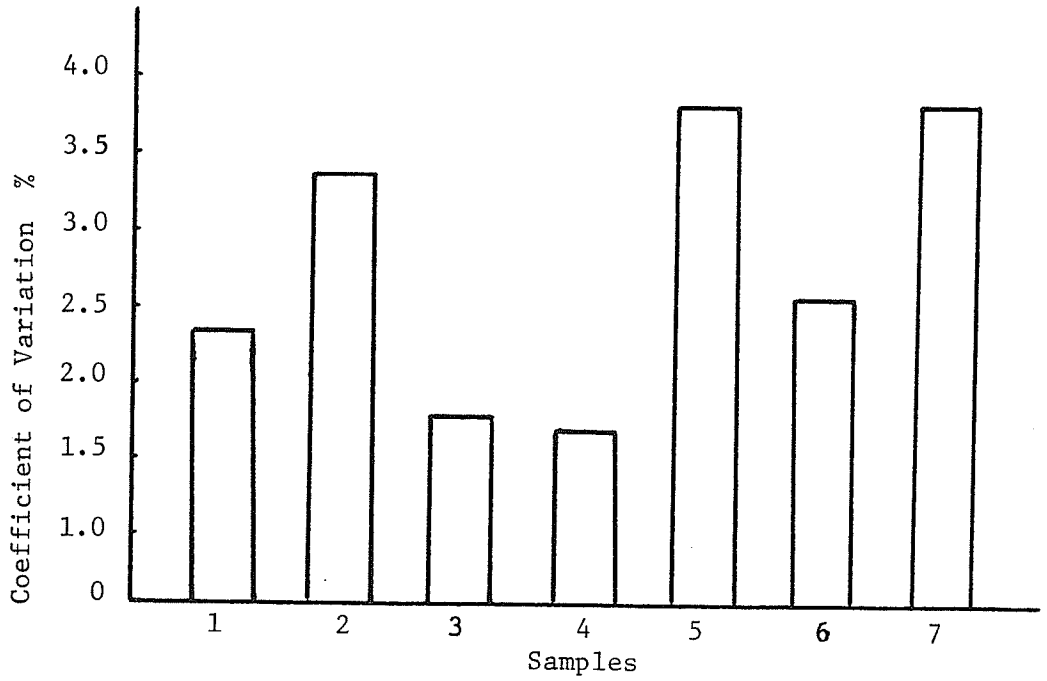

Figure 5. Sample Coefficients of Variation for Linear Density

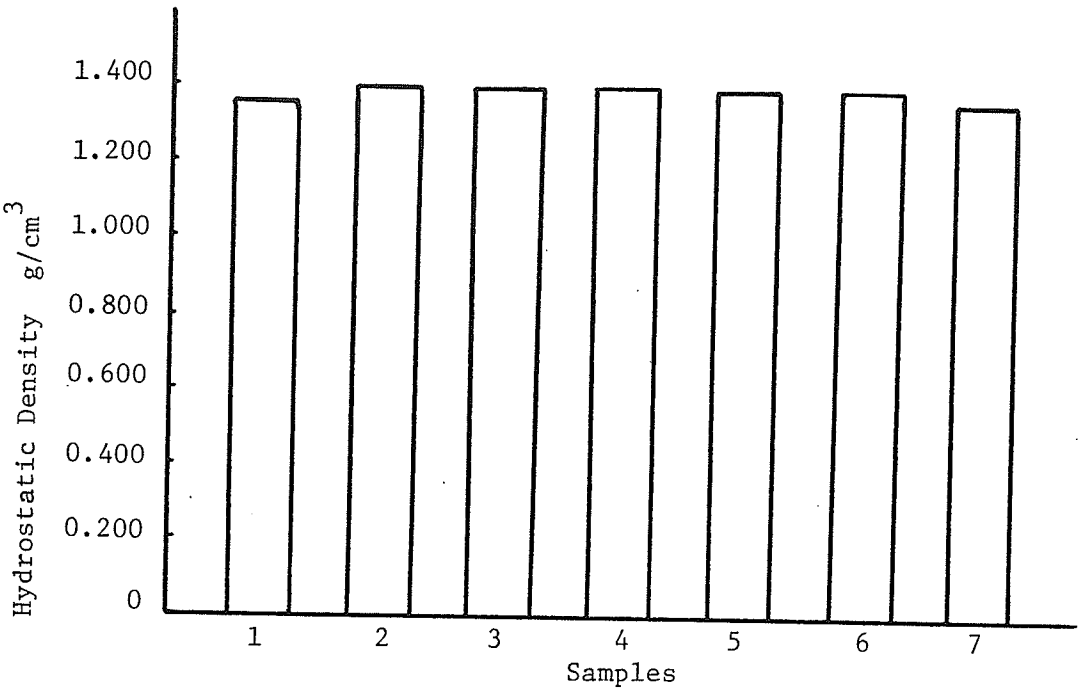

Figure 6. Hydrostatic Density for Each Sample

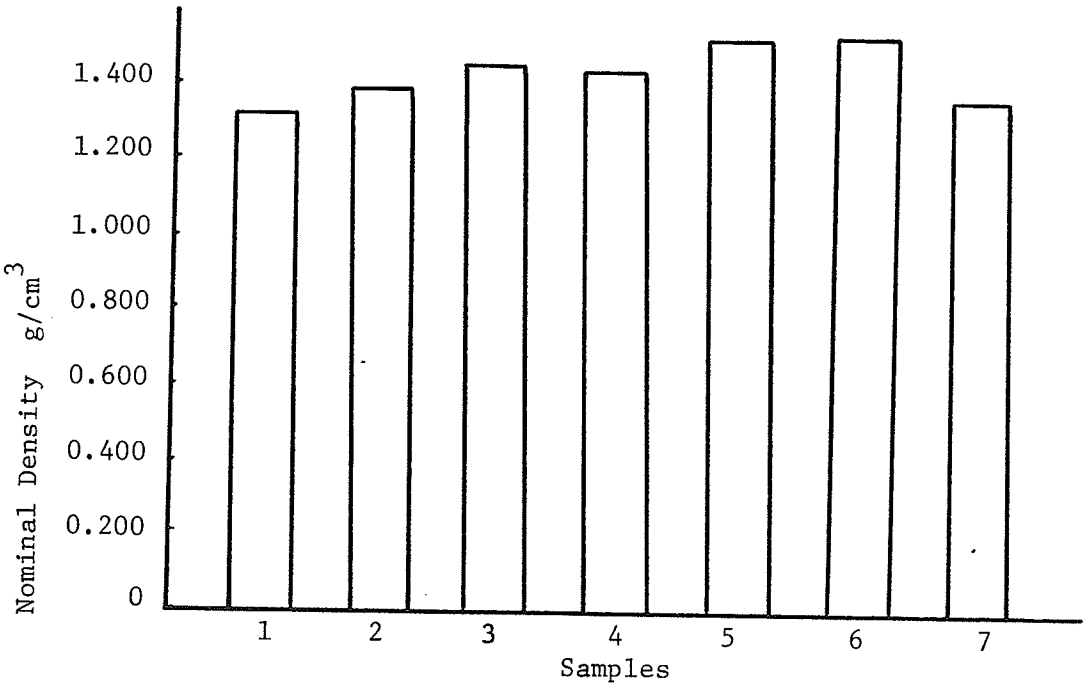

Figure 7. Nominal Density for Each Sample

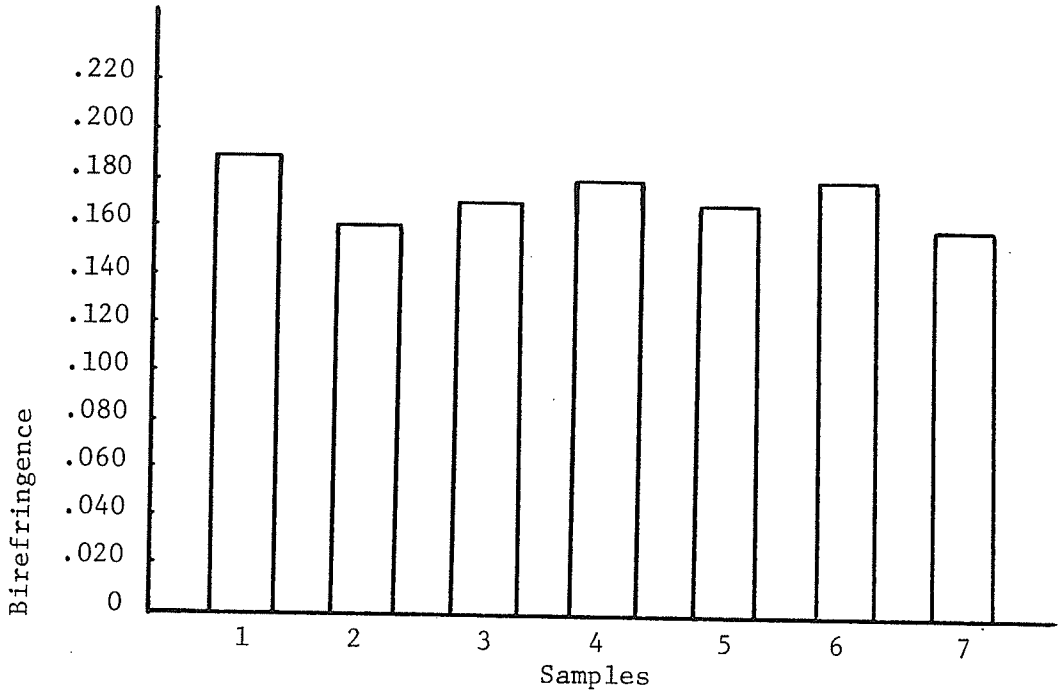

Figure 8. Sample Means for Birefringence

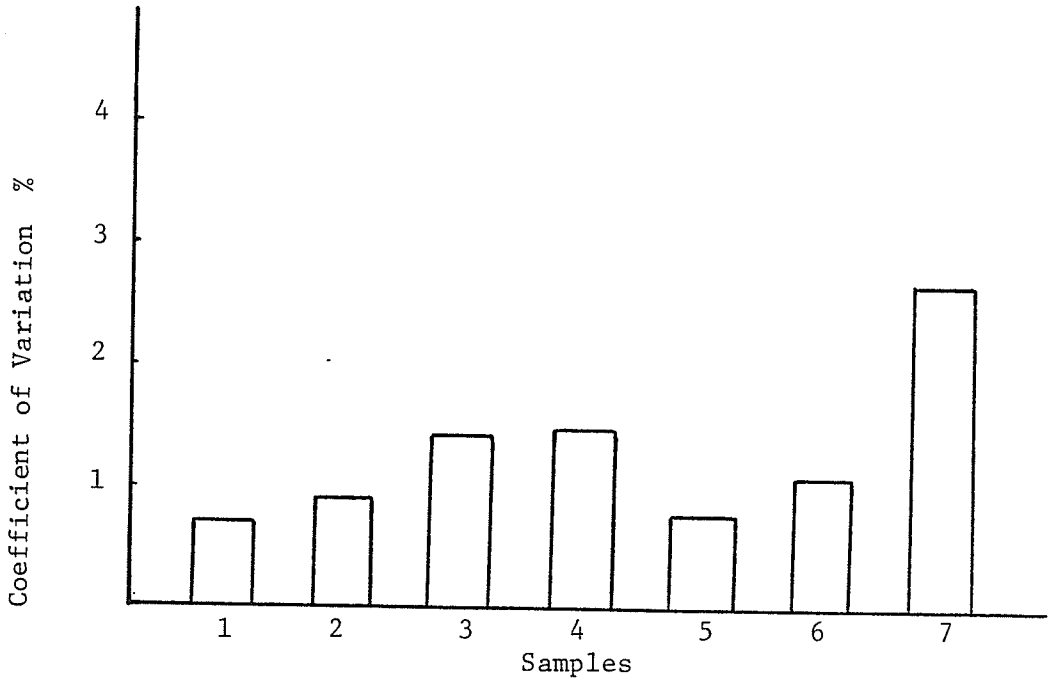

Figure 9. Sample Coefficients of Variation for Birefringence

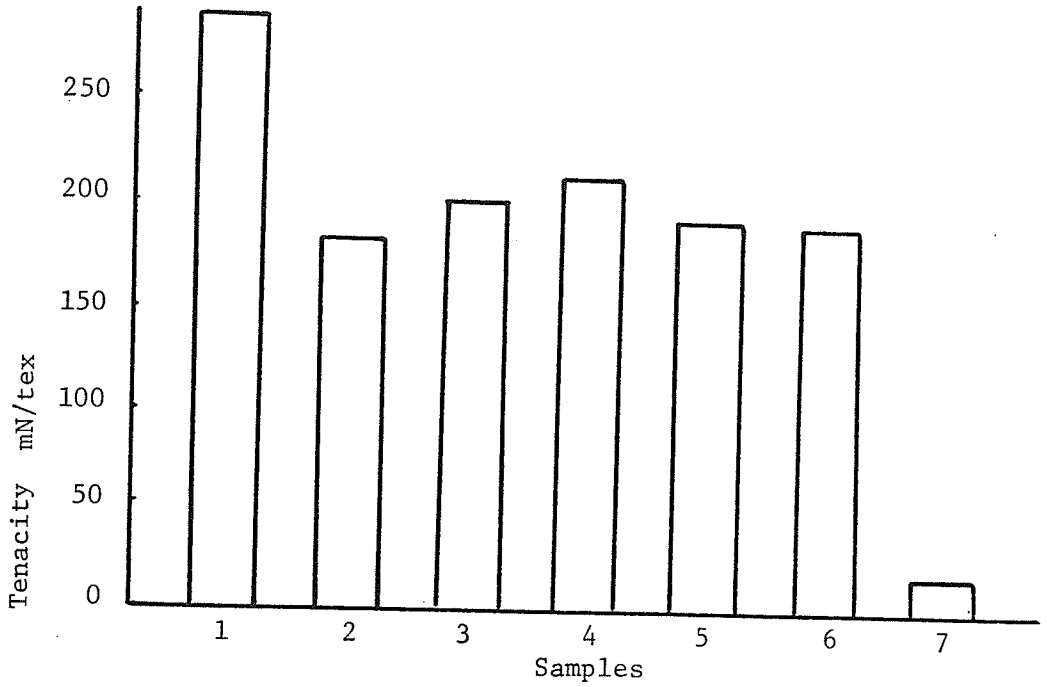

Figure 10. Sample Means for Tenacity

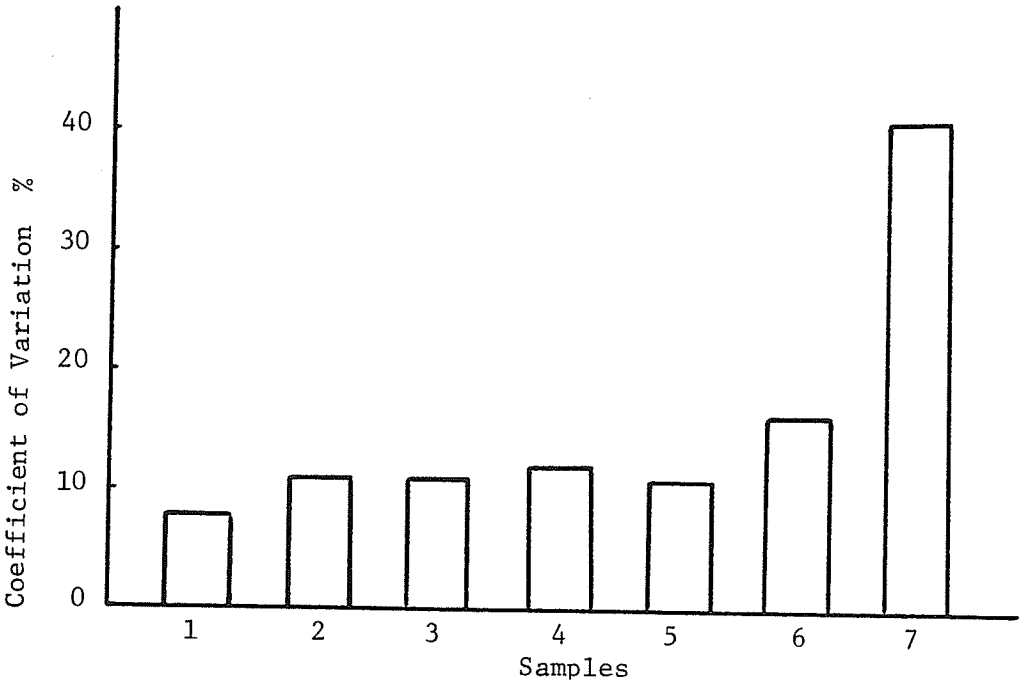

Figure 11. Sample Coefficient of Variation for Tenacity

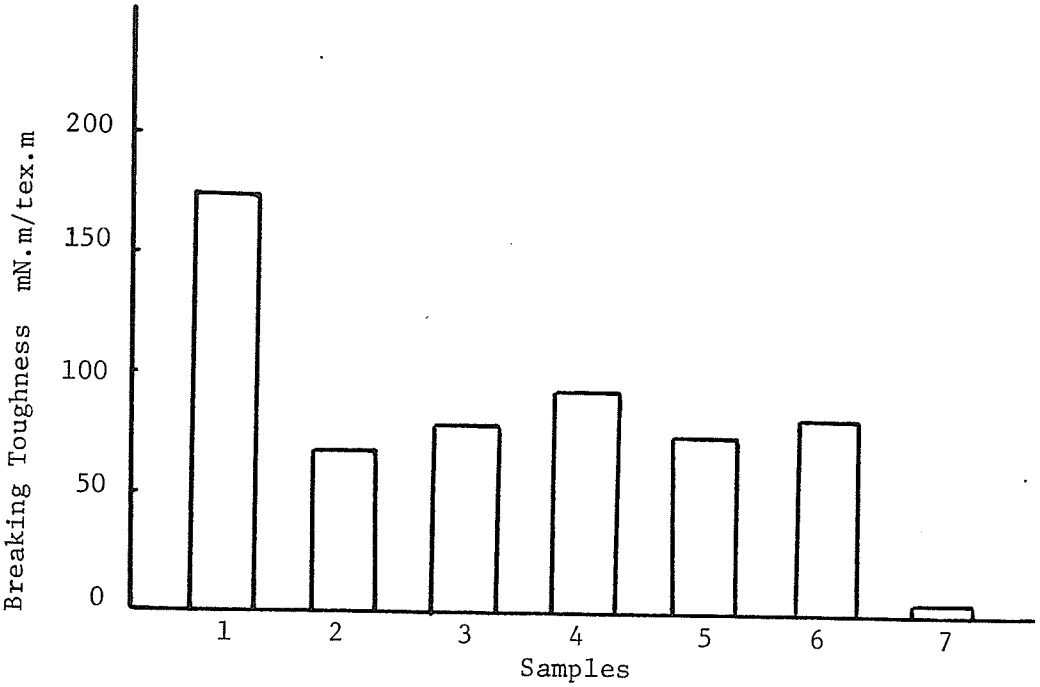

Figure 12. Sample Means for Breaking Toughness

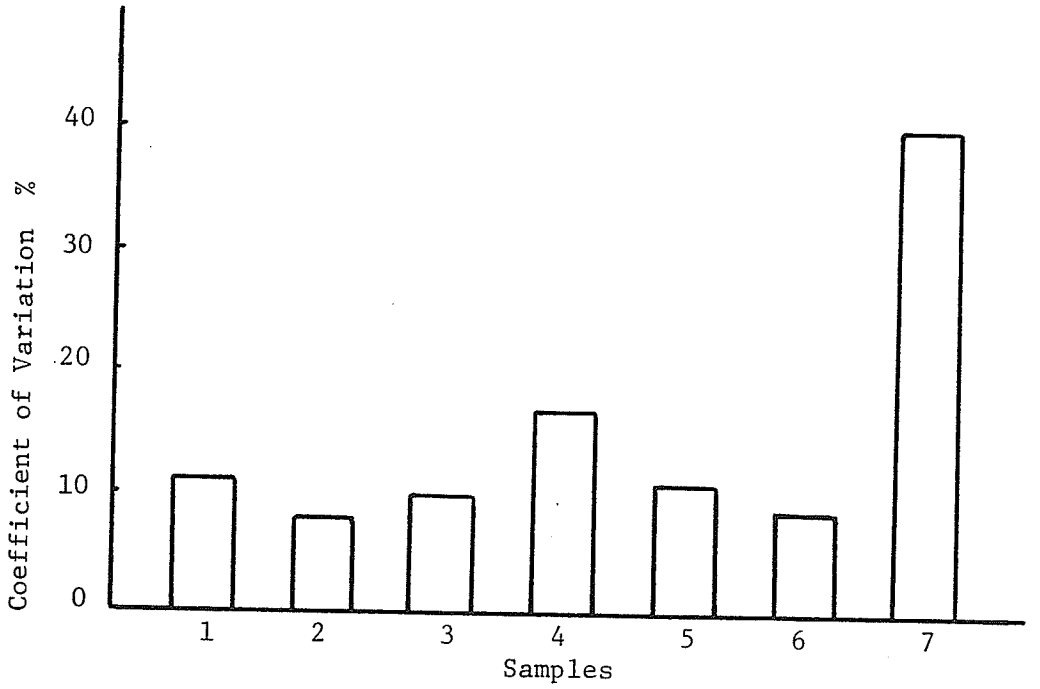

Figure 13. Sample Coefficients of Variation for Breaking Toughness

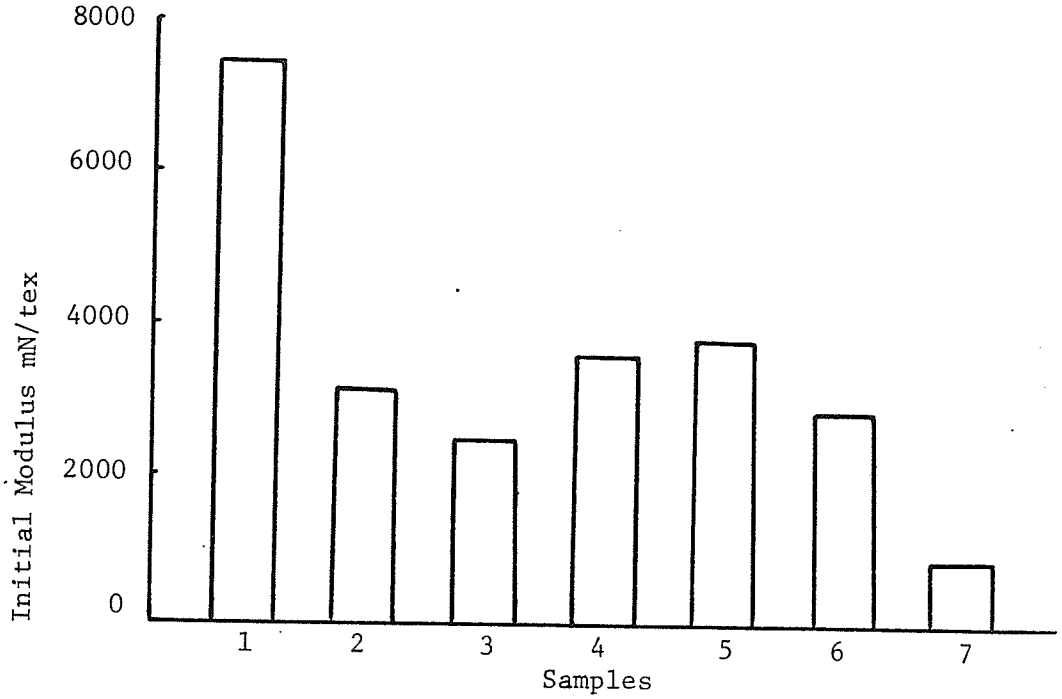

Figure 14. Sample Means for Initial Modulus

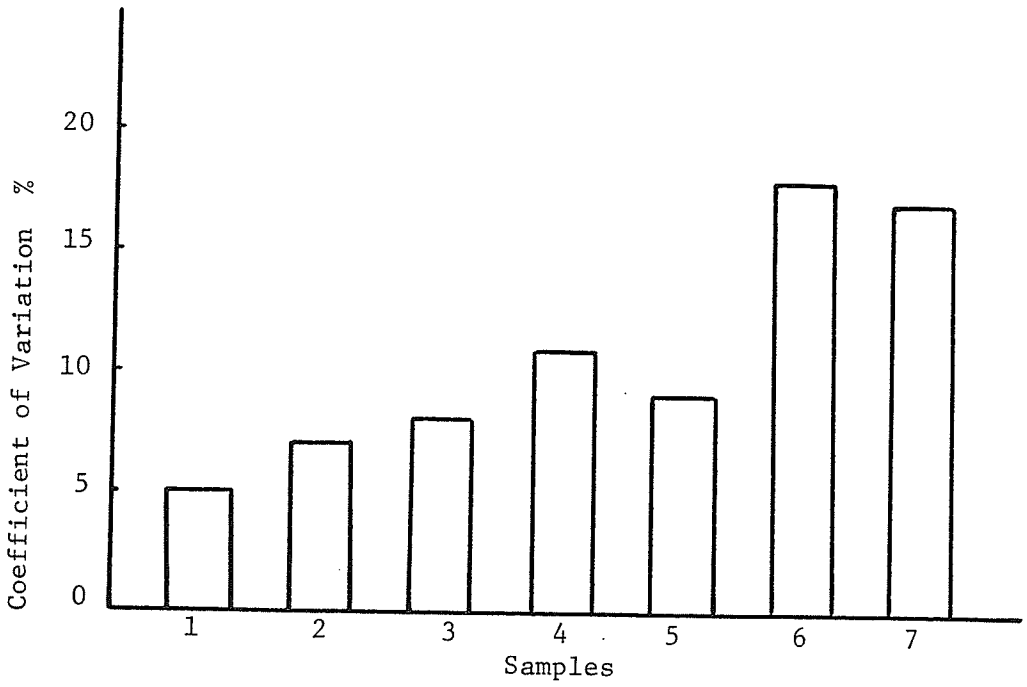

Figure 15. Sample Coefficient of Variation for Initial Modulus

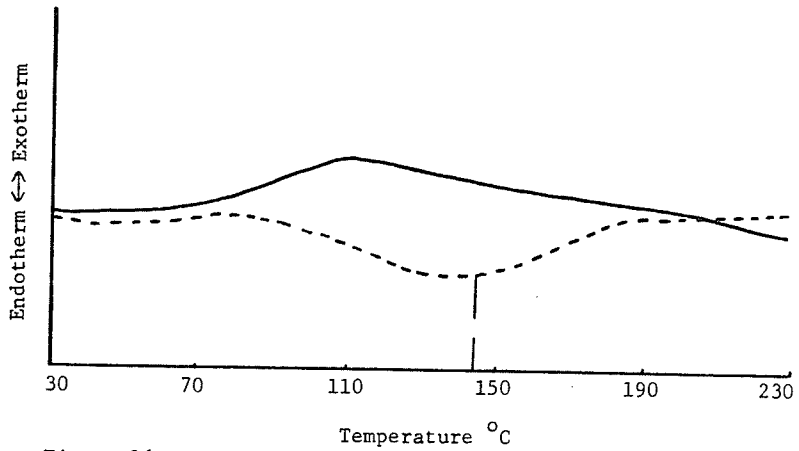

Figure 16. DSC Premelt Endotherm Peak--Effect of Compaction
——— Untreated yarn (sample one)
- - -Yarn compacted (sample two)

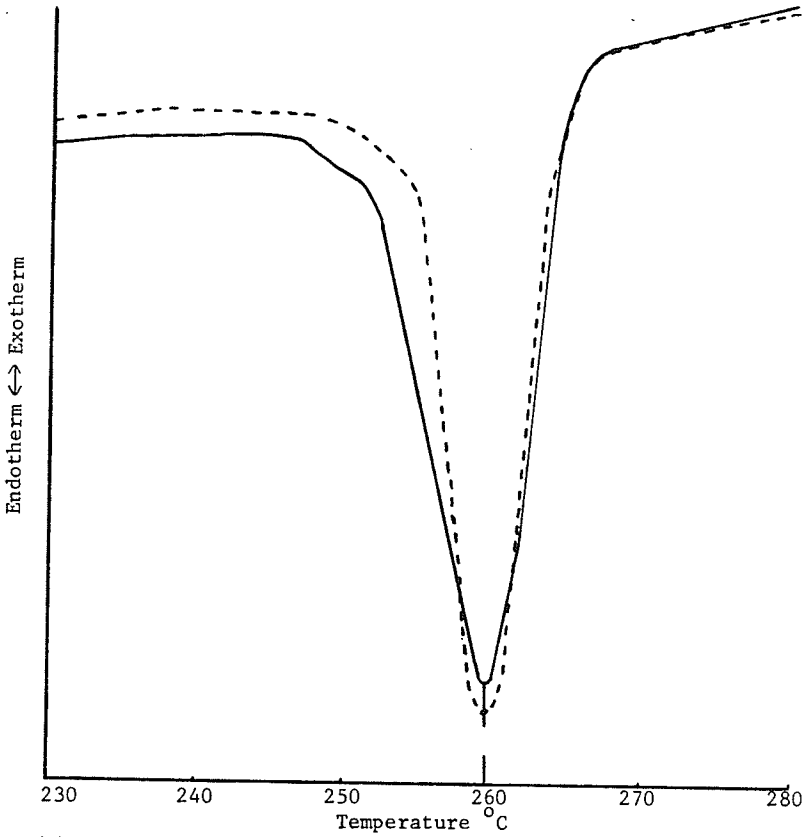

Figure 17. DSC Melt Peaks--Effect of Compaction
——— Untreated yarn (sample one)
- - - Yarn compacted (sample two)

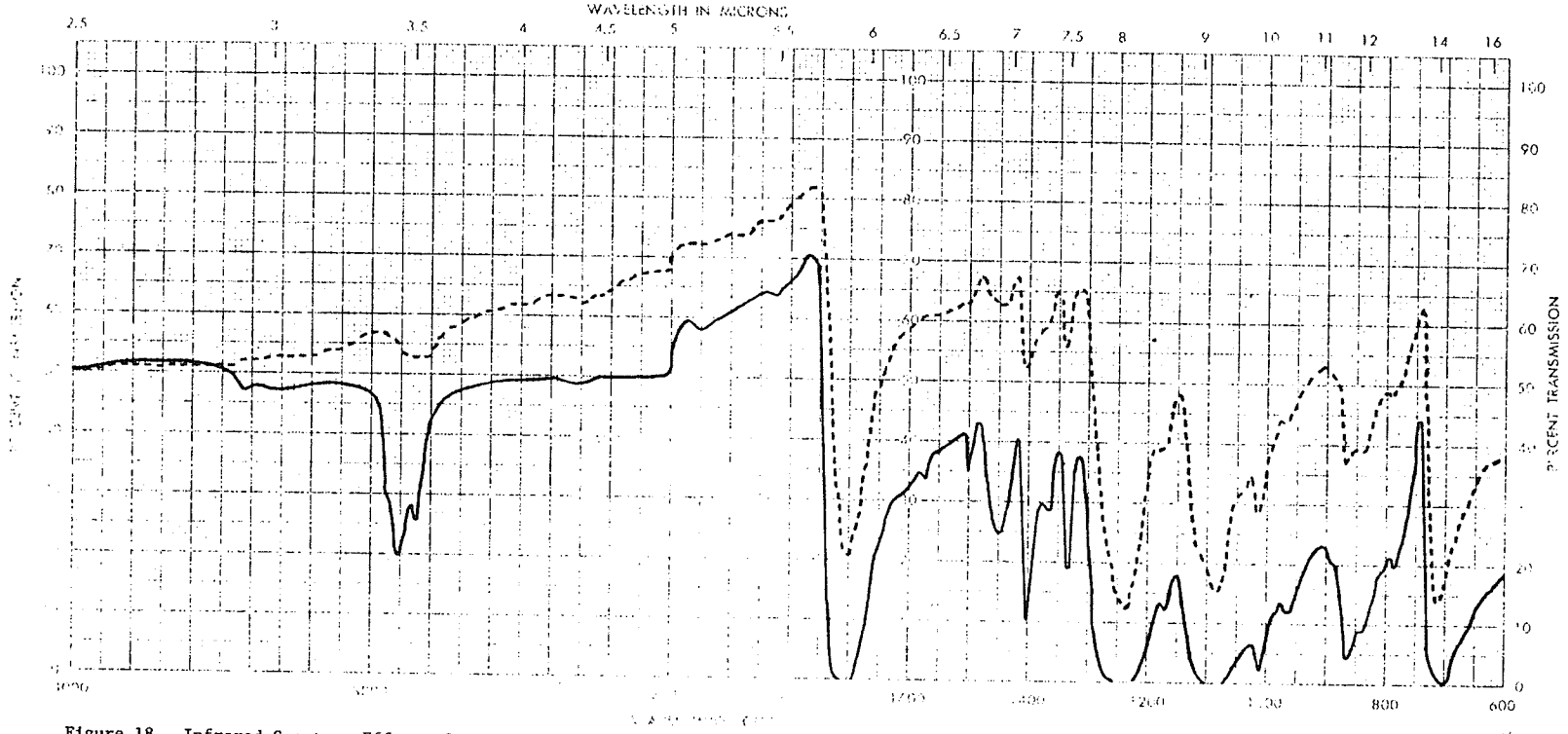

Figure 18. Infrared Spectra--Effect of Compaction
——— Untreated yarn (sample one)
- - - Yarn compacted (sample two)

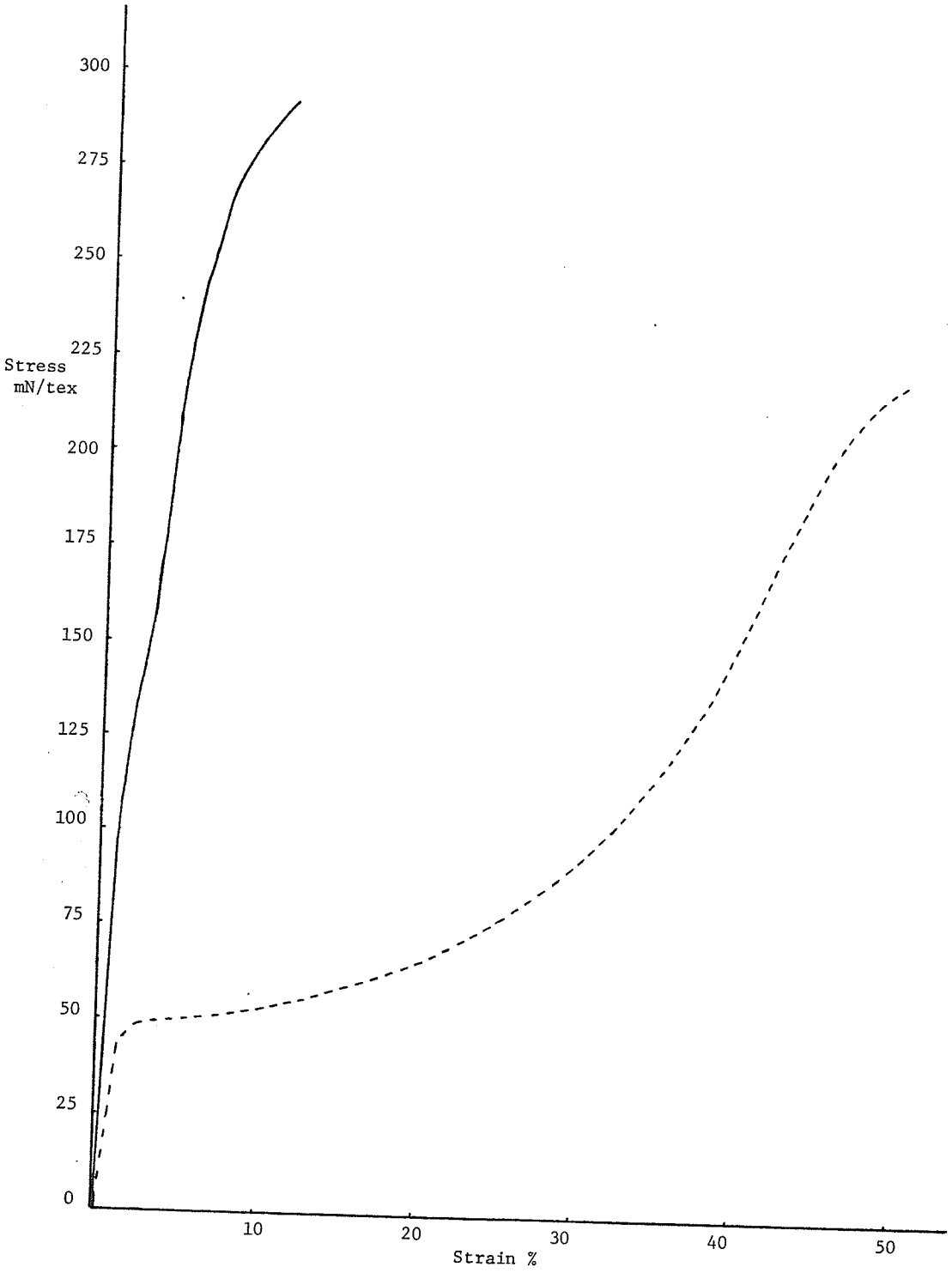

Figure 19. Stress-Strain Curves--Effect of Compaction
—— Untreated yarn (sample one)
--- Yarn compacted (sample two)

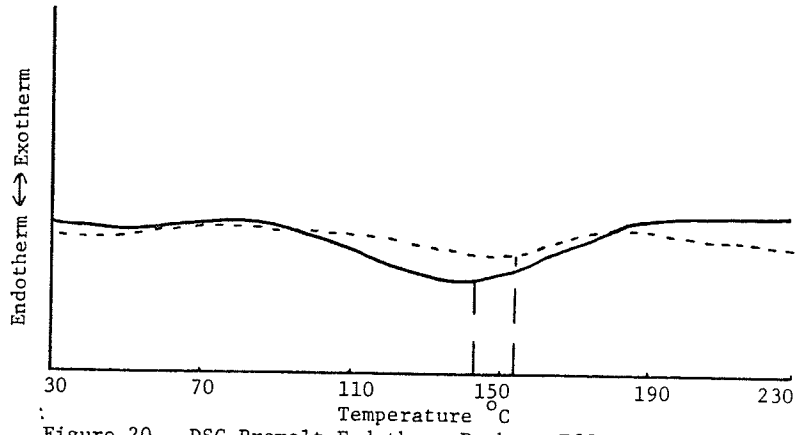

Figure 20. DSC Premelt Endotherm Peaks -- Effect of Crimping at 94°C
—— Compacted yarn (sample two)
--- Yarn compacted and crimped at 94°C (sample three)

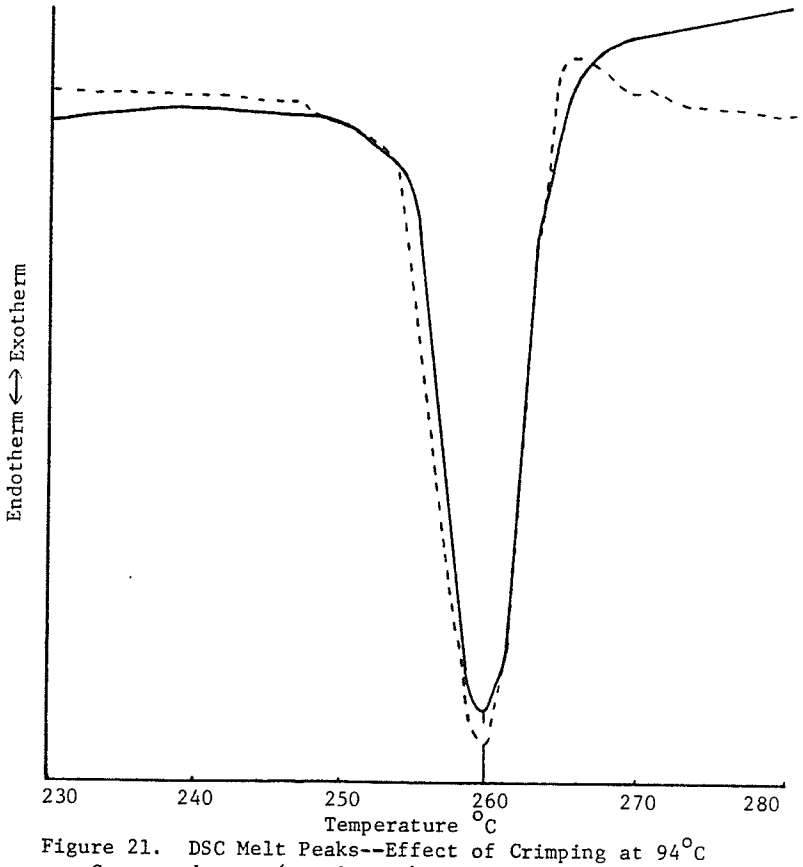

Figure 21. DSC Melt Peaks--Effect of Crimping at 94°C
—— Compacted yarn (sample two)
--- Yarn compacted and crimped at 94°C (sample three)

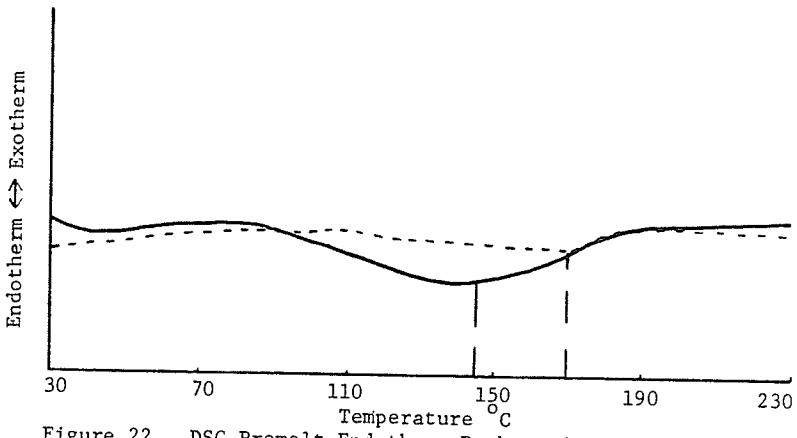

Figure 22. DSC Premelt Endotherm Peaks--Effect of Crimping at 154°C
—— Compacted yarn (sample two)
--- Yarn compacted and crimped at 154°C (sample four)

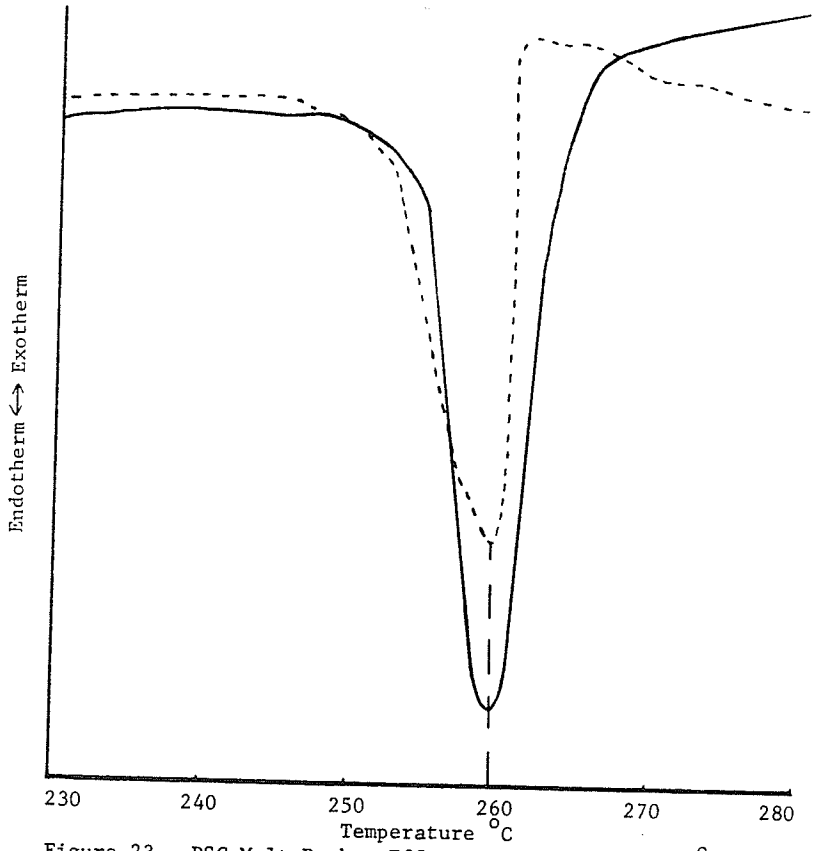

Figure 23. DSC Melt Peaks--Effect of Crimping at 154°C
—— Compacted yarn (sample two)
--- Yarn compacted and crimped at 154°C (sample four)

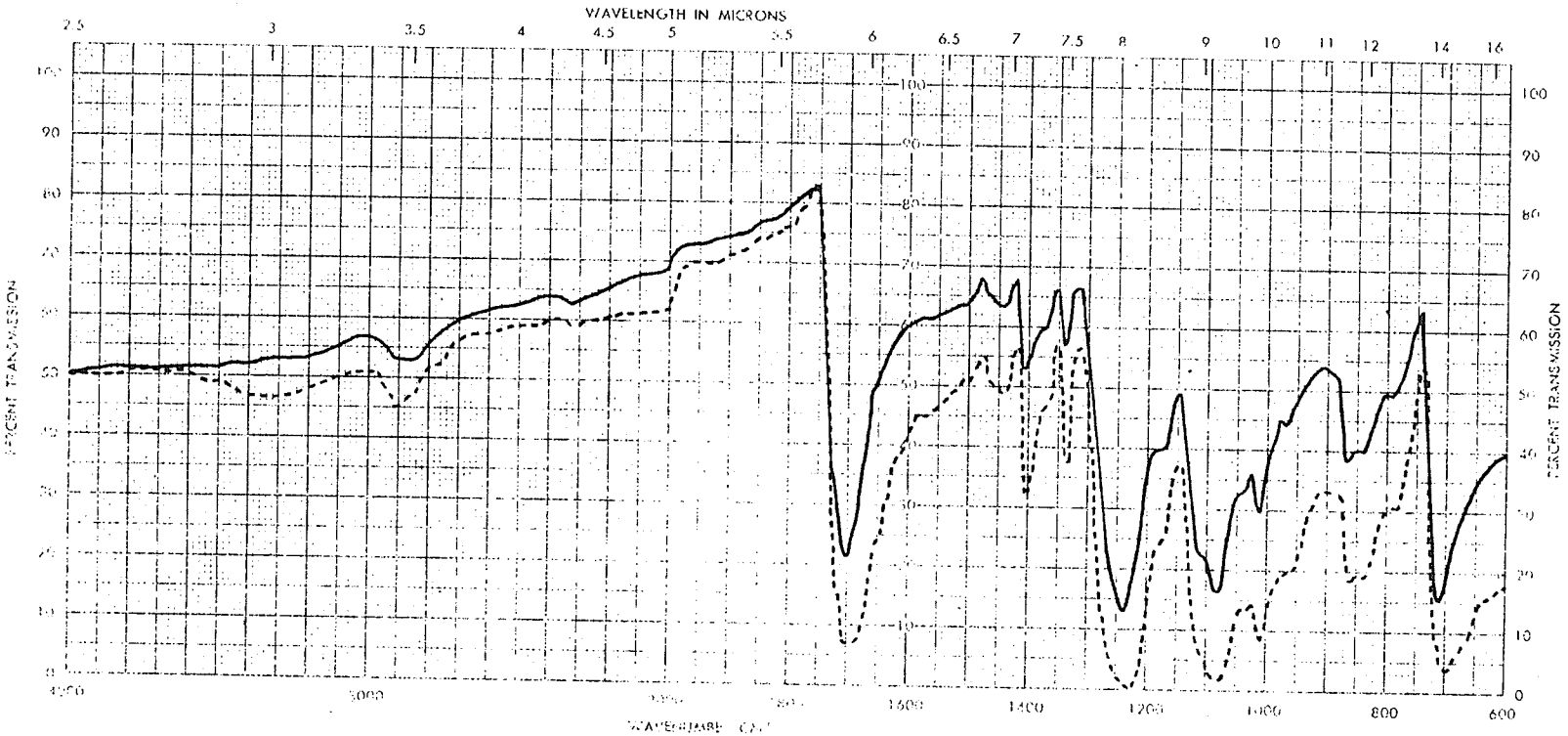

Figure 24. Infrared Spectra--Effect of Crimping at 94°C
—— Yarn compacted (sample two)
--- Yarn compacted and crimped at 94°C (sample three)

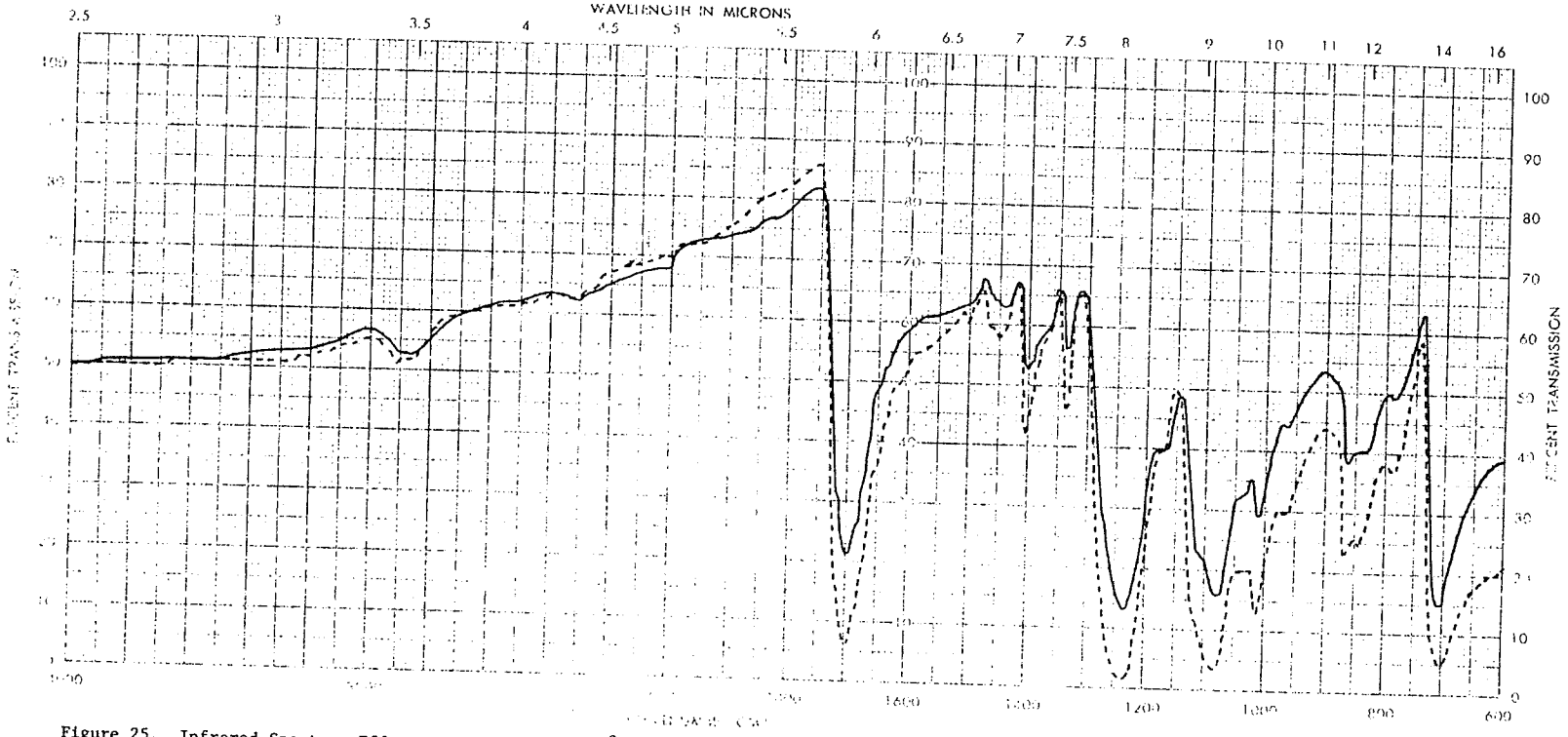

Figure 25. Infrared Spectra--Effect of Crimping at 154°C
—— Yarn compacted(sample two)
--- Yarn compacted and crimped at 154°C(sample four)

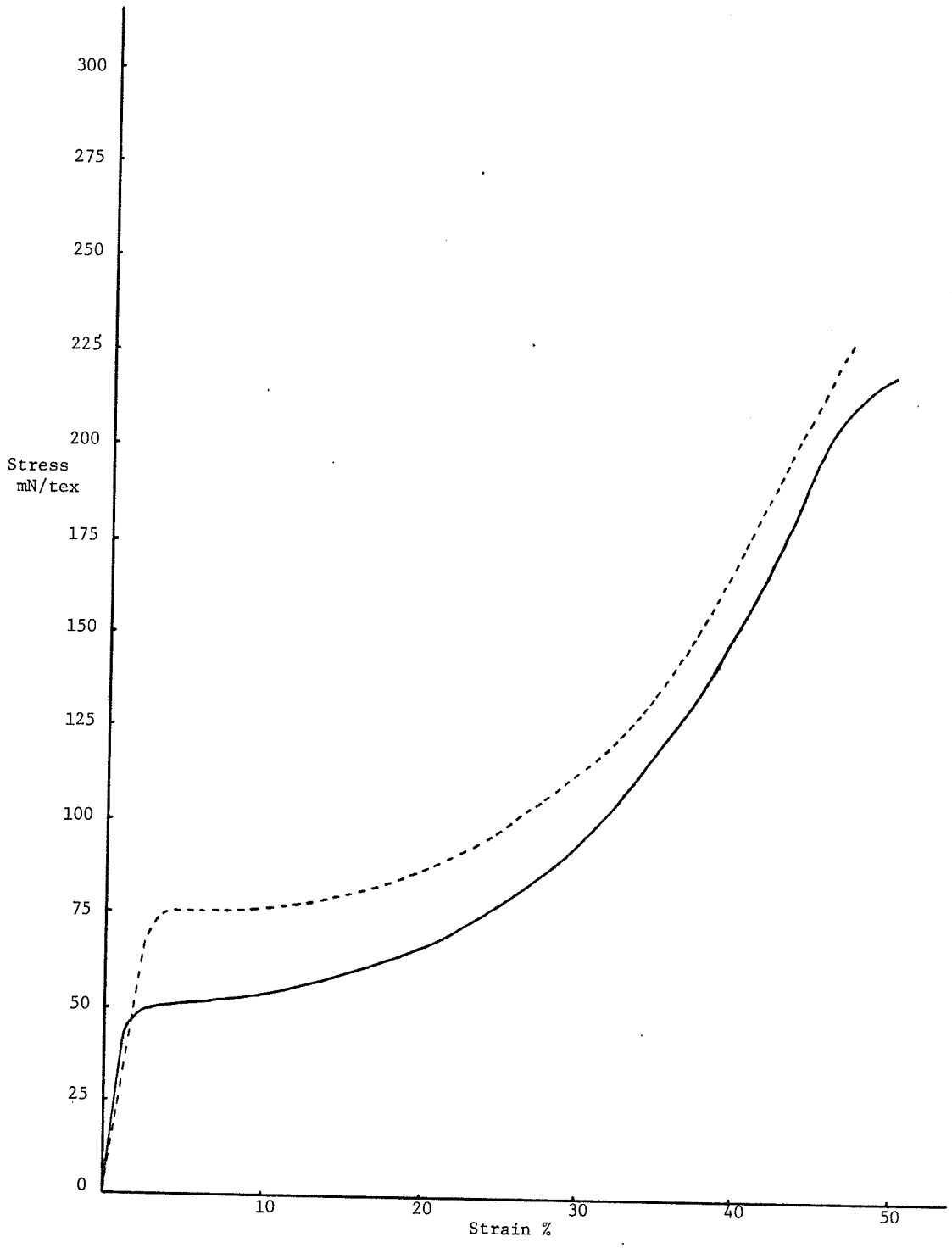

Figure 26. Stress-Strain Curves--Effect of Crimping at 94°C
—— Yarn compacted (sample two)
--- Yarn compacted and crimped at 94°C (sample three)

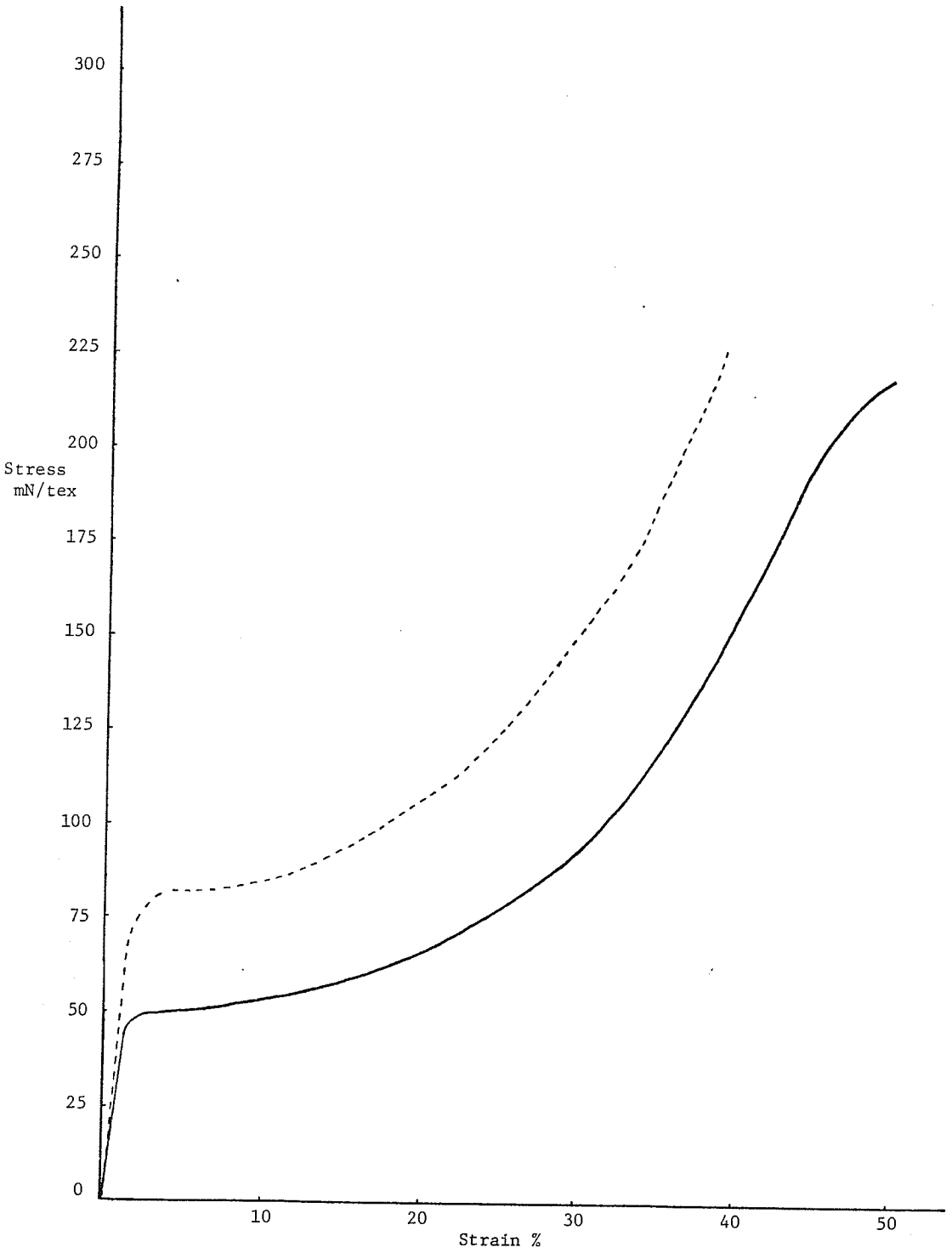

Figure 27. Stress-Strain Curves--Effect of Crimping at 154°C
—— Yarn compacted (sample two)
--- Yarn compacted and crimped at 154°C (sample four)

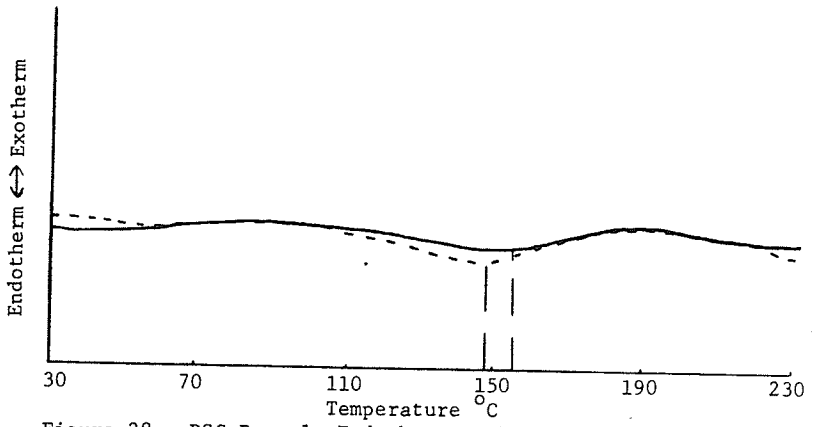

Figure 28. DSC Premelt Endotherm Peaks--Effect of Sterilization on the PET Yarn Crimped at 94°C.
—— Yarn compacted and crimped at 94°C (sample three)
--- Yarn compacted, crimped at 94°C and sterilized (sample five)

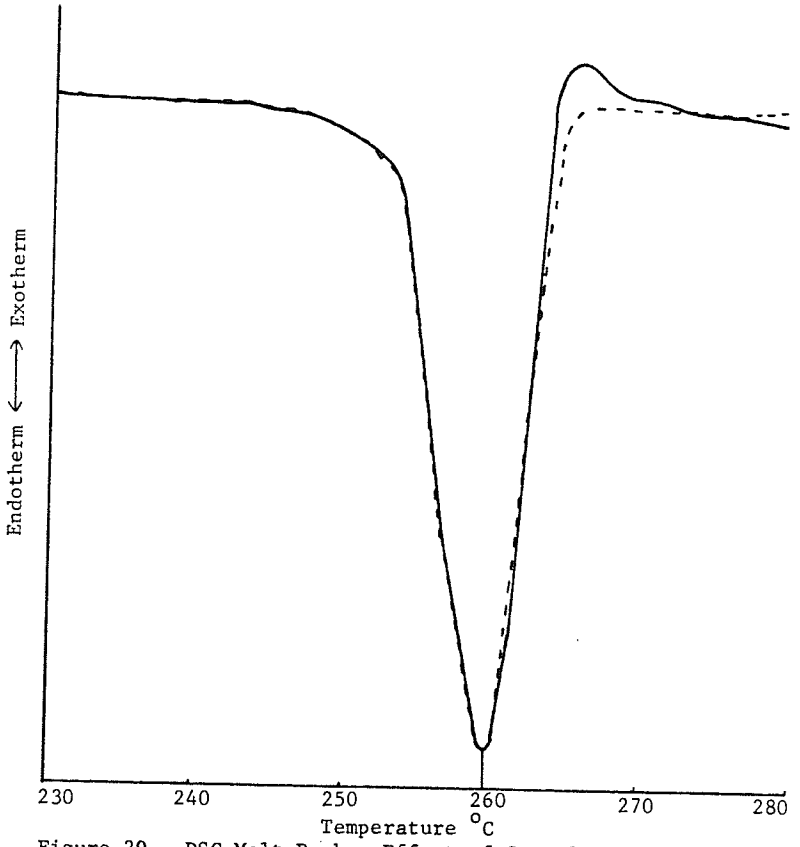

Figure 29. DSC Melt Peaks--Effect of Sterilization on the PET Yarn Crimped at 94°C
—— Yarn compacted and crimped at 94°C (sample three)
--- Yarn compacted, crimped at 94°C and sterilized (sample five)

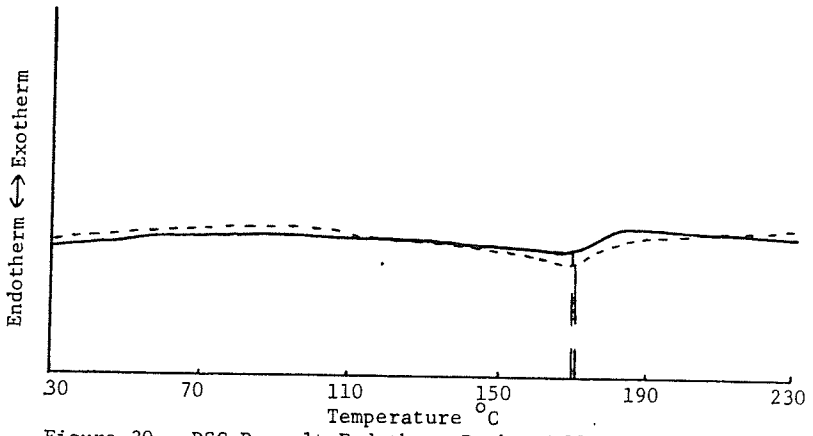

Figure 30. DSC Premelt Endotherm Peaks--Effect of Sterilization on the PET Yarn Crimped at 154°C.
—— Yarn compacted and crimped at 154°C (sample four)
--- Yarn compacted, crimped at 154°C and sterilized (sample six)

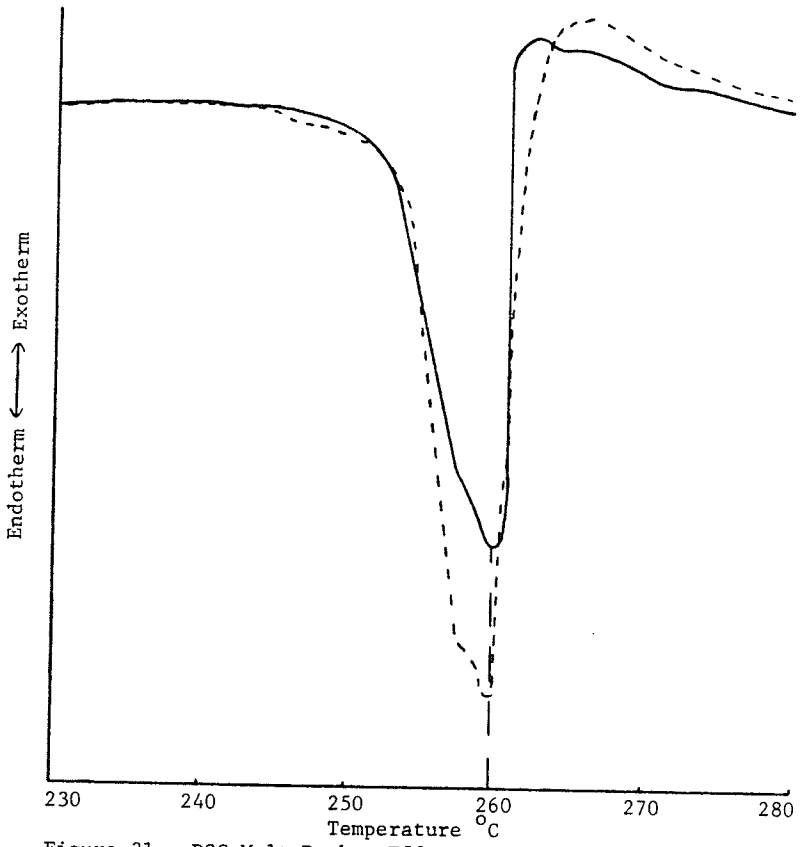

Figure 31. DSC Melt Peaks--Effect of Sterilization on the PET Yarn Crimped at 154°C
—— Yarn compacted and crimped at 154°C (sample four)
--- Yarn compacted, crimped at 154°C and sterilized (sample six)

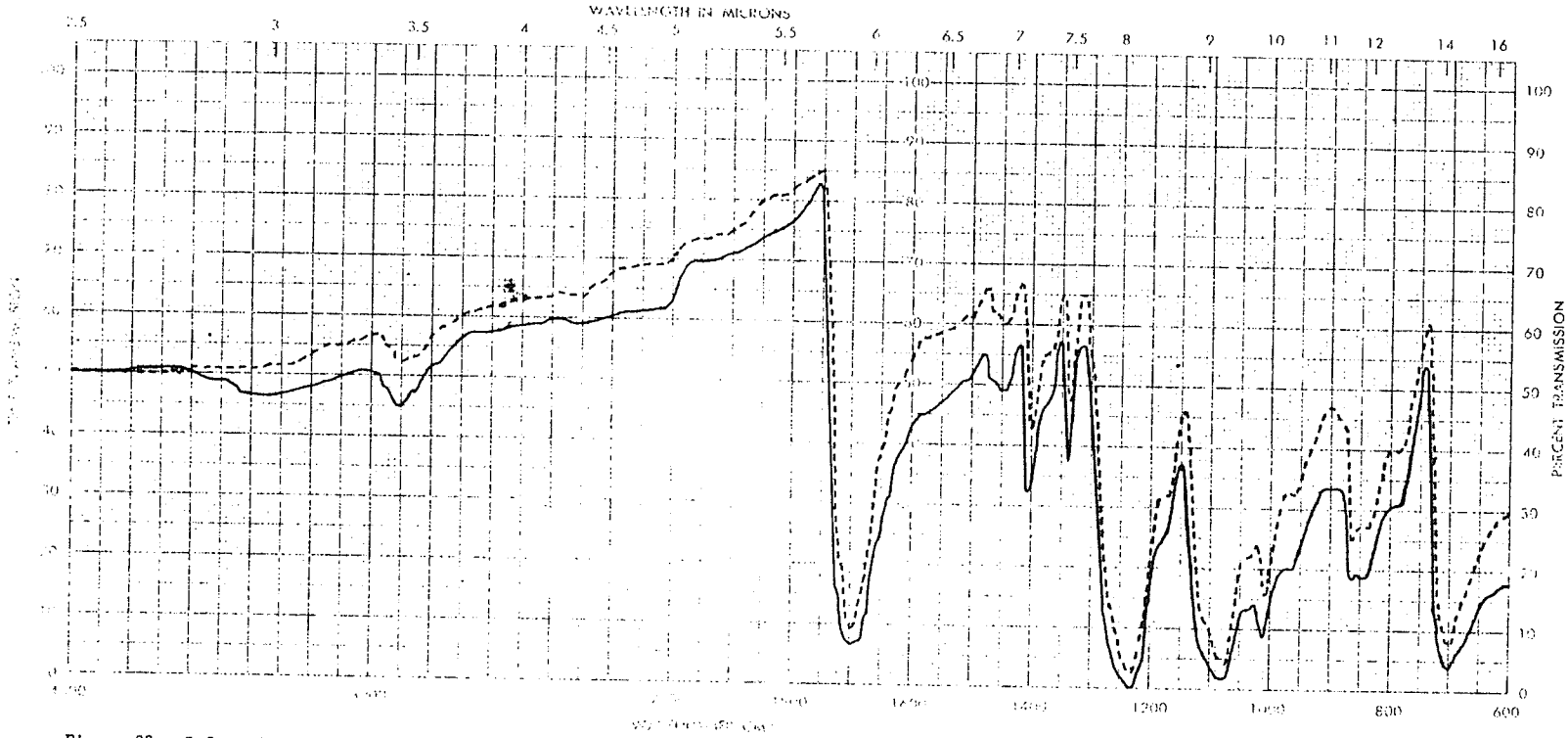

Figure 32. Infrared Spectra--Effect of Sterilization on the Pet Yarn Crimped at 94°C
—— Yarn compacted and crimped at 94°C(sample three)
--- Yarn compacted, crimped at 94°C and sterilized(sample five)

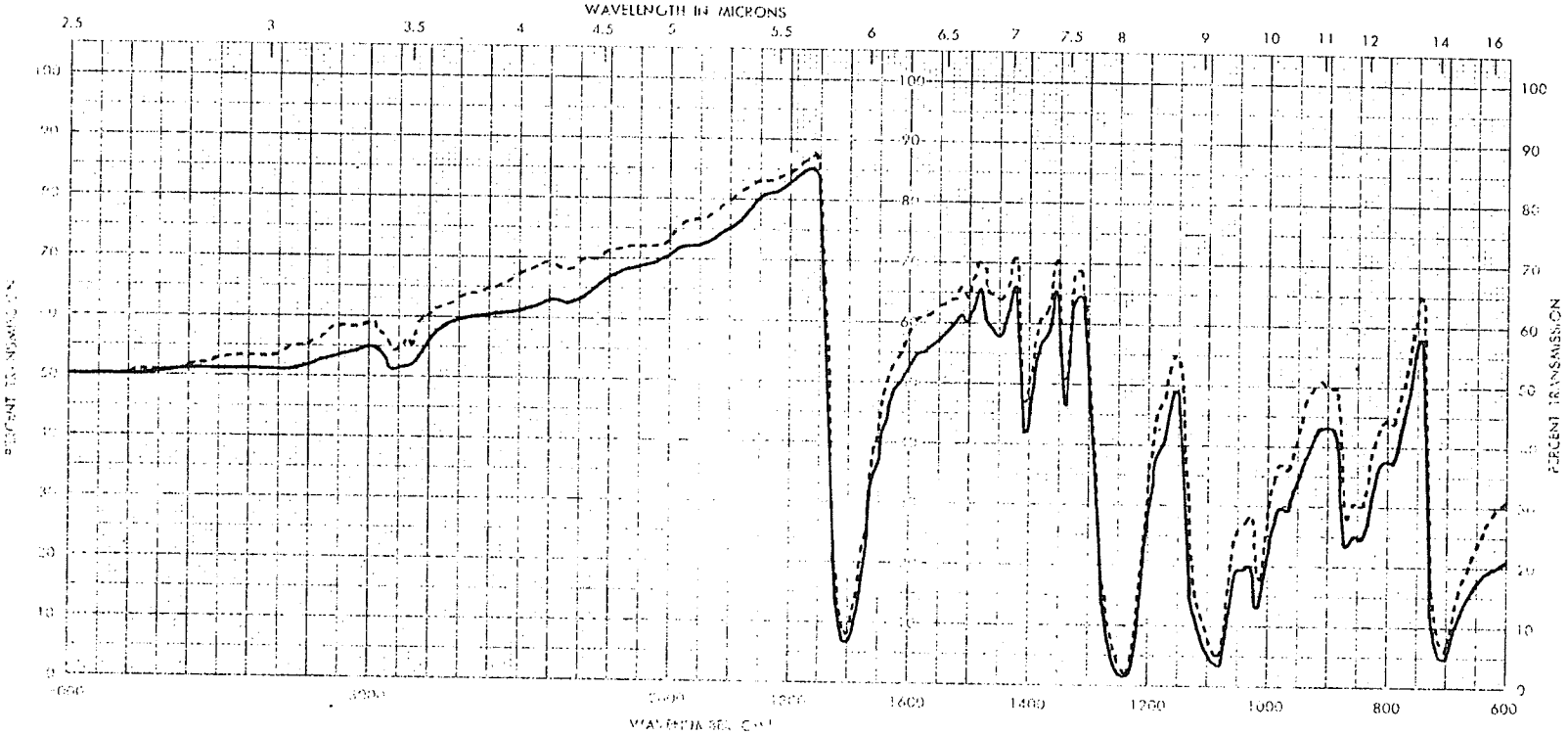

Figure 33. Infrared Spectra--Effect of Sterilization on the PET Yarn Crimped at 154°C
—— Yarn compacted and crimped at 154°C(sample four)
--- Yarn Compacted, crimped at 154°C and sterilized(sample six)

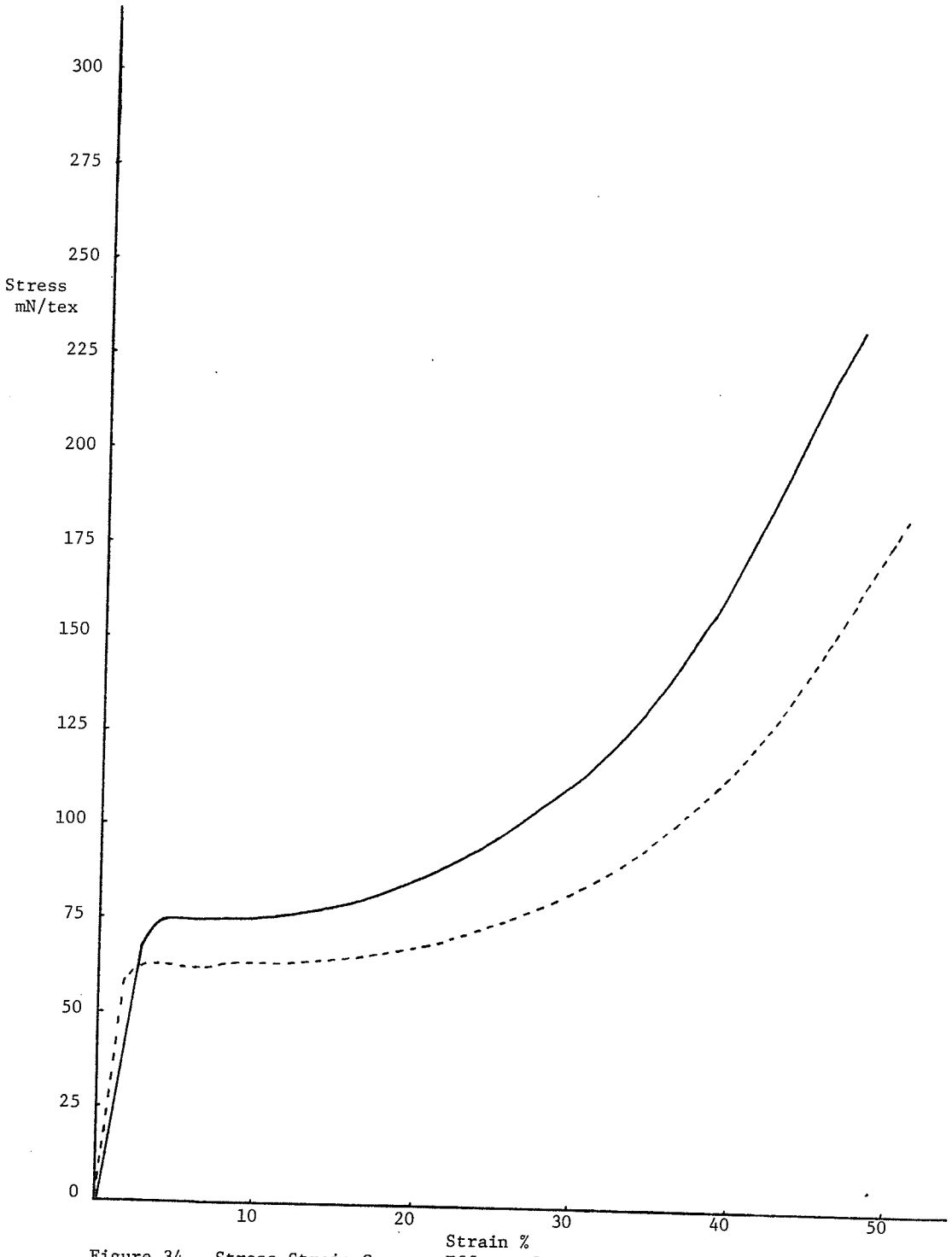

Figure 34. Stress-Strain Curves--Effect of Sterilization on the PET Yarn Crimped at 94°C

—— Yarn compacted and crimped at 94°C (sample three)

--- Yarn compacted, crimped at 94°C and sterilized (sample five)

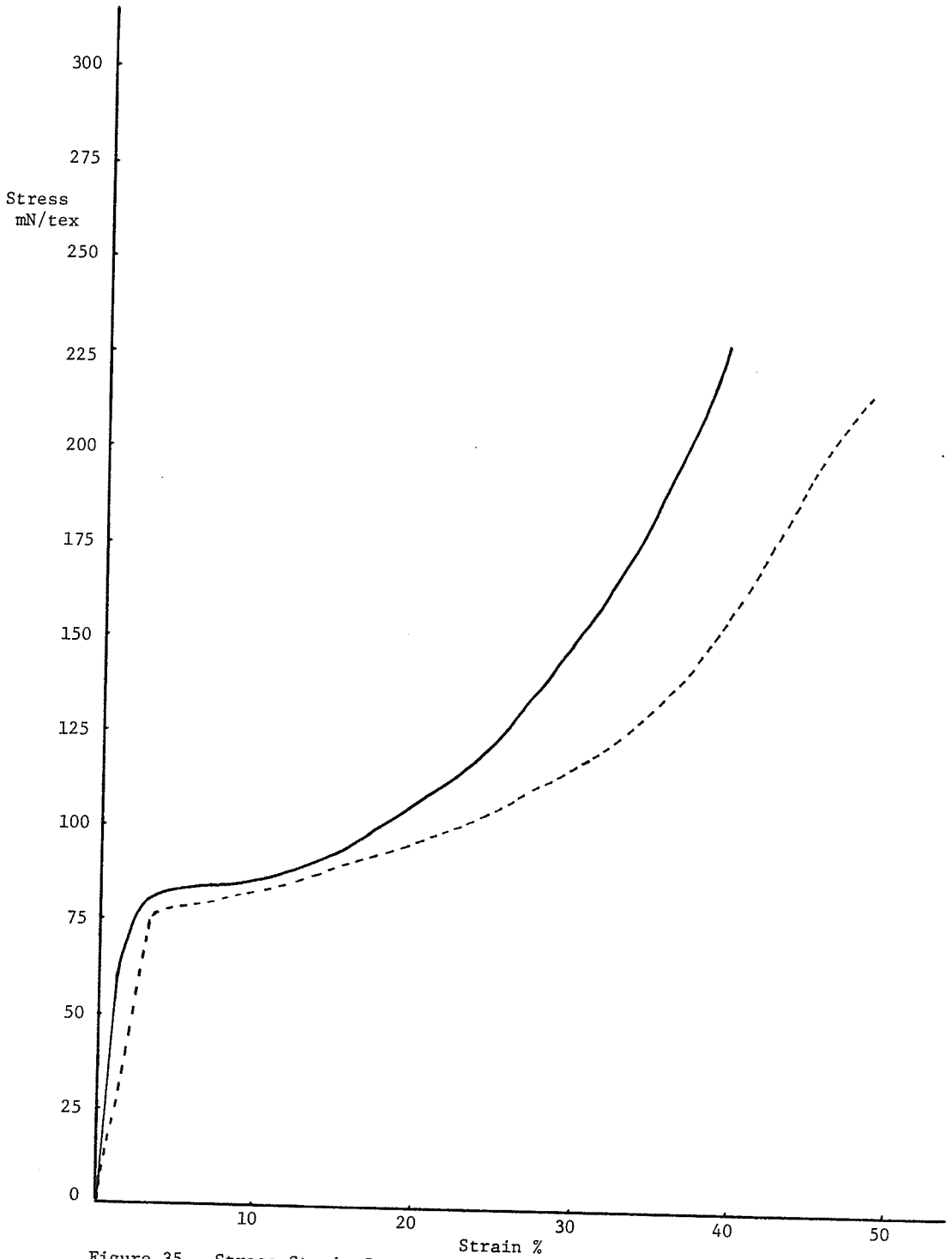

Figure 35. Stress-Strain Curves--Effect of Sterilization on the PET Yarn Crimped at 154°C

—— Yarn compacted and crimped at 154°C (sample four)

--- Yarn compacted, crimped at 154°C and sterilized (sample six)

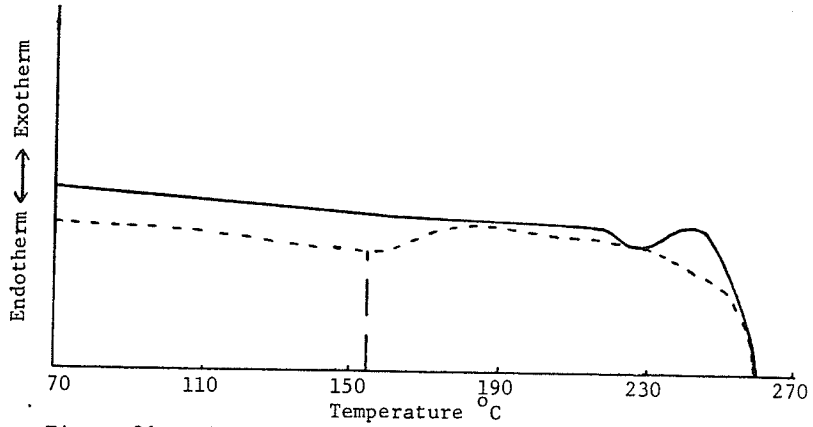

Figure 36. DSC Premelt Endotherm Peak--Commercial Reference Comparison to the PET Yarn Crimped at 94°C
—— Yarn from the Millikni® graft (sample seven)
--- Yarn compacted and crimped at 94°C (sample three)

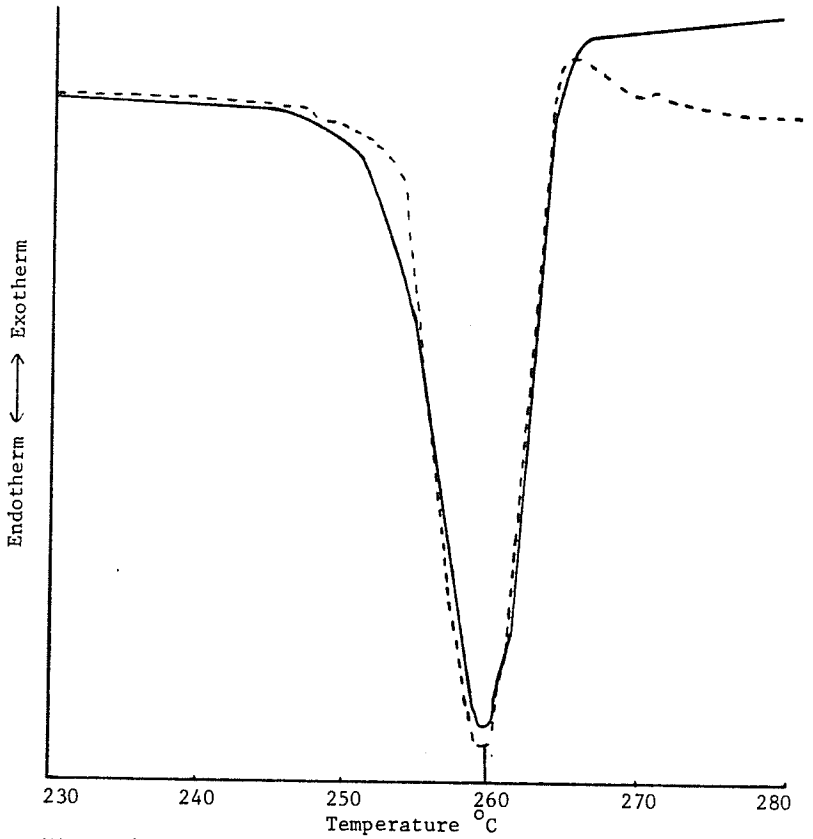

Figure 37. DSC Melt Peak--Commercial Reference Comparison to the PET Yarn Crimped at 94°C
—— Yarn from the Millikni® graft (sample seven)
--- Yarn compacted and crimped at 94°C (sample three)

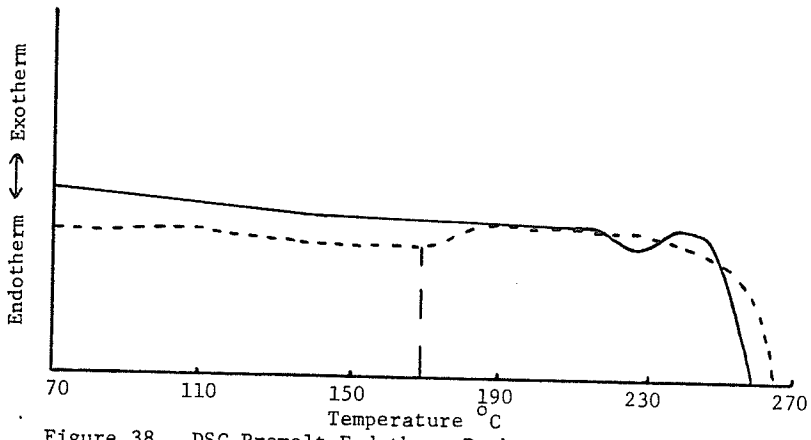

Figure 38. DSC Premelt Endotherm Peak--Commercial Reference Comparison to the PET Yarn Crimped at 154°C
—— Yarn from the Milliknit® graft (sample seven)
--- Yarn compacted and crimped at 154°C (sample four)

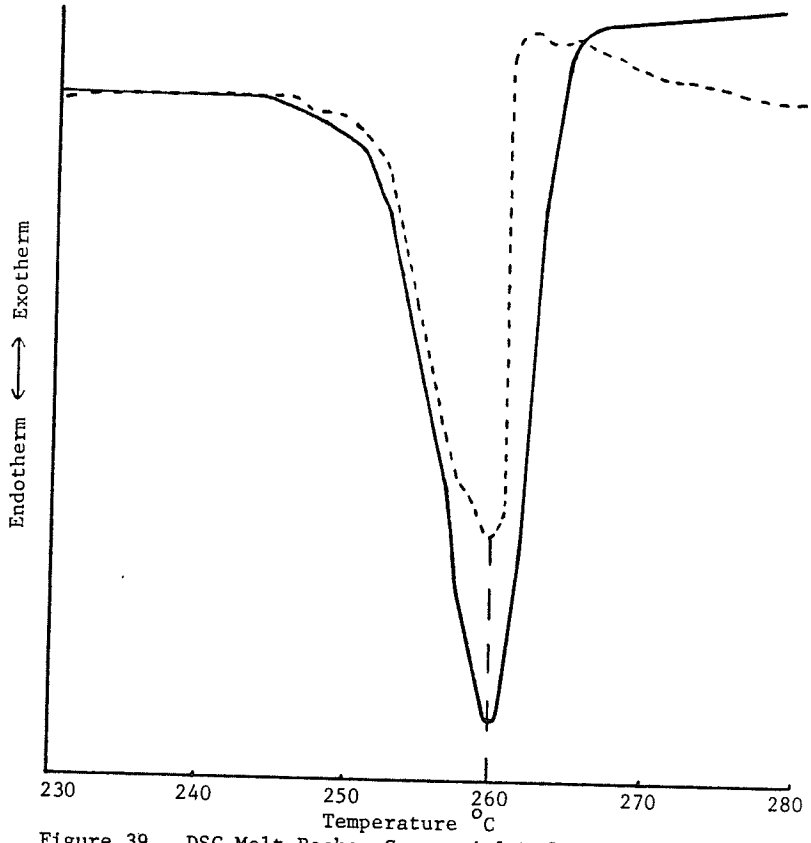

Figure 39. DSC Melt Peaks--Commercial Reference Comparison to the PET Yarn Crimped at 154°C
—— Yarn from the Milliknit® graft (sample seven)
--- Yarn compacted and crimped at 154°C (sample four)

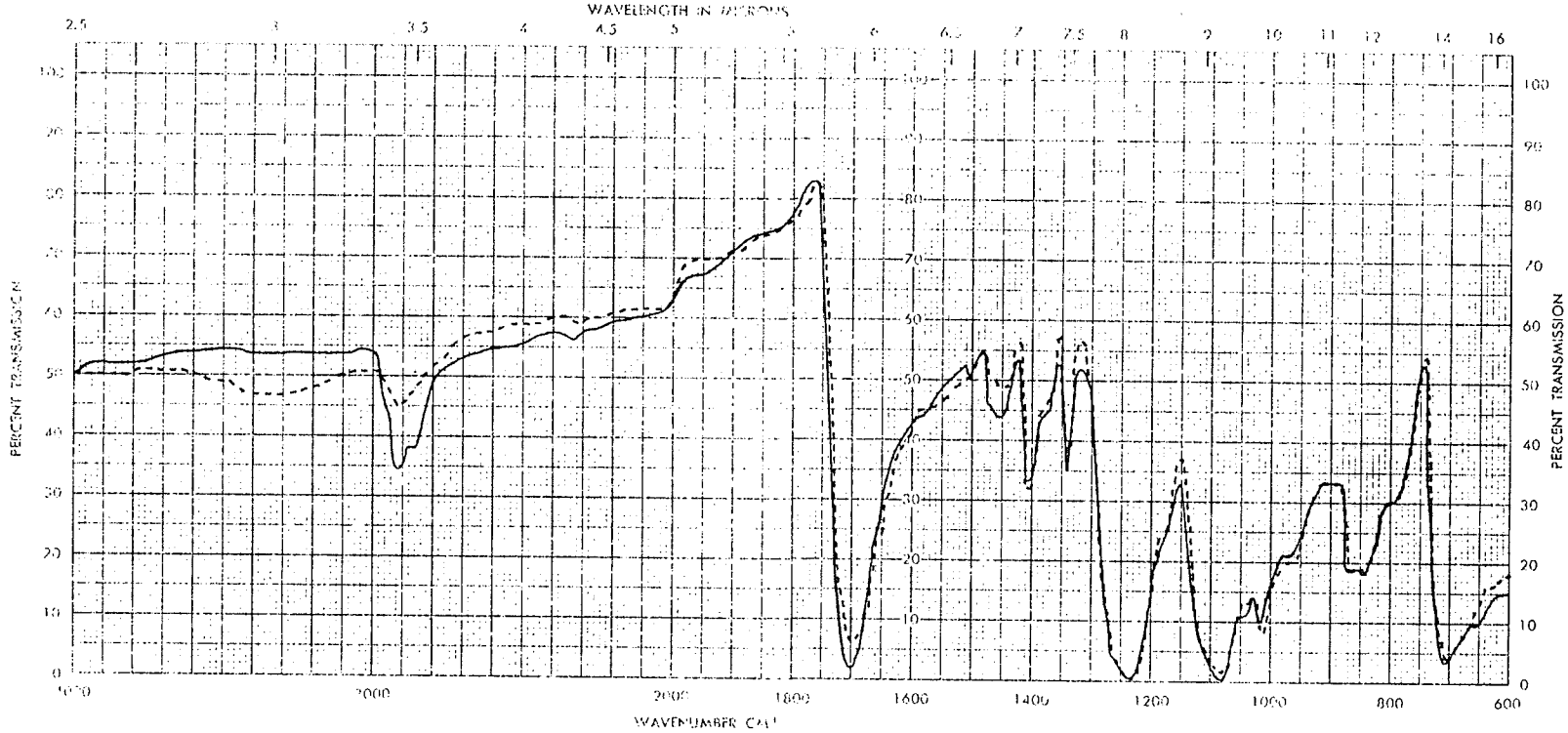

Figure 40. Infrared Spectra--Commercial Reference Comparison to the PET Yarn Crimped at 94°C
——Yarn from the Milliknit® graft(sample seven)
--- Yarn compacted and crimped at 94°C(sample three)

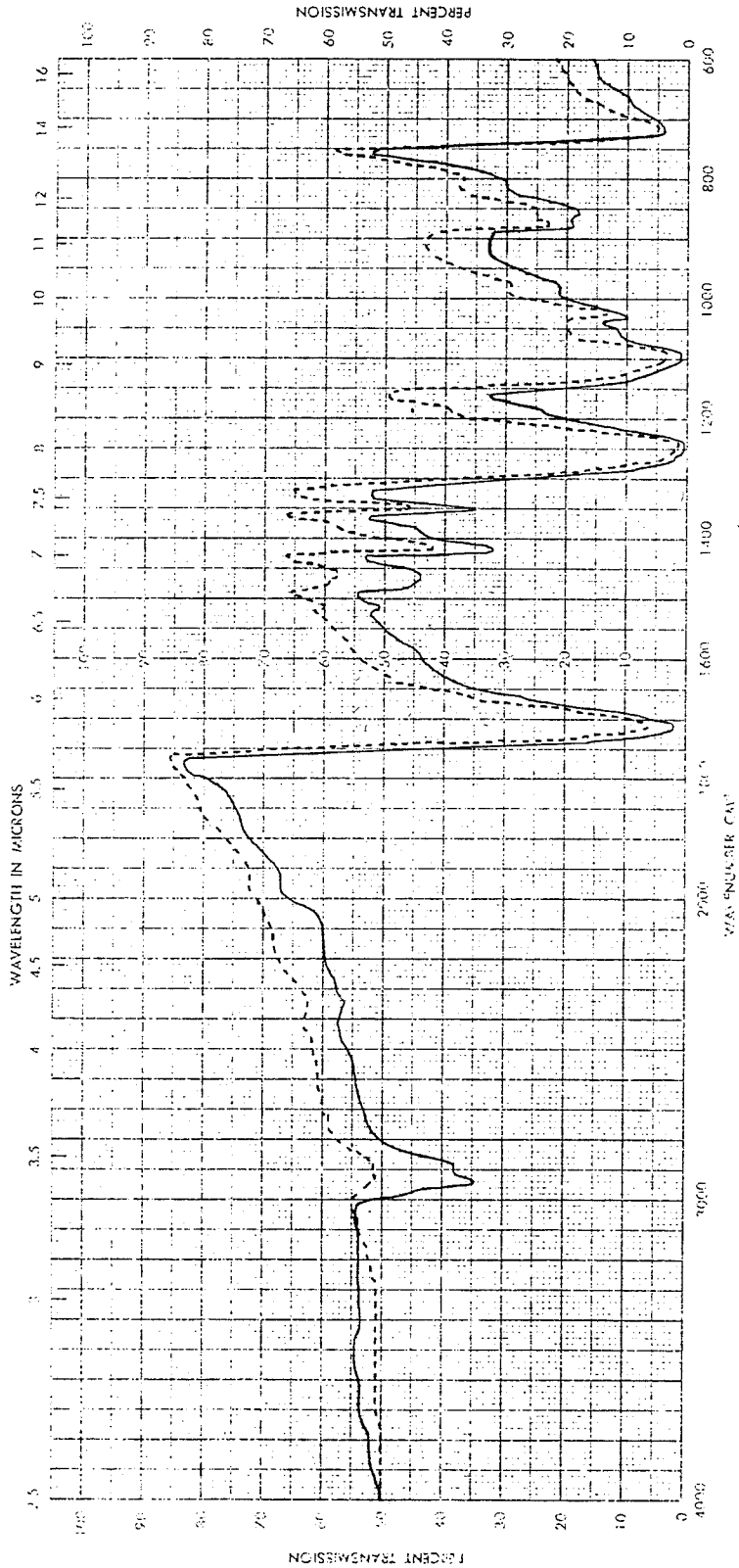

Figure 41. Infrared Spectra--Commercial Reference Comparison to the PET Yarn Crimped at 154°C
—— Yarn from the Millikni®graft(sample seven)
--- Yarn compacted and crimped at 154°C(sample four)

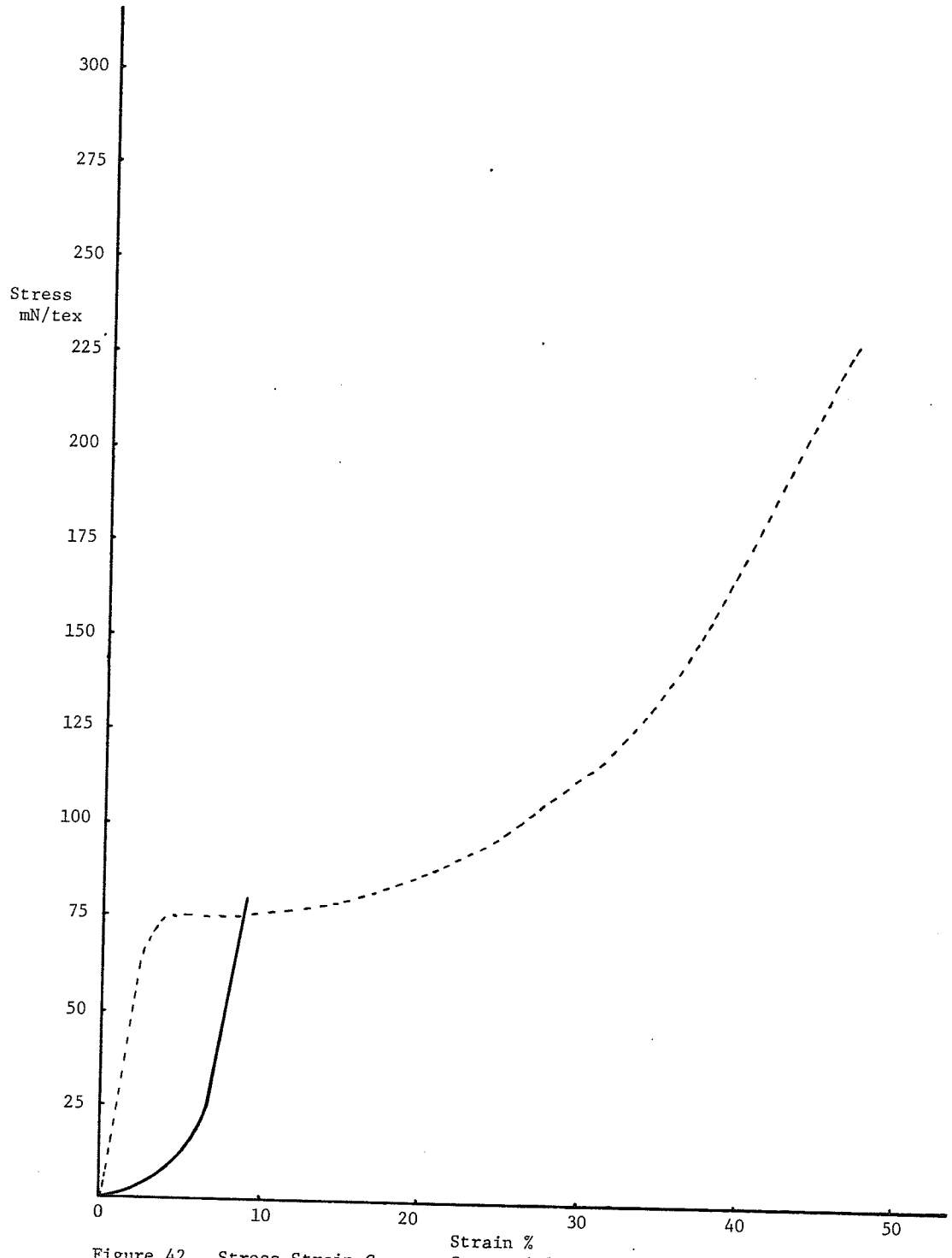

Figure 42. Stress-Strain Curves--Commercial Reference Comparison to the PET Yarn Crimped at 94°C

—— Yarn from the Milliknit® graft (sample seven)

--- Yarn compacted and crimped at 94°C (sample three)

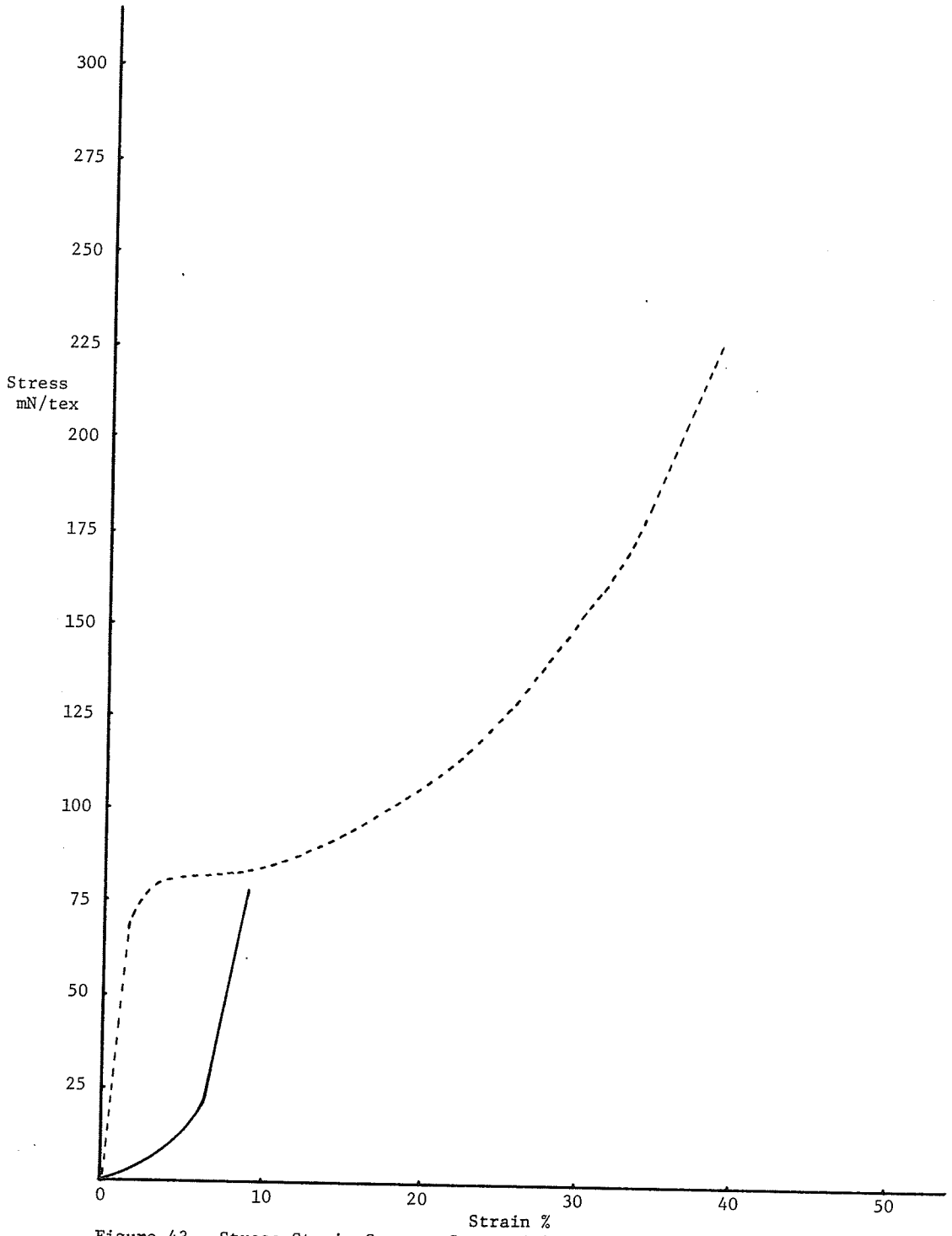

Figure 43. Stress-Strain Curves--Commercial Reference Comparison to the PET Yarn Crimped at 154°C

—— Yarn from the Milliknit® graft (sample seven)

--- Yarn compacted and crimped at 154°C (sample four)

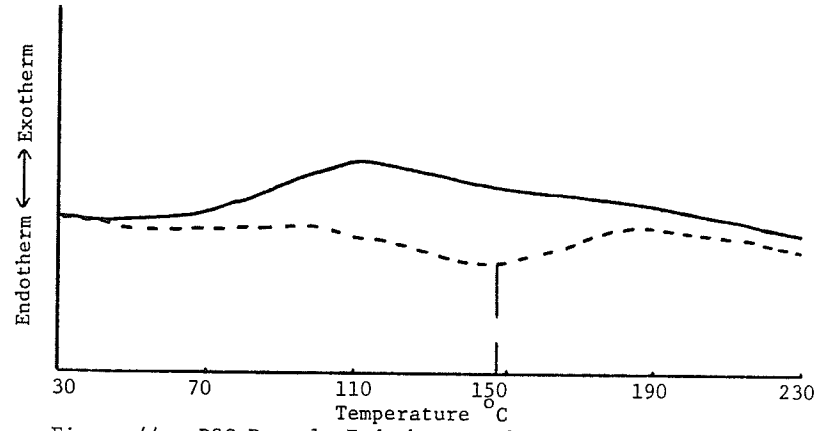

Figure 44. DSC Premelt Endotherm Peak--Comparison of Compacted, Crimped 94°C and Sterilized Yarn to the Untreated Yarn
—— Untreated yarn (sample one)
--- Yarn compacted, crimped at 94°C and sterilized (sample five)

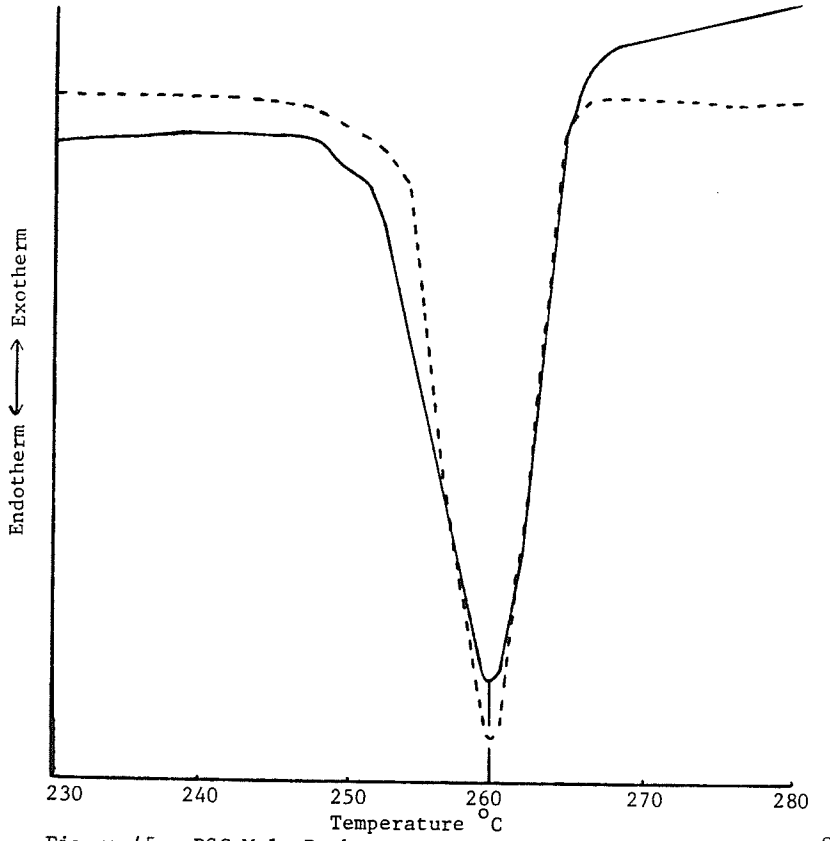

Figure 45. DSC Melt Peaks--Comparison of Compacted, Crimped 94°C and Sterilized Yarn to the Untreated Yarn
—— Untreated yarn (sample one)
--- Yarn compacted, crimped at 94°C and sterilized (sample five)

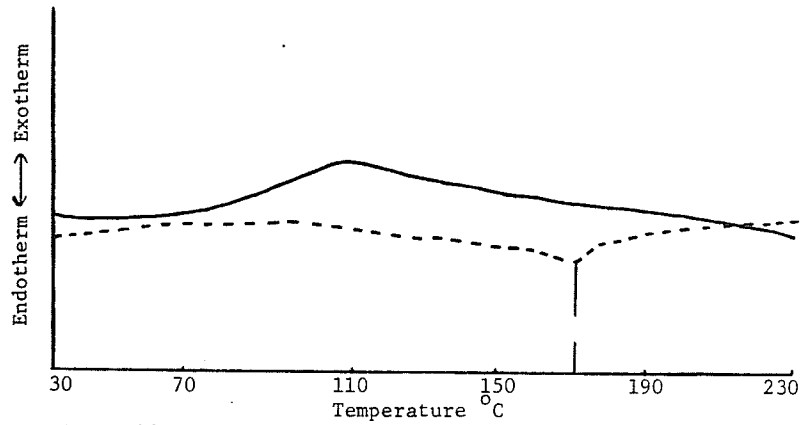

Figure 46. DSC Premelt Endotherm Peak--Comparison of Compacted, Crimped 154°C and Sterilized Yarn to the Untreated Yarn
—— Untreated yarn (sample one)
--- Yarn compacted, crimped at 154°C and sterilized (sample six)

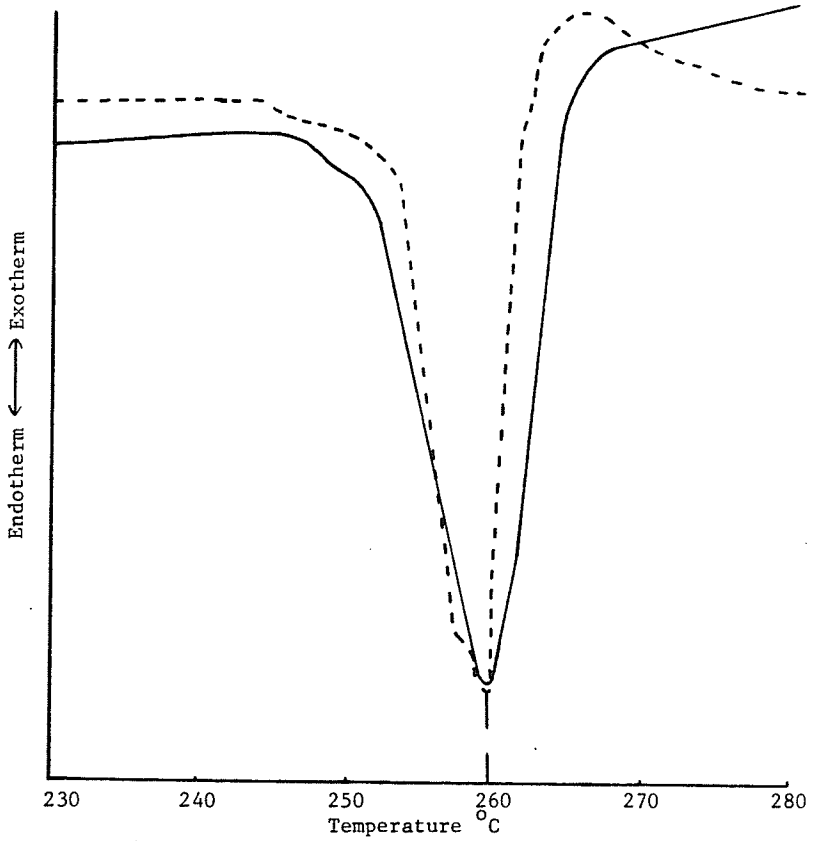

Figure 47. DSC Melt Peaks--Comparison of Compacted, Crimped 154°C and Sterilized Yarn to the Untreated Yarn
—— Untreated yarn (sample one)
--- Yarn compacted, crimped at 154°C and sterilized (sample six)

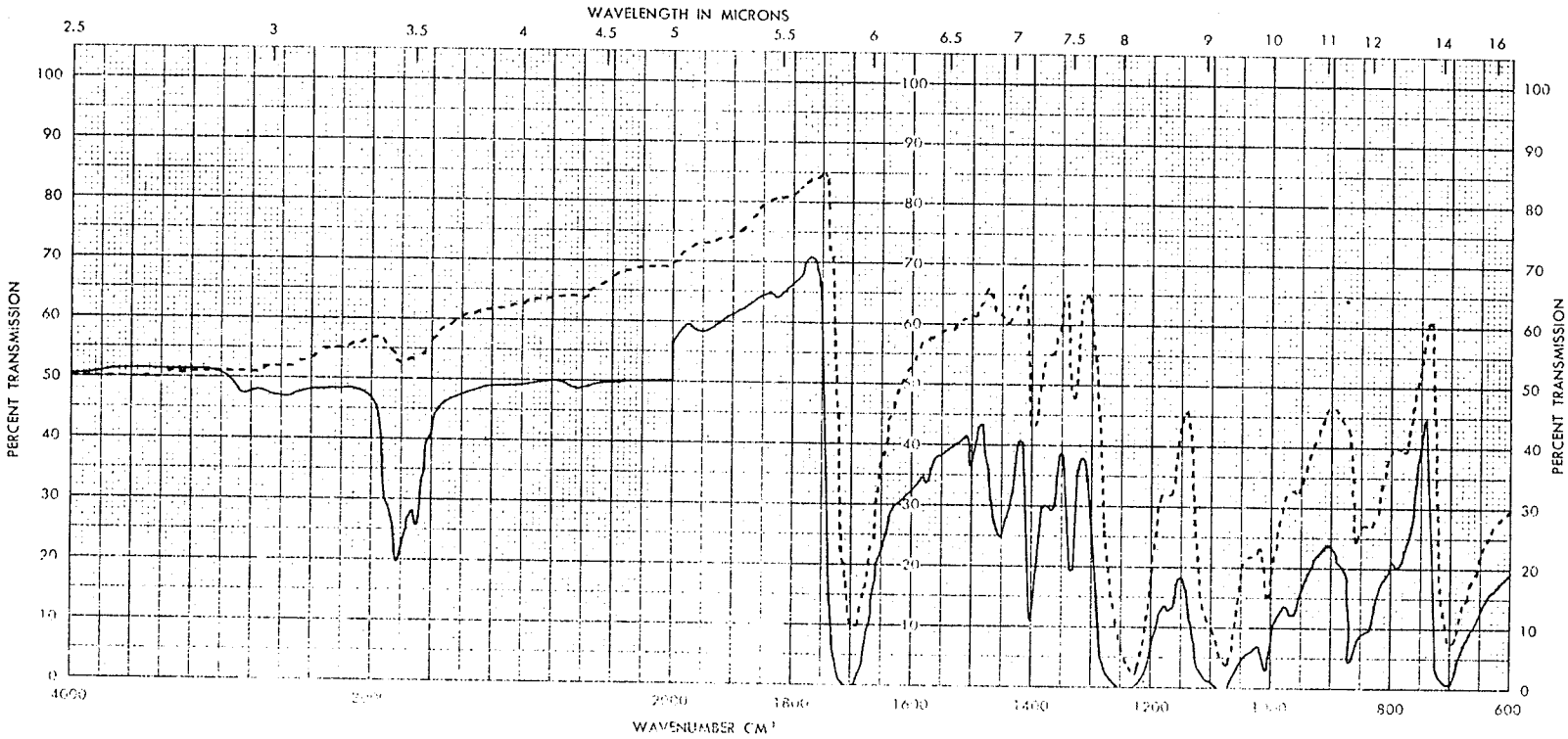

Figure 48. Infrared Spectra--Comparison of Compacted, Crimped 94°C and Sterilized Yarn to the Untreated Yarn
—— Untreated yarn (sample one)
--- Yarn compacted, crimped at 94°C and sterilized (sample five)

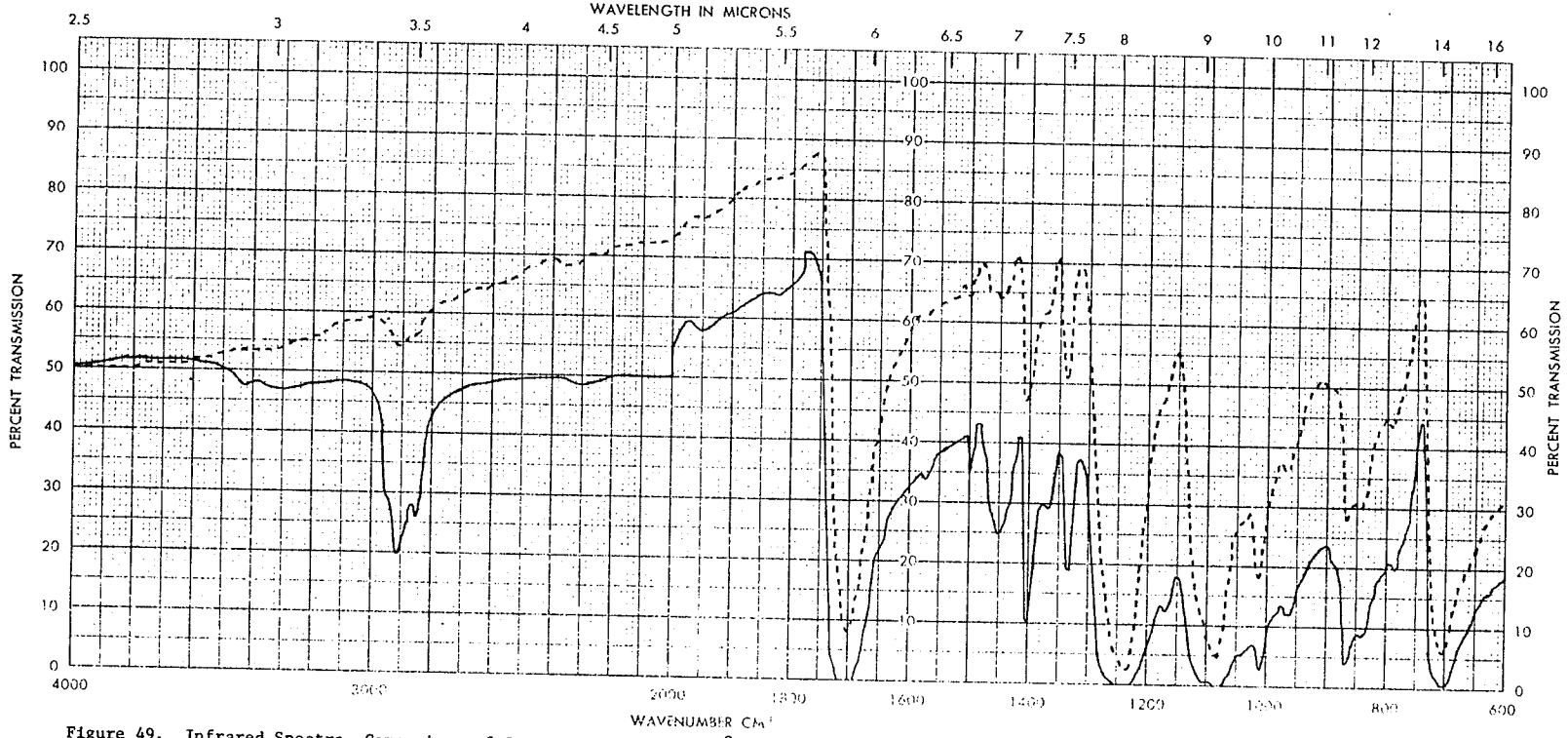

Figure 49. Infrared Spectra--Comparison of Compacted, Crimped 154°C and Sterilized Yarn to the Untreated Yarn
—— Untreated yarn (sample one)
--- Yarn compacted, crimped at 154°C and sterilized (sample six)

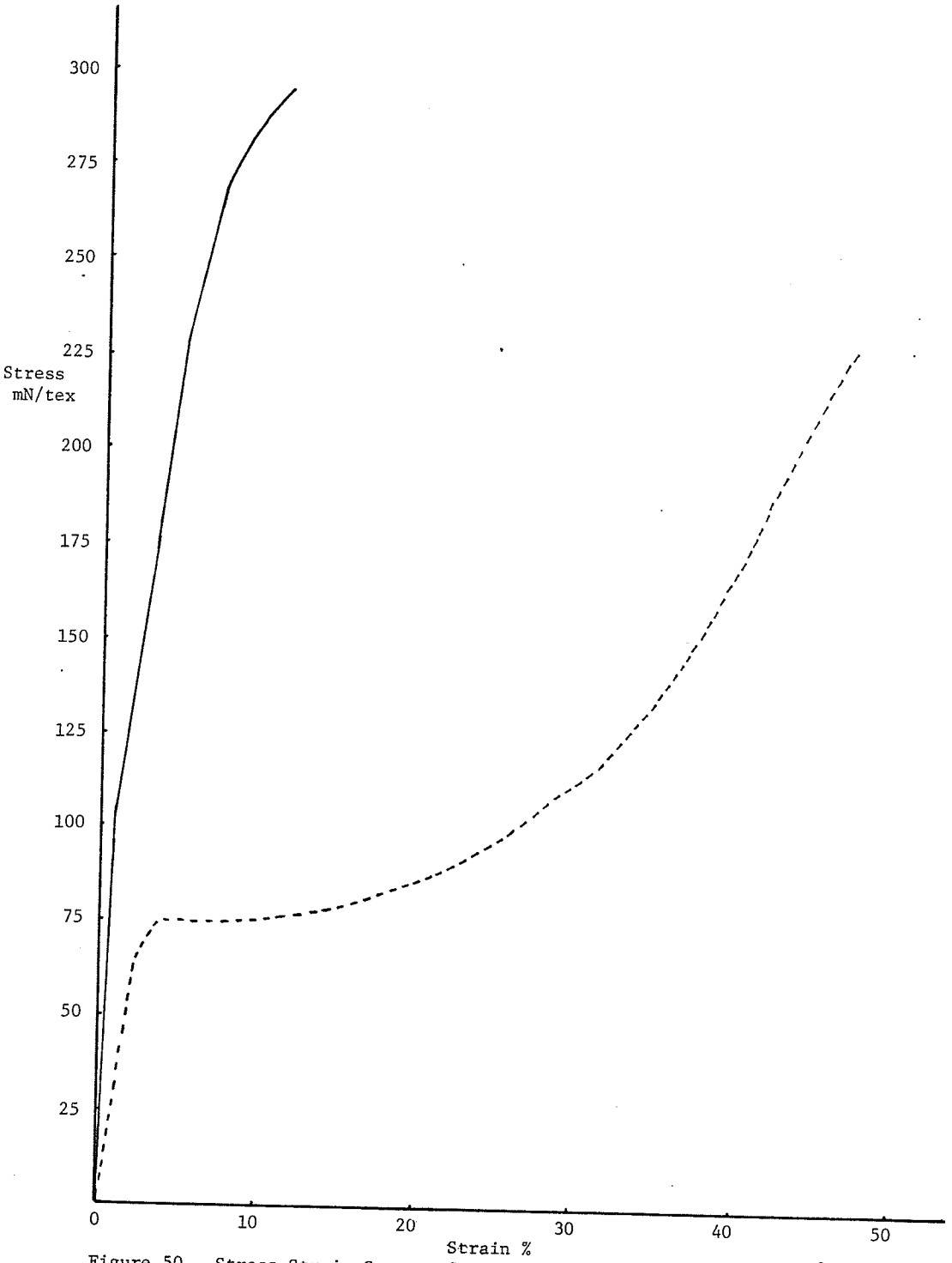

Figure 50. Stress-Strain Curves--Comparison of Compacted, Crimped 94°C and Sterilized Yarn to the Untreated Yarn

—— Untreated yarn (sample one)

--- Yarn compacted, crimped at 94°C and sterilized (sample five)

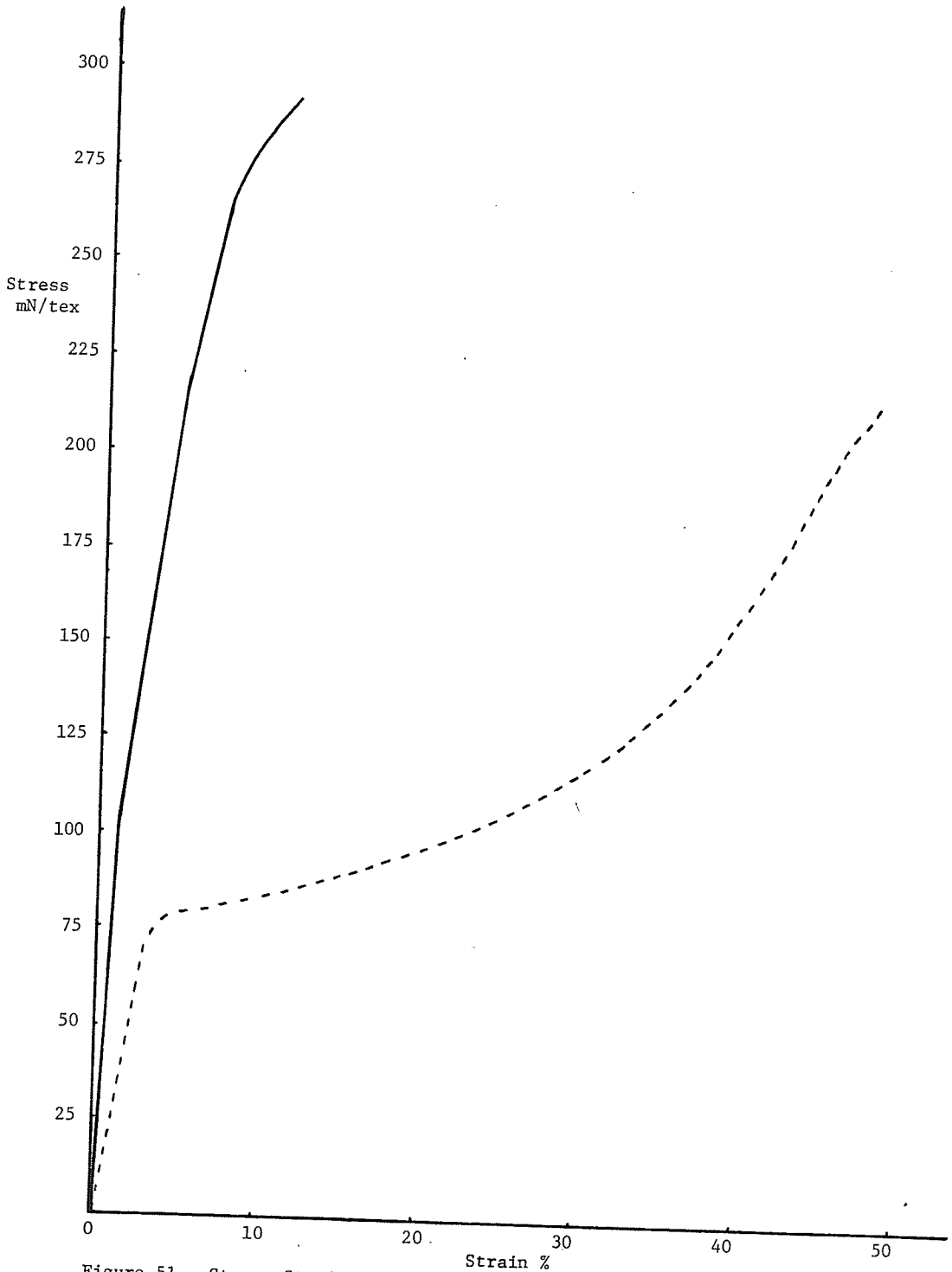

Figure 51. Stress-Strain Curves--Comparison of Compacted, Crimped 154°C and Sterilized Yarn to the Untreated Yarn
—— Untreated yarn (sample one)
--- Yarn compacted, crimped at 154°C and sterilized (sample six)